Energieforschungsprogramm

APPENDIX

Programmsteuerung:
Klima- und Energiefonds

Programmabwicklung:
Österreichische Forschungsförderungsgesellschaft mbH (FFG)

Appendix to Endbericht
erstellt am
11/07/2023

Projekttitel:

Induced Seismicity Risk Estimation

Projektnummer:
FO999888478

InStRikE

Induced Seismicity Risk Estimation in Geothermal Fields

AutorInnen:
Julia Diessl
Nicola Levi
Michael S. Bruno
Jean T. Young
Bastian Roters
Fatimeh Nazari
Christian Rambousek
Jörg Lenneis

Table of Content

Appendix 1. Figures Quoted In The Report

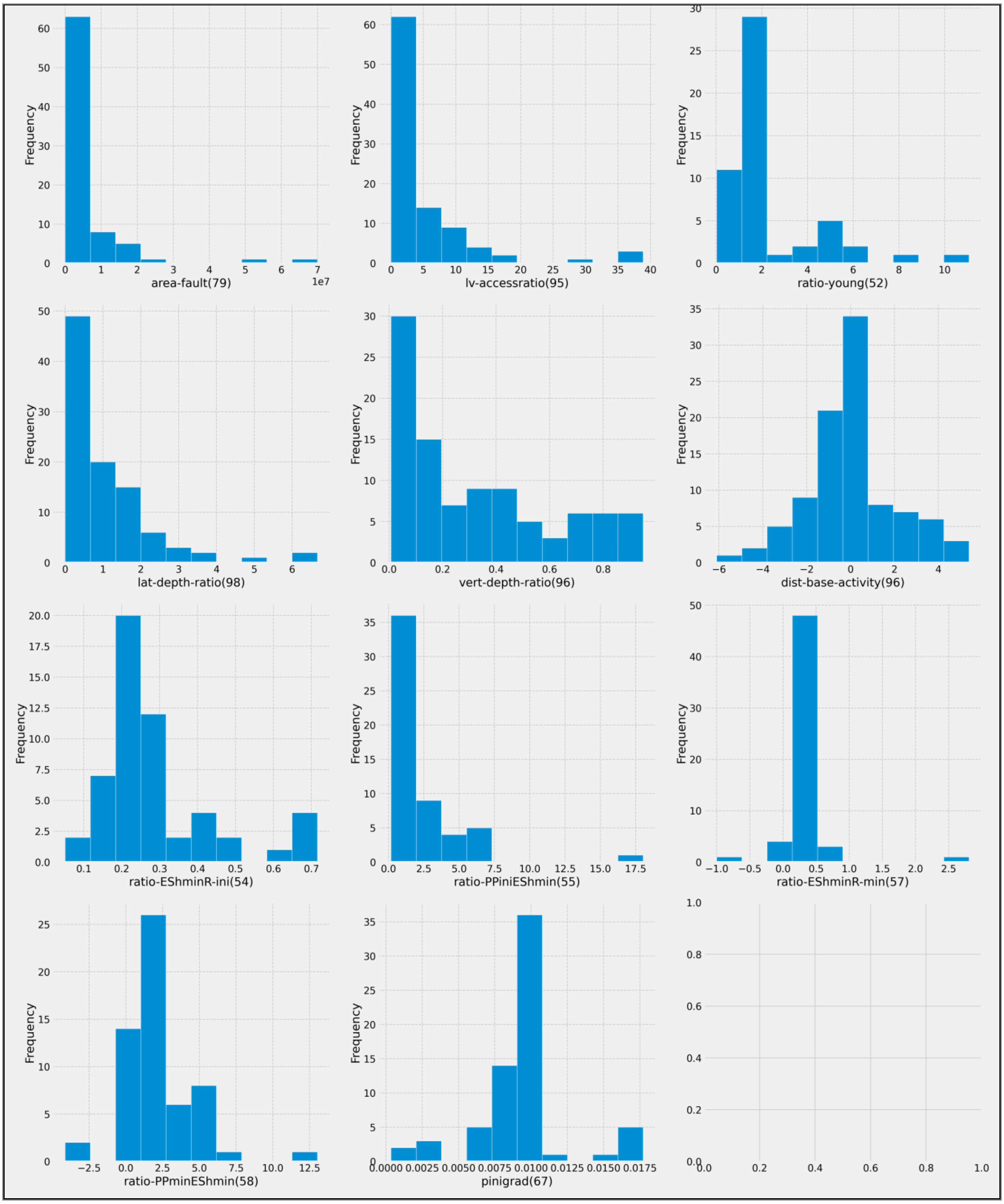

Figure 1. Histograms of the 26 numerical parameters selected for further analysis with the corresponding frequencies.

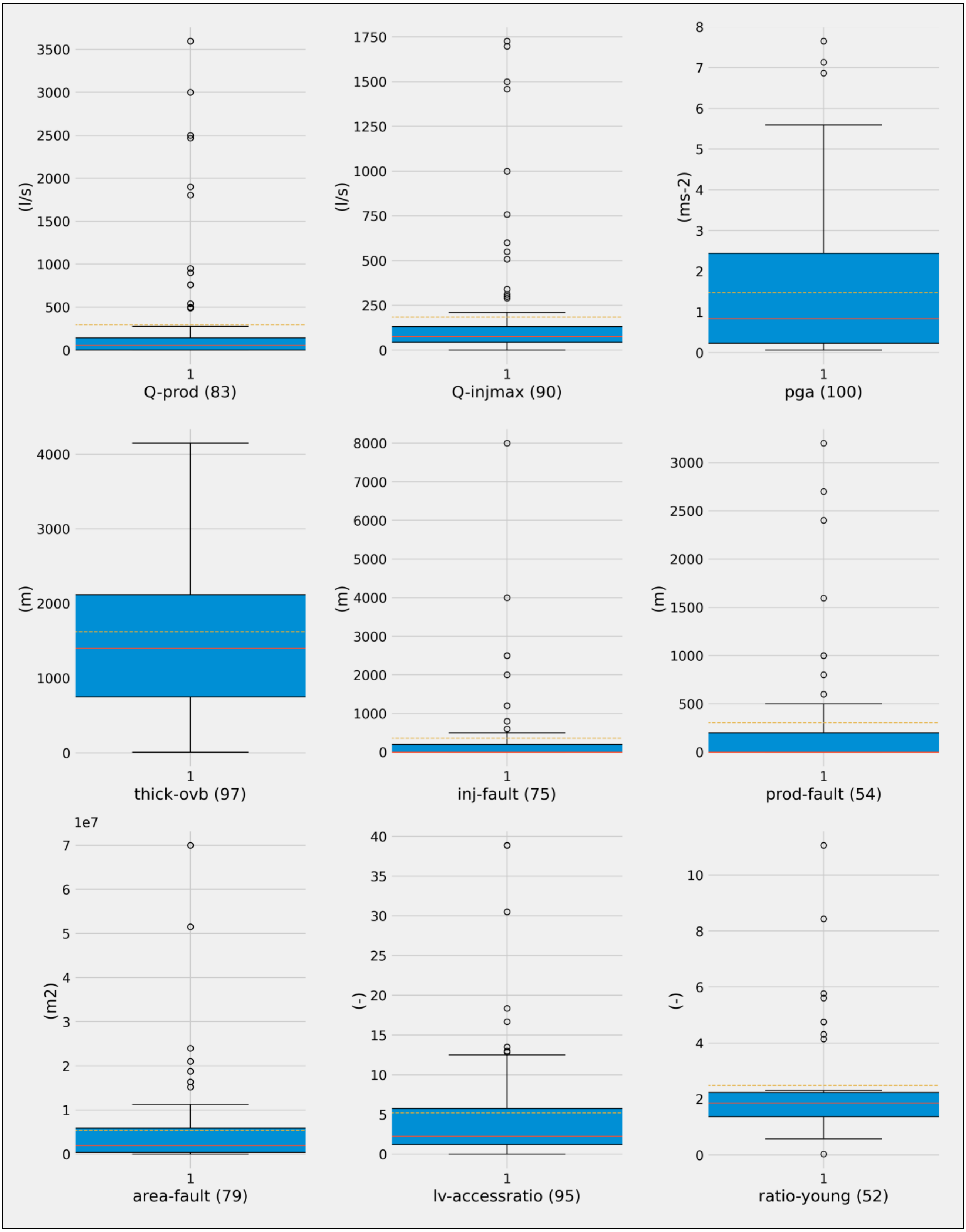

Figure 2. Whisker plot of some of the 26 numerical parameters selected for further analysis. For each plot: blue box, 50% of the data; black lines are max and min values; yellow and orange dashed lines are respectively mean and median; circles are outliners (data far away from the mean). The number next to the parameter name indicates the number of entries in the database.

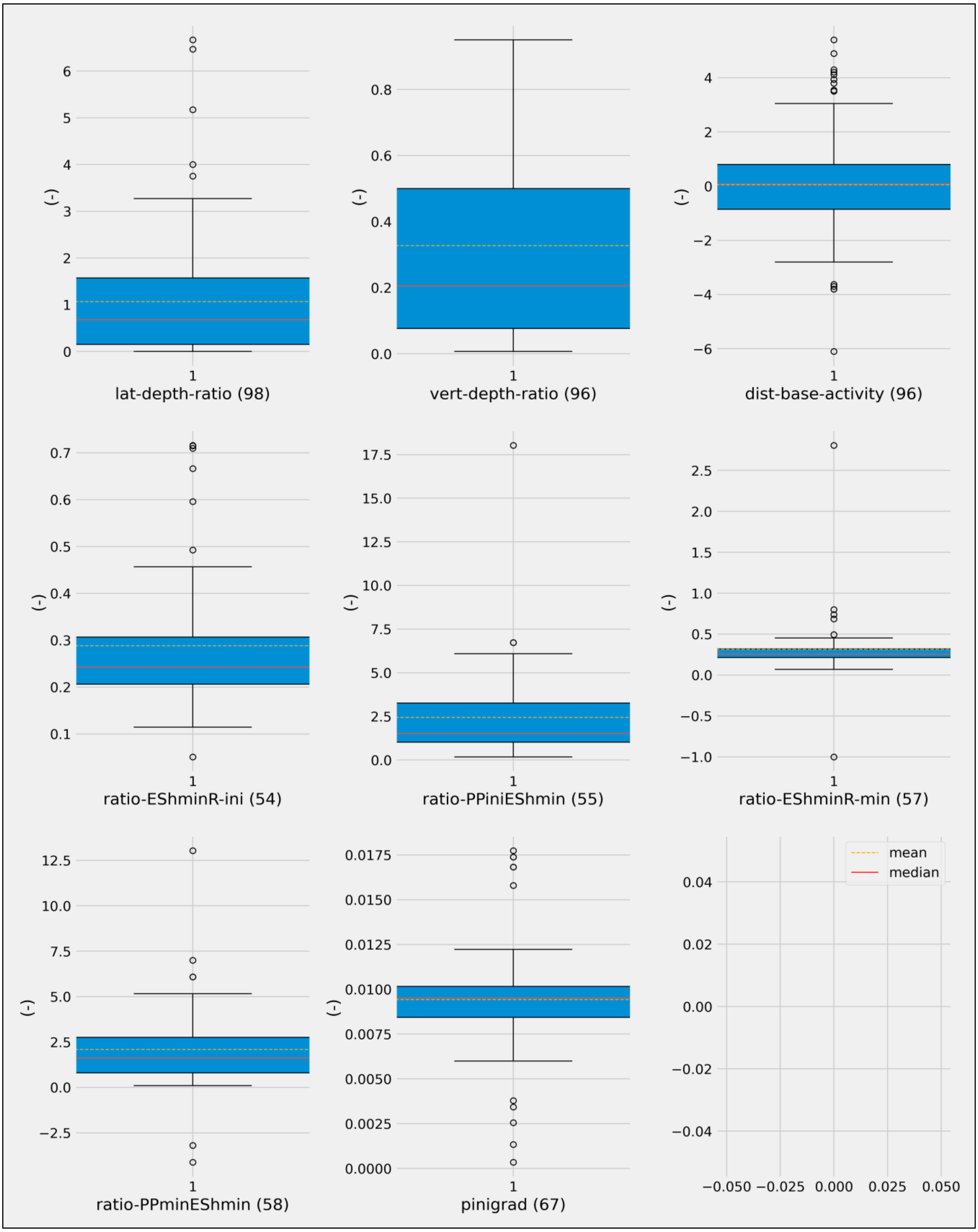

Figure 3. Whisker plot of some of the 26 numerical parameters selected for further analysis. For each plot: blue box, 50% of the data; black lines are max and min values; yellow and orange dashed lines are respectively mean and median; circles are outliners (data far away from the mean). The number next to the parameter name indicates the number of entries in the database.

Appendix 2. Short Names of the Parameters in the Database

Table 1 List and Description of the parameters in the InStriKe Database that were originally also in the Buize et al. (2020).

short name	Unit	
play		
play-type		according to Moeck et al. 2014.
cond-conv		
system		HS: hydrothermal system, PS: petrothermal system, HSA: hot sedimentary aquifer
balance		net fluid/mass balance. DEP: depletion, DEP-REINJ: depletion-reinjection, BAL: balanced circulation, INJ: injection
depth-act	km	maximum depth of the activity (0 = surface)
T	°	initial reservoir temperature
dT	°	temperature difference in-situ T and (re)injected fluids
rock		rockype in which the activity takes place
depth-base	km	Depth of basement below the reservoir
por		initial reservoir porosity
start-operation	M/D/Y	start date (and time) of the activity
start-rein	M/D/Y	start of (re)injection. For geothermal fields this can be years later than the start of prodction
end-of-activity	M/D/Y	end data (and time) of the activity. Ongoing (01-01-2019)
datemmax	M/D/Y	date of occurrence of mmax
mmax		magnitude of mmax. -9999 for no seismicity; maximum magnitude associated with a certain project. Mostly relating to induced events, but for a number of sites where natural seismicity was abundant and correlation between operations and seismicity was not straightforward, it was the maximum magnitude at a certain geothermal site. We based this on publicly available literature/documents.
mag-scale		scale used to determine magnitude
Mc		magnitude of completeness of monitoring network
dV-prod	m3	produced volume
dV-inj	m3	(re)injected volume
dV-net	m3	net injected volume (negative = net depletion volume)
date-dV	M/D/Y	date at which produced or injected volume was taken
dP-inj	MPa	wellhead injection pressure
pini	MPa	initial pressure at activity depth
Q-prod	l/s	maximum production rate (in case of multiple wells it is the cumulative production rate of all wells)
Q-injmax	l/s	maximum injection rate (in case of multiple wells it is the cumulative production rate of all wells)
tectonic		Stress Regime
pga		seismic hazard related to natural seismicity from Pagani et al., 2020

Table 2 List and Description of the parameters in the new InStRiKE Database that are not in Bujize et al. (2020).

short name	Unit	
l-access	m	maximum well distance, laterally
v-access	m	maximum well distance, vertically
perm-min	mD	min permeability
perm-max	mD	max permeability
strength-res-min	MPa	min reservoir strength (UCS)
strength-res-max	MPa	max reservoir strength (UCS)
young-res-min	GPa	min reservoir stiffness (Young's mod.)
young-res-max	GPa	max reservoir stiffness (Young's mod.)
heterogen		Field heterogeneity (reservoir/overburden)
strength-ovb-min	MPa	min strength of first overlying formation, (UCS)
strength-ovb-max	MPa	max strength of first overlying formation,(UCS)
young-ovb-min	GPa	min stiffness of first overlying formation, (Young's modulus)
young-ovb-max	GPa	max stiffness of first overlying formation, (Young's modulus)
thick-ovb	m	overburden thickness
fault-bound		fault boundaries one / multiple)
fault-res		reservoir faults
inj-fault	m	dist to injector perforations - fault
prod-fault	m	dist to producer perforations - fault
csf		critically stressed faults
area-fault	m2	fault area
sigma3-min	MPa	min minimum stress (sigma 3)
sigma3-max	MPa	max minimum stress (sigma 3)
sigma1	MPa	maximum stress (sigma1)
pp-min	MPa	minimum reservoir pressure
pp-max	MPa	max reservoir pressure
shmax-orient	deg	sHmax orientation clockwise from N (0-180)
fault-orient1	deg	main fault orientation clockwise from N (0-180)
fault-orient2	deg	fault orientation clockwise from N (0-180)
fault-orient3	deg	fault orientation clockwise from N (0-180)
fault-dip1	deg	fault dip
oper-current		current operator
num-events		Number of Seismic Events 50 years before starting of operations
depth-Average		Average depth of Seismic Events 50 years before starting of operations
Magnitude-Average		Average Mag. of Seismic Events 50 years before starting of operations
Magnitude-Max		Max Mag. of Seismic Events 50 years before starting of operations

Table 3 Overview of the parameters derived from other parameters present in the InStRikE Database.

name	formula
l-access-v-access-ratio	=(lateral access/vertical access)
strength-res-avg	=(strength-res-min+strength-res-max)/2
strength-ovb-avg	=(strength-ovb-min+strength-ovb-max)/2
ratio-strength	=strength-res-avg/strength-obv-avg
young-res-avg	=(young-res-min+young-res-max)/2
young-ovb-avg	=(young-ovb-min+young-ovb-max)/2
ratio-young	=young-res-avg/young-obv-avg
l-access-depth-act-ratio	=(lateral access/depth of activity)
v-access-depth-act-ratio	=(vertical access/depth of activity)
dist-base-activity	=depth-base-depth-act
sigma3-avg	=(sigma3-min+sigma3-max)/2
ratio-EShminR-ini	=(sigma3-avg-pini)/(sigma1-pini)
ratio-PPiniEShmin	=(pini)/(sigma3-pini)
ratio-EShminR-min	=(sigma3-avg-pp-min)/(sigma1-pp-min)
ratio-PPminEShmin	=(pp-min)/(sigma3-pp-min)
ratio-EShminR-max	=(sigma3-avg-pp-max)/(sigma1-pp-max)
ratio-PPmaxEShmin	=(pp-max)/(sigma3-pp-max)

Appendix 3. Risk Parameter Details

The risk parameters here described are subdivided in 3 main groups:

A. Geothermal reservoir system factors
B. Geomechanical Risk Parameters
C. Operational Risk Parameters

The first two groups consist of parameters that depend on the geologic and geodynamic setting of the site, whereas the last group consists of factors that can be changed by the operators, based on various requirements.

Geothermal reservoir system factors

3.1.1 Type of Reservoir (A)

Following the geothermal play categorization by Moeck (2014) the risk for inducing seismicity is estimated to be high for the types CD3 and CV2, medium for CV3, CD1 and CD2 and low for CV1 types (Table 4). We derive this information from literature on general description of the geothermal field.

Entry: **BT** (basement type), **EDT** (Extensional Domain Type), **IBT** (Intracratonic Basin Type), **OBT** (Orogenic Belt Type), **PT** (Plutonic Type), **VF** (Volcanic Field). **CD** (Conductive Type), **CV** (Convective Type) (Figure 4).

Table 4. Geothermal Play types after Moeck et al. (2014).

Table 3
Catalog of geothermal play types applying the scheme from Figs. 2 and 5. Examples represent typical geologic systems in which geothermal reservoirs are already discovered and developed. These examples might act as typus localities for respective geothermal play types. Reservoir characteristics host rock, fluid type and temperature range refer to the examples and do not reflect necessarily general characteristics. Categories of fluid types: Basinal fluids are saline brines and NaCl-dominated, infiltration fluids are carbonate waters and HCO_3-dominated, crustal fluids are acidic and H_2S/HCl-dominated (modified from [80]).

Heat transfer	Geologic controls	Geologic system plate tectonic setting	Geothermal play type	Index	Examples	Characteristics		
						Host rock	Fluid	Temperature in (°C)
Convection Dominated (CV)	Magma chambers in active volcanic fields	Volcanic arc regions at subduction zone Mid oceanic Ridges (MOR) Mantle plumes (hot spots)	Volcanic type	CV1	Java - Kamojang (Indonesia) [99] Taupo – NZ [100] Reykjanes – Iceland [101] Hawai (USA) [102]	Andesites Rhyolithes Basalt	Crustal fluids mixed with infiltration fluids (meteoric, seawater)	70–320
	Crystallizing magma, intrusions + active faulting	Decrescent volcanism in steep terrain at young orogenic belts	Plutonic type	CV2	Larderello (Italy) [103] The Geysers (USA)	Sediments Granite, Grabbo	Infiltration and crustal fluids	100–350
	Active faulting (natural seismicity)	Metamorphic core complexes Pull-apart basins Back-arc basins Intracontinental rifts (grabens)	Extensional domain type	CV3	Great Basin (Basin and Range) – USA [22] Western Turkey Soultz-sous-Forêt (France) [71]	Volcanic sedimentary rock	variable	150–240
Conduction Dominated (CD)	Lithofacies (grain size, mineralogy) Biofacies (fossil content)	Intracontinental rift basins Passive margin basins	Intracratonic Basin Type (hydrothermal)	CD1	North German Basin [27]	High–low permeability fluvial sediments	Basinal fluids	< 150
	Litho-/biofacies + faults/ fractures	Fold-and-Thrust-belts Foreland basins	Orogenic belt type (hydrothermal)	CD2	Molasse Basin (South Germany) [23]	High–low permeability marine sediments	Infiltration fluids (basinal fluids possible)	< 160
	Faults/fractures	Intracontinental intrusion in flat terrain	Basement type (petrothermal hot dry rock)	CD3	Cooper Basin (Australia)	Granite rock with high radiogenic heat production	–	150–320

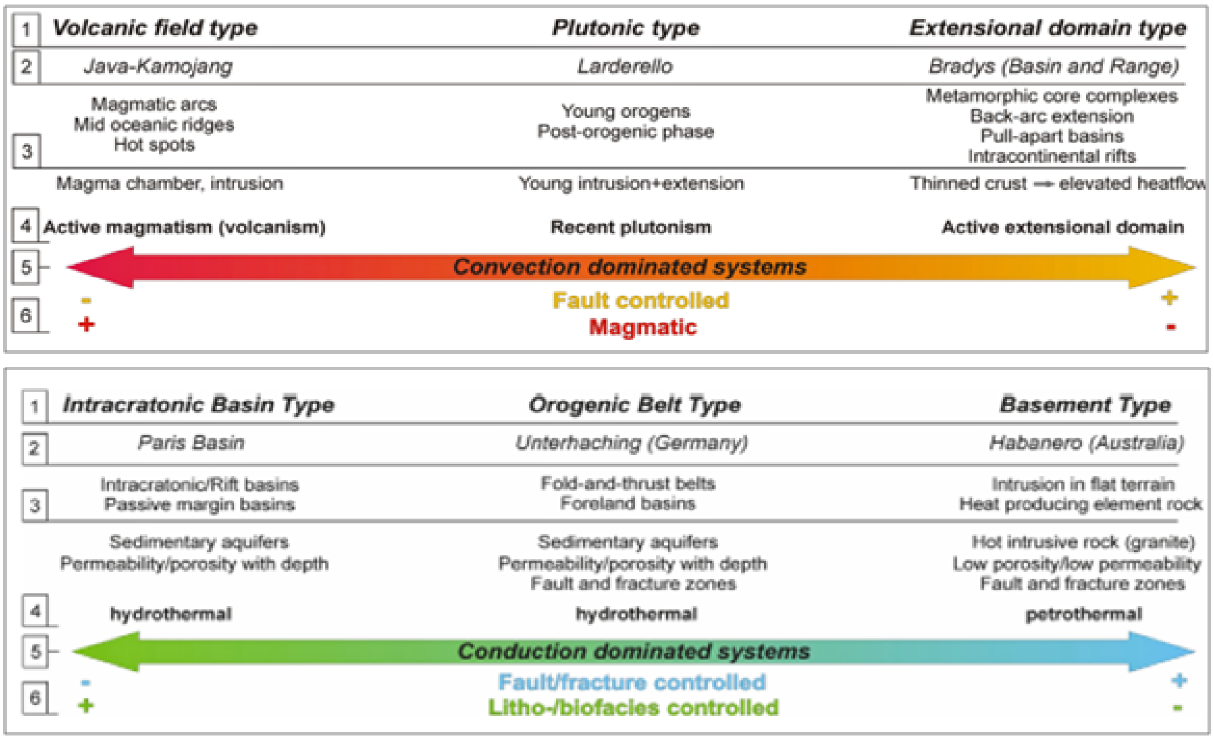

Figure 4. Convection and conduction dominated geothermal play types, according to Moeack et l., (2014)

3.1.2 Reservoir Zone Porosity / Permeability (A)

Porosity determines the volume for fluids as well as the potential for moving these fluids, thus heat convection, in the reservoir. The permeability in the end is the factor that determines the possibility of migration of fluids through the reservoir. We collect initial reservoir porosity. Since permeability is often not determined, well established porosity-permeability functions can be used to estimate this parameter from the porosity.

The permeability of the reservoir mainly influences the fluid migration in the reservoir. Also, the larger the permeability, the less the pressure build up surrounding the injection area; and therefore, the lower the risk to cause the development of shear or tensile fractures. On the other hand, a high permeability allows the transport of fluids further away from the injection area. Thus, changes in effective stresses can occur in a larger area that could result in reactivation of existing faults.

Buijze et al. (2019, 2020) found a trend of porosity with induced seismicity for conduction dominated plays, but no significance of that parameter for convection dominated plays. However, these relationships could derive from the commonly observed correlation between reservoir porosity and stiffness, which in turn might result in higher seismicity.

The parameter reservoir permeability must be reported in Mili-Darcy (mD). In case multiple values in the reservoir section are recorded, an average value is used. If only hydraulic conductivity is reported (cm/s), the corresponding permeability can be derived using a simple formula. In case permeability is derived from other parameters, this shall be highlighted.

Entry: porosity in %, permeability in mD.

Long description: initial reservoir porosity, reservoir permeability

3.1.3 Rock strength and strength ratio (A)

Rock strength is the property of the rock to withstand fracturing induced by external stresses, both reservoir and overburden and here considered. A fracture develops only when the unconfined compressive strength (UCS) in a rock is overcome, so the higher the unconfined compressive strength of the reservoir the lower the risk for the development of fracture networks for a specific stress change. Fracture networks influence the permeability, thus the potential of induced seismicity as discussed above. The compaction is not affected by strength, but rather by the stiffness that is shown in the next paragraph.

The overburden is subject to poro-elastic stresses induced by the fluid injection in the underlaying reservoir rocks, resulting from both thermal and pressure components. In these conditions the strength (UCS) of the overburden must withstand these stresses. Furthermore, the overburden must also be capable of containing the increase of pore pressure resulting from fluid injection.
A high rock strength ratio indicates a stronger overburden compared with the rocks of the geothermal reservoir, thus failure due to stress changes is more likely to occur inside the reservoir. Levels of high stress will thus dissipate within the reservoir. In case the reservoir strength is higher than that of the overburden or surrounding rock, more energy will be stored in the reservoir rock and the propagation energy can be dissipated further away from the point of perturbation. This increases the likelihood of affecting larger areas once reaching weaker overburden rock, thus inducing bigger seismicity.

In case overburden and reservoir strength values cannot be retrieved, they can be estimated from other parameters using various empirical equations for specific rock types. To estimate UCS from the rock stiffness (E) the following equations were used: volcanics Dinçer et al. (2004); carbonates Sachpazis (1990); sandstones and shales Zoback (2007); granites Tuğrul and Zarif (1998); gneiss Kesonen (2015). In case open hole logs are available, UCS can be estimated from these data using one of the various lithology-calibrated equations listed in Zoback (2007). For some locations, the entries for the UCS were derived from the PetroPhysical Property Database P³ (Bär et al. 2020).

Unconfined compressive strength (UCS) of both reservoir and the first overlying formation is collected and expressed in MPa. In case of multiple values within one of the intervals (overburden and reservoir), maximum and minimum values will be used.

Entry: UCS in MPa.
Long description: Unified compressional strength or rock strength for both reservoir and overburden rocks.

3.1.4 Rock stiffness and stiffness ratio (A)

The stiffness (or Young's modulus E) of a rock describes its inability to deform under growing stress load. The stiffer a rock the less the strain experienced based on added stress. On the contrary a less stiff, thus soft rock will exhibit/show more deformation under the same stress load.
As stiff rocks can store more energy, a lot more energy can be released once they reach failure (its strength limits). A numerical study by Mehrabifard et al. (2021) shows, that the frequency of events and the number of events with relatively large magnitude triggered due to water injection increases with rock stiffness. Additionally, as Vilarrasa et al. (2019) discuss, the thermal stresses are directly linked to the stiffness of a rock. Thus, a stiffer rock can absorb stresses for the same amount of thermal stress (= change in temperature) applied to the formation. This factor again provides bigger potential for induced seismicity once the rock reaches its failure criterion.

Variations of stiffness in the geothermal field between reservoir and overburden rocks may lead to differential responses to the induced stresses, resulting into potential stress concentrations on the boundary surfaces between them, increasing the likelihood of inducing seismicity there.

For our study we are collecting information of the prevailing stiffness in the geothermal field additional to the stiffness of other relevant rock types in the reservoir or the overburden. If we have a heterogeneous reservoir in regard to high stiffness contrast, the interfaces between such rock types are prone for stress concentration, increasing the risk for inducing seismicity.

In case no stiffness if found, this parameter can be estimated from the rock strength (UCS) using the same equations listed in the previous paragraph, or in case OHL are available, it can be estimated from the combination of sonic and density logs (Zoback, 2007). For some locations, the entries for the rock stiffness were derived from the PetroPhysical Property Database P^3 (Bär et al. 2020). The source of the UCS entries is listed in the database.

Min and max rock stiffness shall be collected for the reservoir (1) and for the first overlying formation layer (2).

Entry: Young's modulus (E) in GPa.
Long description: Young's modulus describes the stiffness of a rock. If applicable and possible, provide two values for reservoir and overburden each.

3.1.5 Field heterogeneity (A)

A rock volume is not necessarily a homogeneous body, in which the properties are similar everywhere. Several factors can produce heterogeneity in the rock, meaning that locally the rock volume is more susceptible to induce seismicity. I.e., heterogeneity in the rock may lead to stress concentrations due to poro- and thermo-elastic perturbations, rendering these interfaces or points prone to tensile or shear failure. At a bedding plane such failures might induce seismicity (Guglielmi et al. 2008).

Types of heterogeneities are:

- Zones of different porosity/permeability (i.e., due to cementation)
- Fault/fracture zones
- Unconformities
- Differences in lithology (i.e., varying clay content)
- Differences in facies (i.e., reef facies vs. layered facies in carbonates)
- Differences in rock stiffness
- Changes in pore pressure
- Changes in horizontal stress orientation.

etc.

The above given factors are just examples of heterogeneities. Actual factors encountered in a specific geothermal field shall be taken from available literature. Furthermore, a quantitative measure, by how much a certain heterogenic factor will alter the risk for induced seismicity is impossible to distinguish. Likely, several heterogenic factors are recorded for a field. The idea is to compare the heterogeneity of the collected geothermal fields in a relative manner between each other.

Entry: Low/Moderate/Strong

Long description: Qualitative level of heterogeneity in the rocks as described from the literature about the field. If minimum two of the types of heterogeneity are found we consider a moderate heterogeneity, if more than four are present, we consider it strong.

3.1.6 Overburden thickness (A)

This parameter is strongly linked to the ratios discussed in paragraph 3.1.10. In general, there is a trend that induced seismicity tends to occur in greater depths as discussed in Das and Scholz (1983). This can indicate that shallow geothermal operations are at lower risk in regard to induced significant seismicity compared with deep geothermal operations.

With increasing depths, rocks tend to become stiffer and stress gradients tend to be also higher. Additionally, the risk of intercepting a fault increases with longer distances at depth. If a fault slip occurs under these conditions, a larger seismic event might occur.

Entry: TVD in meter

Long description: Overburden thickness can be inferred from information from literature or from geologic cross-sections. We define it from surface down to the top of shallowest reservoir access of any well in the geothermal field.

3.1.7 Depth to basement (A)

As shown by Buijze et al. (2020), there is a statistical relationship between the depth to basement and induced magnitude, as shown in Figure 5. Thus, in general, there is a higher risk to induce seismicity if the basement is closer. Moreover, if the operation occurs in the basement itself, the risk of inducing seismicity is higher compared with operations well above the basement.

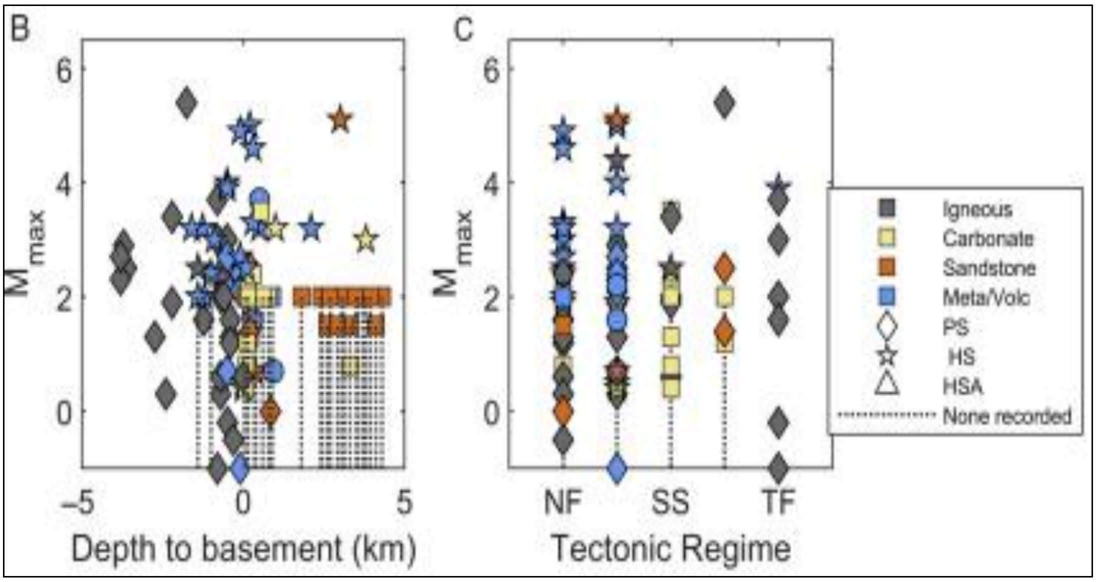

Figure 5. Induced seismicity in correlation with depth to basement (left) and tectonic regime (to the right) (Buijze et al. 2020)

To be able to calculate it, we collect both the base of activity in (km) and top of basement (km).
Entry: Automatically calculated from base of activity (I) and top of basement (M)
Long description: The depth to basement is defined as the base of activity to top of basement.

3.1.8 Natural seismicity depth (A)

Commonly, geothermal fields are explored and operated in regions with constant natural seismicity, such as subduction zones as the geothermal gradient in such regions is higher than the average. High natural seismicity indicates an active geodynamic setting, associated to significant tectonic stresses and close to critically stressed conditions (at least along seismically active faults). Even if natural seismicity occurs usually in a deeper interval than the usual geothermal activities, tectonic stresses can propagate also into shallower structural levels, leading to close to critically stressed conditions. Thus, a perturbation of pore pressure and stresses due to geothermal operation could impose the risk of further seismicity, when large faults with favorable orientation to the stress field are present in the vicinity of the wells. Furthermore, seismically active faults proved to represent preferential fluid pathways, capable of propagating pore pressure over great distance and to influence the natural seismicity (Goebel et al. 2018).

Thus, there is a need to assess the level of the natural seismicity to filter out the background seismicity and to range the (possible) seismicity induced due to the geothermal operations. Seismicity data are collected from publicly available sources (i.e., the USGS) to learn about the natural seismicity in the vicinity of a geothermal field. Average magnitudes and average depths of the earthquakes will be collected. The following factors shall govern the data collection:

- The radius in which seismic events have been recorded shall be 3 times the maximum distance between the wells in the field.
- 50 years before the start of geothermal operation and beyond shall be considered.
- Only seismic events greater than magnitude 2 shall be considered.
- If the number of events is not big enough either the radius or the observation period or both shall be extended.

Entry/units: Magnitude, Depth in km
Long description: Average magnitude value of natural seismicity events near the geothermal plant, Average depth of seismic events nearby the geothermal plant.

3.1.9 Reservoir faults (B)

Stable faults are in equilibrium with the stresses acting on the fault plane. An increase or decrease in fluid pressure due to injection or production during geothermal operation will change the effective normal stress on a fault plane in the reservoir section. Depending on the stress regime, when the fault plane approaches the critical stress needed to initiate fault movement, this pore pressure change may activate the fault. Furthermore, Orlic et al. (2011) have demonstrated that stress concentrates on fault planes offsetting interfaces between different lithologies, such as the boundary between reservoir and overburden rocks. Therefore, fault reactivation may be more likely when they intersect/offset the boundary between reservoir and overburden. In general, faults through boundaries might increase the seismicity risk.
Fault slip will occur once the ratio of shear stress to normal stress reaches the coefficient of friction [μ]. μ depends on the rock type, typically it is between 0.6 and 1. Rising pore pressure on a fault reduces the effective normal stress on it, and can lead to fault slip (Zoback, 2007).
Entry: none, one, multiple
Long description: The presence of reservoir faults is defined by three options: none, one, multiple.

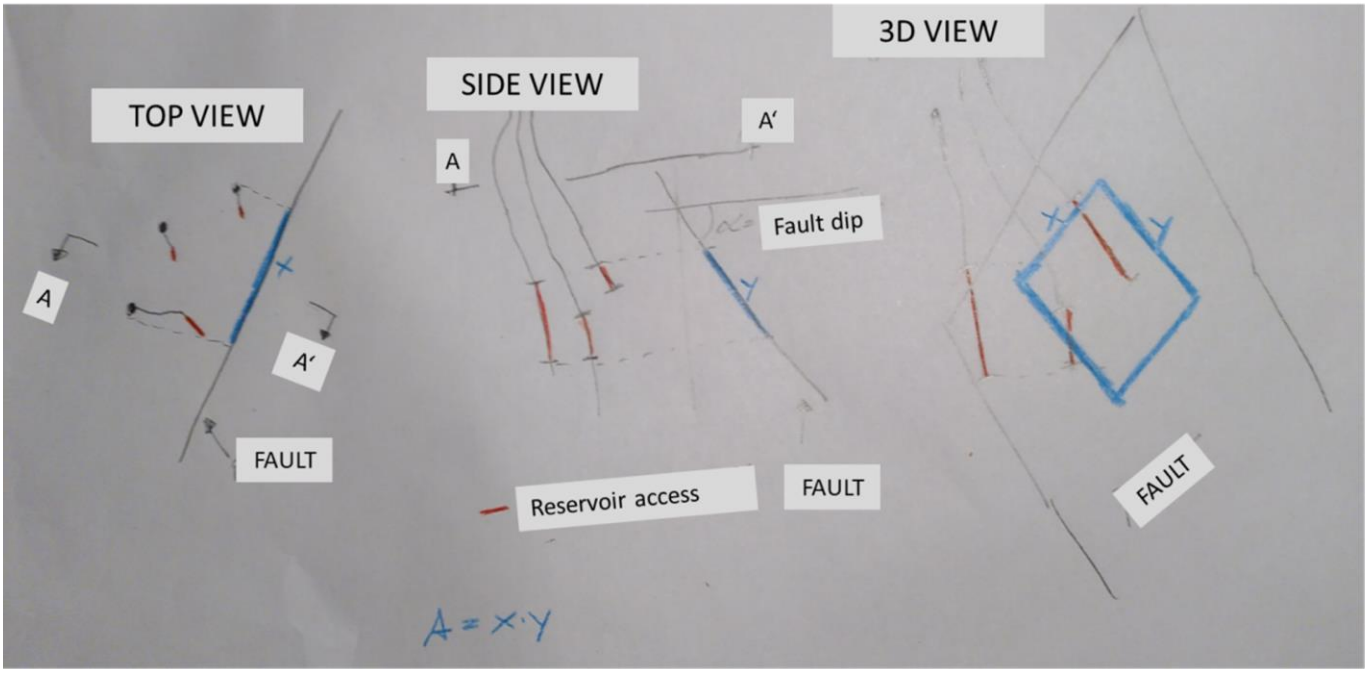

Figure 6. Estimate minimum perturbated fault area.

3.1.10 Bounding Fault Existence and Contact Area (A)

When a reservoir is bounded laterally by a fault, there tends to be a sharper contrast in pressure across the fault. The greater the number of bounding faults, the higher the risk for fault (re-) activation. The size of the fault contact area is also a factor, as for the same amount of slip, larger faults release a much higher amount of energy. That is expressed by the definition of the seismic moment Mo (Maruyama, 1963):

$$M_0 = \mu A d = 10^{(1.5M + 16.05)}$$

With µ the coefficient of friction; A: fault area; d: the fault slip; M: seismic magnitude.
Thus, if the area where the mechanical equilibrium is perturbated by the geothermal field includes a large section of a fault, if favorably oriented to the stress field, the risk of inducing larger earthquakes is higher. On the contrary, the reactivation of isolated small faults could lead to smaller magnitudes.

Entry: none, one, multiple; area in m²

Long description: the parameter Bounding Faults defined by three options: none, one, multiple. The contact area (m2) is defined by the vertical and lateral overlap between zone of impact and fault. The calculation takes into account the dip of the fault (Figure 6).

Geomechanical Risk Parameters

3.1.11 Stress regime (A)

In reservoirs managed with both producers and injectors, fluid injection in the reservoir can induce poro-elastic stresses in the surrounding rocks, including the overburden. In these conditions, the stress regime can play a role in inducing seismicity. In case of a thrust faulting regime, the poro-elastic stresses induced close to the injector wells can facilitate the reactivation of suitable oriented thrust faults. In a normal faulting regime, the induced poro-elastic stresses tend to stabilize the faults that could potentially slip (Figure 7). In a strike-slip regime there is no particular effect related to poro-elastic stresses induced in the overburden.

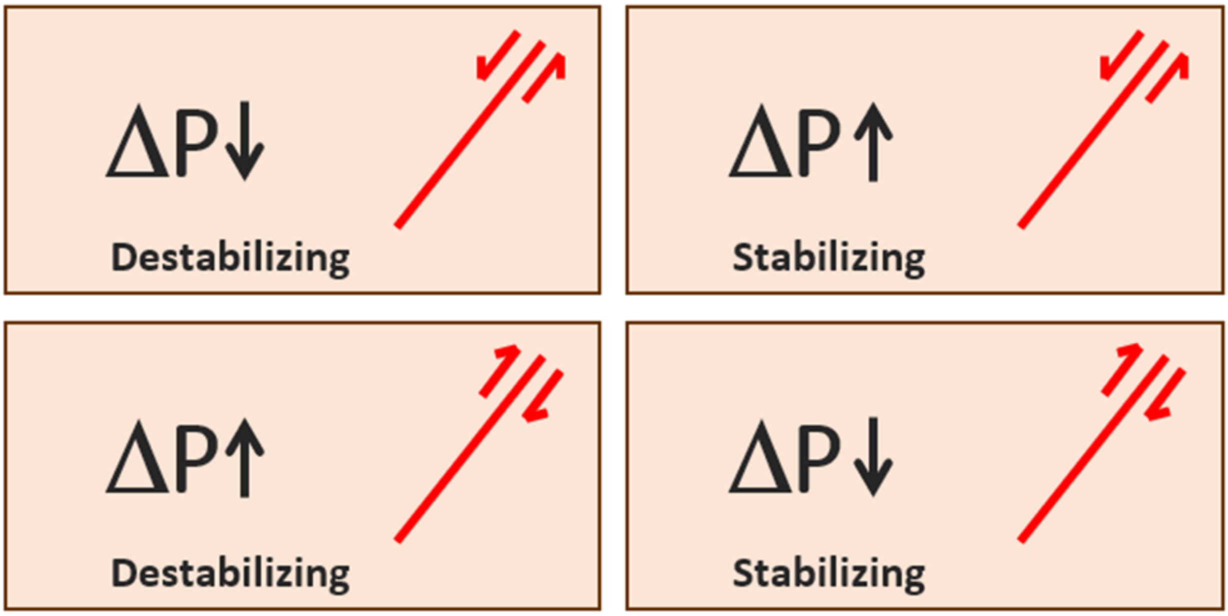

Figure 7. Poro-elastic effect of production and injection on fault stability in different stress regimes.

In fields that are managed just with producers, a certain drop of pore pressure is expected around the production wells, which could induce pro-elastic stresses in the overburden. In this case a thrust faulting regime should tend to stabilize suitable oriented thrusts, whereas in a normal faulting the risk of induced slip is increased.

Entry: NF, NF-SS, SS, SS-TF, TF

Long description: We collect the stress regime in categories. Information sources are the world stress map database, literature, or detailed analysis in case well logs (BHI, Calipers) are available.

3.1.12 Effective Stress ratio (A)

Effective stress (σ) is defined as total stress, S, minus pore pressure, PP. We consider the ratio between the largest effective principal stress and the smallest effective principal stress with a ratio, defined as:

$$\sigma3/\sigma1 = (S3-PP)/(S1-PP)$$

The stress difference also defines the maximum shear stress. The larger the difference between the two stresses, the smaller the stress ratio, and the higher the shear stress. Modelling studies for extensional stress regimes have shown that lower stress ratios lead to larger absolute fault slip magnitudes (Mazzoldi et al. 2012; Rutqvist et al. 2013; Figueiredo et al. 2015). In general, effective stress ratios are on the order of 0.5-0.7 (Bruno et al. 2014). Lower stress rations lead to higher shear stress and lower normal stress acting on favorably oriented faults, increasing the risk of critically stressed conditions and induced seismicity.

In case stress magnitude are not available, they can be extrapolated from gradients in nearby wells or from existing stress databases (for example Morawietz et al. 2020). In case of NF or TF regimes, when either S1 or S3 are vertical, the corresponding magnitude can be computed from high resolution density data (in case OHL are available) or from mean values reported for the specific field/area, using commonly used equations (Zoback, 2007).
All stress and pore pressure measurements must be referred to the depth of activity. We collect both initial pore pressure, and max and min pore pressures during operations (see paragraph), and for the stress magnitudes, we collect min and max S3 and the magnitude of S1.

Entry: Absolute values in MPa. Effective stress ratio is calculated automatically.
Long description: We collect stresses for minimum and maximum principal stresses at the reservoir depth and initial formation pressure, all in units of MPa. Using those values, we will derive the effective stress ratio.

3.1.13 Critically stressed faults (strike & dip in relation to principal stresses) (A)

Critically stressed faults are faults that are orientated in respect to the current stress regime in such a way that they are close to failure i.e., very likely to be (re)activated in case of stress perturbation. Orientation of the maximum principal stress (S1) is a crucial parameter for the identification of potentially critically stressed faults, together with the stress regime. This orientation can be retrieved from the World Stress Map. It should be kept in mind, however, that the data is not always accurate. Better data might be found in published papers on the specific area. Another source to determine the parameters (principal stress orientations, fault strike & dip) is direct data from borehole images (BHI) or oriented calipers.

Faults that are not favorably oriented to the stress field, in regard to being critically stressed, can be reactivated only in case of very high pore pressure (Leclère and Fabbri, 2013). As larger faults are more prone to induce seismicity with a higher magnitude, the orientation and dip only of the main structures will be considered. In case more sets of faults with other/different orientation exist in the area, they all will be considered.

Entry: AQ: Flag YES, NO, UNSURE.

AX: orientation of Shmax from North
AY: orientation in degrees from N, for each fault set (we assume maximum 2 will be encountered), divided by a slash, i.e., 50/130
AZ: fault dip in degrees from horizontal

Long description: Ideally we find a study about critically stressed faults indication and can set a clear YES or NO flag in AQ. If that is not available, the parameters we are collecting in our study to estimate whether critically stressed faults are prevailing in the current stress field or not are fault(s) strike & dip and the stress regime (already collected), including SHmax orientation.

3.1.14 Pore pressure gradient and formation pressure/effective Shmin stress ratio (B)

Generally, the pore pressure depends on fluid density and depth. During geothermal operations pressure differences exists near the wells. In the vicinity of the producing well a decrease in pore pressure is expected, while around the injection well higher pore pressure is expected. Reservoir porosity and permeability determine how large the zones of different pore pressures are.

In compartmentalized reservoirs the pore pressure in certain intervals can vary from the natural pore pressure. Compartmentalization can occur due to the presence of impermeable formations that impede the generation of the natural pore pressure state. The fluid pressure in over-pressured formations may exceed the natural shear strength of the rock and cause rock failure (Zoback, 2010).

Furthermore, higher pore pressure also increases the risk of inducing shear failures along already existing structures, by diminishing the effective stresses acting on them.

After estimating the pore pressure and effective minimum horizontal stress gradients, a ratio will be derived from these parameters. The higher this ratio, the higher the risk for fracturing or inducing shear failures, resulting into seismicity. This number is a measure of how close the pore pressure in the formation is to the failure pressure, as fracturing occurs when the minimum horizontal stress is exceeded by the pressure in the reservoir.

Entry: All values in MPa.
Long description: Initial pore pressure in the reservoir is collected in the database as P_initial as absolute measurement (MPa). During operations, maximum and minimum pore pressures in the reservoir are listed as max and min pressures (MPa) in the InStRikE database. After filling the tables, pressure gradients will be computed by diving by the corresponding depth (TVD).

Operational Risk Parameters

3.1.15 Zone of impact (A)

The zone of impact determines the volume of rock mass that is perturbated by the geothermal operations in the subsurface. The larger this volume the higher the risk to induce seismicity. Thus, the higher the risk to interfere with critically stressed faults and the larger the areas that can be stressed due to pressure and temperature gradients. Bruno et al. (1998) have shown the influence of lateral and thickness extents for gas reservoirs in a numerical study.

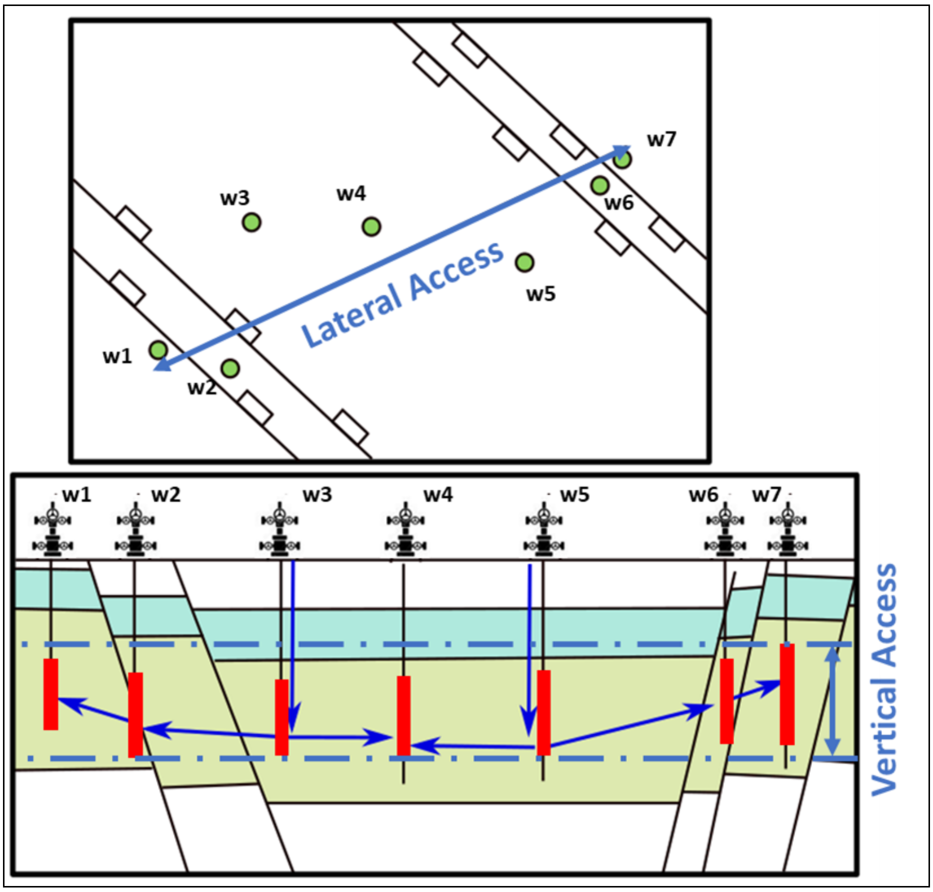

Figure 8. Estimation of lateral and vertical reservoir access.

Since the geothermal reservoir extent is not a parameter easily to be determined, we take the areas of the reservoir access as a proxy parameter for the InStRikE tool. We will determine the lateral and the vertical extent of reservoir access. The lateral extent is determined by the furthest horizontal distance of perforated or open hole access to the reservoir – considering producers and injectors at the same time. The vertical extent is determined by the largest vertical distance of reservoir access (Figure 8).

Entry: All values in meters.

Long description: Lateral and vertical extent of the geothermal field.

3.1.16 ΔT relative to initial temperature (A)

A geothermal plant operates at best efficiency, if the highest amount the energy contained in the fluids is used. This means, the fluid shall be reinjected as cold as possible. However, colder reinjected fluids induce higher thermal stress to the reservoir rocks. Therefore, a dilemma exists between production efficiency and operational safety.

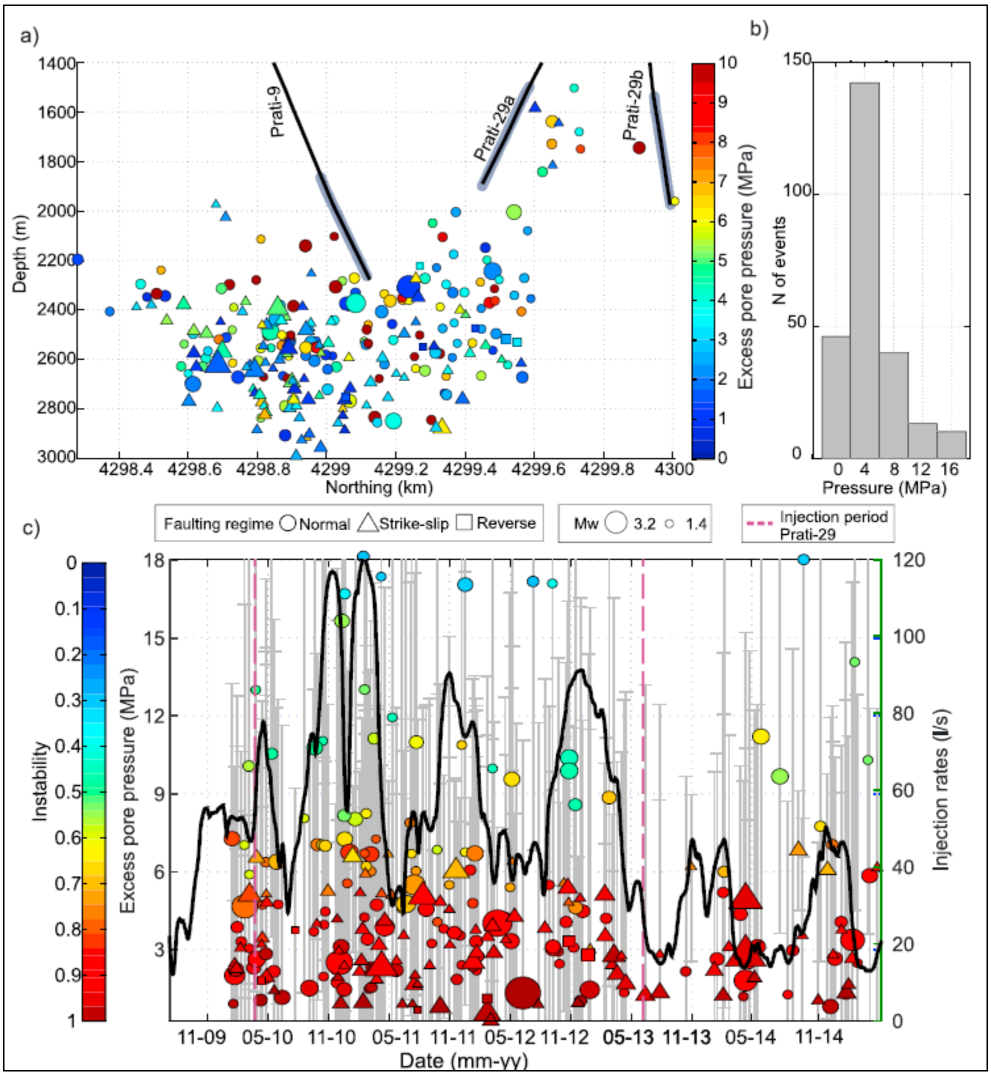

Figure 9. Induced seismicity in the Geyser field, resulting from injection of colder fluids in the reservoir (Martínez-Garzón et al. 2016).

Injection of cold liquids into the reservoir combined with production of hot fluids leads to a progressive cooling of the reservoir rocks, which might lead to poro-elastic and thermo-elastic stresses induced in the surrounding rocks, increasing the risk of induced seismicity (Martínez-Garzón et al. 2016). The higher the temperature difference, the higher the stresses induced, thus the higher the risk for inducing seismicity (Figure 9).

Only injector wells are prone to thermal stress, production wells are not affected.

$$\Delta Trel=(Tini-Tinject)/Tini$$

Entry/Unit: ∆T temperature of initial reservoir fluid (T-initial) – temperature of reinjected fluid (T-inj) in °C.

Long description: ∆T relative to initial temperature.

3.1.17 ∆ P relative to initial pressure (A)

This ratio is a measure of the pressure increase (decrease) in the reservoir. The higher this ratio, the larger the pressure increase in the geothermal reservoir system. Vice versa the lower this ratio the higher the depletion of the reservoir pressure. The magnitude of pressure change controls the potential for tensile and shear failure in the reservoir. Therefore, the further away the ratio from 1, the higher the risk of inducing seismicity.

$$\Delta Prel=(Pini-Pinject)/Pini$$

Entry: All values in MPa.
Long description: We are collecting the information about initial reservoir pressure (P_initial), maximum depletion and pressure increase observed at any well in the reservoir (MPa) and maximum well head injection pressure (DP_inj).

3.1.18 Distance of producers and injectors to closest faults (A)

Most of the geothermal fields are based on a system of both producers and injectors, in order to keep the reservoir pressure constant over long periods, whereas in a few cases only production wells are present. In petrothermal and/or enhanced geothermal systems (EGS), where hydraulic stimulation is often planned prior to production to increase the permeability, the distance between wells and large faults proved to be a critical parameter controlling the development of induced seismicity (Häring et al. 2008; Kwiatek et al. 2019).
The distance of both production and injection wells from large faults, in particular those favorably to the in-situ stress, is very important as during regular production activities the volume next to the boreholes can experience both pressure accumulation and pressure drop, but also poro-elastic stresses (Chang and Segall, 2016; Chang et al. 2020). Furthermore, injection of cold fluids into hot formations can result into thermal stresses (Rutqvist and Oldenburg, 2007; Martínez-Garzón et al. 2016; Jeanne et al. 2017). Thus, the minimum distance of both producers and injectors from larger faults, potentially generating significant seismic events, in particular of those favorably oriented to the stress field, might be a crucial parameter (Figure 10).

Entry: All values in meters.

Long description: We are collecting the distance for the closest injector and closest producer we find in the field to a large fault. The fault must not be the same for injector and producer.

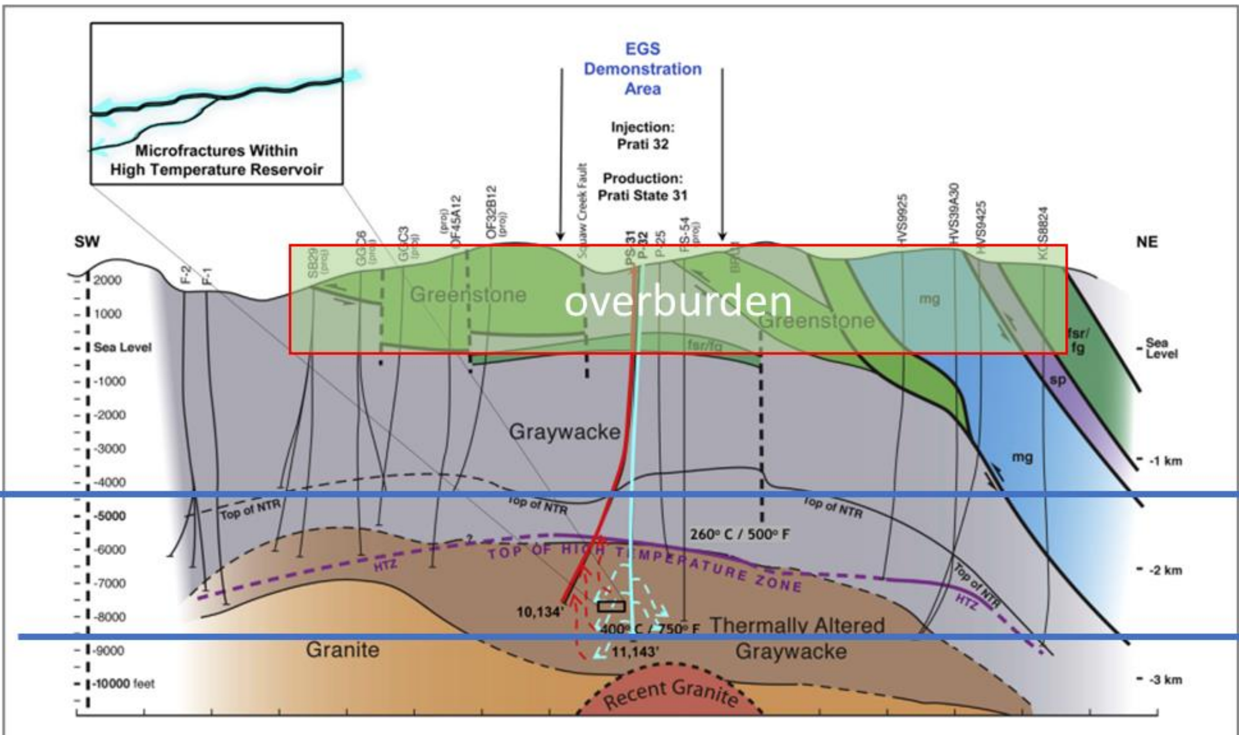

Fig. 1. NE-SW geologic cross-section through the northwest Geysers including the two wells P-32 and PS-31 that were reopened and recompleted as an injection/production pair within the HTR (Garcia et al., 2012).

Figure 10. Structural model of the Geyser geothermal site, where both injectors and producers go through several faults (Garcia et al. 2012).

3.1.19 Injection volume and production volume (B)

Greater amounts of injection and production creates larger pressure and temperature change over a larger volume, increasing seismicity risk. Total depletion relates to net production, or production minus injection, which can increase seismic risk. Furthermore, injection by itself seems to correlate with induced seismicity. McGarr (2014) presents data from waste injection operations showing a correlation between larger injection volumes and induced seismicity.

Entry: All values in cubic meters.

Long description: The volumes are collected in m3 over the period of interest (e.g., hydraulic stimulation period or operation period).

3.1.20 Type of operation (A)

Buijze et al. (2020) distinguish between three geothermal play types. Besides different operating procedures, they are also associated to different levels of seismicity risk. The play types are (Figure 11):

- petrothermal plays and EGS (PT)

- hydrothermal plays (HS)
- hot sedimentary aquifer plays (HSA)

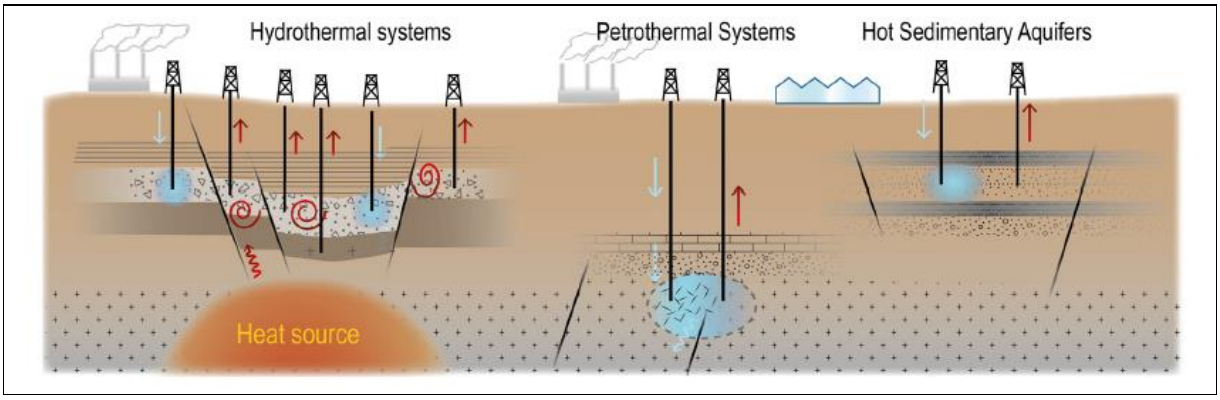

Figure 11. Types of geothermal fields according to Buijze et al. (2020).

As shown in figure 3, there is a higher risk of seismicity in hydrothermal and petrothermal (EGS) systems. Hydrothermal plays are often located in (recently) seismic active regions which generally have a higher risk of seismic activity. If the geothermal systems are enhanced (EGS) the risk rises, as more fractures are generated in the formation and cold fluids are pumped down to the formation. By doing so, the fluids (1) may circulate on otherwise dry faults, (2) they alter the existing pore pressure, and (3) they introduce thermal stress as the temperature difference between the pumped fluids and the rock is significant. Hydrothermal plays are connected to volcanic or plutonic activity, either recent or medium-recent. As magmatic activity is mostly bound to plate boundaries, thin crust regions or faults in general, also seismic activity occurs here.
This also affects any geothermal plants that are constructed in these places. The fluids are moved in the subsurface between production and injection wells and may also circulate on fault surfaces. The wells themselves may penetrate inactive faults and (re-)activate them. Hot sedimentary aquifer plays are situated far away from plate boundaries or magmatic regions and are not penetrating deeper parts of basins. However, these plays may be placed near orogens or in intra-orogenic basins. Depending on the state of activity of the orogen, HSA might be more or less exposed to seismicity risk.

Entry: HS, HSA, PS, HS-PS
Long description: Type of geothermal play

Appendix 4. Summary of simplifications/abstractions used in Appendix 3

E	Rock Stiffness or Young’s Modulus (GPa)
mD	MilliDarcy
MD	Measured Depth
Mo	Seismic moment

NF	Normal Faulting
µ	Coefficient of Friction
OHL	Open Hole Logs
PP	Pore Pressure
σ	Effective Stress
T	Temperature (°C)
∆T	Difference between T of reservoir and injected fluids (°C)
S1	Maximum Stress (MPa)
S3	Minimum Stress (MPa)
SS	Strike Slip
Svert	Vertical Stress
TF	Thrust Faulting
TVD	True Vertical Depth
UCS	Unconfined Compressive Strength or just Rock Strength (MPa)

Appendix 5. Database and Parameters

In this paragraph all the references used to derive the various parameters in each of the 100 geothermal sites in the InStRikE database are listed in the same order used in the database. The same references are also shown in the Tab "References" of the Database, which indicates also for which parameter each of these references was used.
For each field in the database some data are derived always from the same sources that are listed in each field: PGA, from Pagani et al. 2020; Strain Magnitude, Kreemer et al. 2014; Shmaxorientation, WSM database Heidbach et al. 2018; natural seismicity is from USGS Database).
Each field is indicated here with name and number as listed in the database.

35 Los Humeros (Flores-Armenta et al. 2014; Urban and Lermo, 2013; Lermo et al. 2008; Prol-Ledesma and Zenteno, 2019; Kruszewski et al. 2022; Arellano et al. 2003; Wedyt et al 2018; Bär et al. 2020; Urban and Lermo, 2017)

48 Gross Schoenebeck water-frac (Blöcher et al. 2010; Blöcher et al. 2018; Kwiatek et al. 2008; Kwiatek et al. 2010; Moeck et al. 2009; Zimmerman et al. 2010; Zimmermann and Reinicke, 2010)

76 Kawerau (Sherburn et al. 2015 ; Milicich et al. 2011; McNamara et al. 2014; White, 1995; Wyering et al. 2014; Wallis et al. 2012; New Zealand Geothermal Association, 2023; GeoMechanics Technologies, 2020)

156 Newberry (Davatzes and Hickman, 2011 ; McLeod et al. 1995 ; Dinçer et al. 2003 ; Cladouhos et al. 2015 ; Cladouhos et al. 2016 ; AltaRock Energy, Inc., 2011)

6 Honselersdijk (Vrouwe and Rutten, 2012; Vondrak et al. 2014; Schmid et al. 2012; Bender, 2011; Worum et al. 2004; Van Gessel et al. 2021, HIKE Database; trans-European PERFORM Project, 2023)

7 Koekoekspolder (Veldkamp et al. 2015; Verweij et al. 2012; Van Gessel et al. 2021, HIKE Database; Van Wees et al. 2014)

75 Basel (Haering et al. 2008; Deichmann et al. 2014; Kushnir et al. 2018; Valley and Evans , 2019; Mukuhira et al. 2016; Schill et al. 2012; Ulrich et al. 2007; Monsees, 2021)

33 Fenton Hill MHF EE-2 1983 (Phillips et al. 1997; Brown, 2009; Norbeck et al. 2018; Kelkar et al. 2015; Rinaldi and Rutqvist, 2019; Tuğrul and Zarif, 1998)

45 Unterhaching (Megies and Wassermann, 2014; Wolfgramm et al. 2007; Seithel et al. 2019; Richter, 2010; Rojas et al. 2017; Budach et al. 2018; Lueschen et al. 2014; Ziegler and Heidbach, 2020; Dussel et al. 2016; Zoback, 2007; Sachpazis, 1990; Ziegler et al. 2016; Seithel et al. 2015)

139 Riem (Dussel et al. 2016; Geotis Database, Agemar et al. 2014a/b; Geothermal energy, 2023;)

140 Unterschleissheim (Dussel et al. 2016; Seithel et al. 2019; Geotis Database, Agemar et al. 2014a/b; Informatonsportal Tiefe Geothermie, 2023; Stadt Unterschleissheim, 2023; Birner et al. 2012; Levi et al. 2021)

145 Ismaning (Dussel et al. 2016; Geotis Database;)

147 Oberhaching (Grünwald) (Dussel et al. 2016; Rojas et al. 2017; Geotis Database, Agemar et al. 2014a/b)

150 Unterföhring (Schulz et al. 2017; Dussel et al. 2016)

16 The Geysers (Majer et al. 2017 ; Trugman et al. 2015 ; Garcia et al. 2016; Rutqvist et al. 2016; Martínez-Garzón et al. 2014; Boyle and Zoback, 2014; Garcia et al. 2012; Brown, 1989; Jeanne et al.2014; Boyd, 2018; Martínez-Garzón et al. 2016)

15 Helsinki OTN-3 injection (Kwiatek et al. 2019; Juhlin and Sandstedt, 1989; Hillers et al. 2020; Palmström, 2011)

138 Straubing (Evans et al. 2012; Jaehn, 1999; Sachpazis, 1990; Levi et al. 2021)

151 Waldkraiburg (Baisch et al. 2016; Goldbrunner and Vasvari , 2016; Ziegler and Heidbach , 2020; Sachpazis, 1990; Levi et al. 2021)

14 Fjällbacka Stimulation Fb1 (Jupe et al. 1992; Saadati et al. 2018; Eliasson et al. 1990;)

71 Californië CLG + CWG (Baisch and Vörös., 2019; Reith, 2018; Vörös and Baisch., 2019; Mijnleff, 2020; ter Heege et al., 2020; Zoback, 2007; Sachpazis, 1990; Livingstone et al., 2013; Brinkgreve, 2016)

72 Californië CWG (Baisch and Vörös., 2019; Vörös and Baisch., 2019; Mijnleff, 2020; Zoback, 2007; Reith, 2018; Livingstone et al., 2013; Brinkgreve, 2016; Heege et al., 2020;)

19 Desert Peak EGS 2011 (Lutz et al. 2010; Zemach et al. 2010; Benato et al. 2016 ; Drakos, 2010; Dempsey et al. 2013; Bauer et al. 2018)

20 Desert Peak EGS 2013 (Lutz et al. 2010 ; Drakos, 2010 ; Dempsey et al. 2013 ; Robertson-Tait and Morris, 2003 ; Bauer et al. 2018)

47 Gross Schoenebeck 4120 gel (Zimmerman et al. 2010 ; Kwiatek et al.2008 ; Kwiatek et al. 2010 ; Blöcher et al. 2010 ; Blöcher et al. 2018 ; Moeck et al. 2009 ; Trautwein and Huenges, 2005 ; Jacquey et al. 2016 ; Zimmermann and Reinicke, 2010 ; Zoback, 2007)

98 Soultz-sous-Forets GPK1 1993 (Cornet et al. 1997 ; Aichholzer et al. 2016 ; Vallier et al. 2018; Azzola et al. 2019 ; Glaas et al. 2021 ; Glaas et al., 2018 ; Valley and Evans, 2007 ; Mouchot et al. 2018 ; Morawietz et al., 2020)

99 Soultz-sous-Forets GPK2 1995 (Evans et al. 2005 ; Aichholzer et al. 2016 ; Vallier et al. 2018 ; Azzola et al. 2019 ; Glaas et al. 2021 ; Glaas et al., 2018 ; Valley and Evans, 2007 ; Baria et al., 2000 ; Morawietz et al., 2020 ; Mouchot et al. 2018)

100 Soultz-sous-Forets GPK2 2000 (Dorbath et al. 2009 ; Aichholzer et al. 2016 ; Azzola et al. 2019 ; Vallier et al. 2018 ; Glaas et al. 2021 ; Glaas et al., 2018 ; Valley and Evans, 2007 ; Mouchot et al. 2018 ; Morawietz et al., 2020)

101 Soultz-sous-Forets GPK3 2003 (Cornet et al., 1997 ; Dorbath et al. 2009 ; Charlety et al. 2007 ; Vidal and Genter, 2018 ; Tischner et al. 2007 ; Vallier et al. 2018 ; Azzola et al. 2019 ; Glaas et al. 2021 ; Aichholzer et al. 2016 ; Dezayes et al. 2010 ; Morawietz et al., 2020)

102 Soultz-sous-Forets GPK4 2004 (Cornet et al., 1997 ; Dorbath et al. 2009 ; Charlety et al. 2007 ; Vidal and Genter, 2018 ; Tischner et al. 2007 ; Vallier et al. 2018 ; Azzola et al. 2019 ; Glaas et al. 2021 ; Aichholzer et al. 2016 ; Dezayes et al. 2010 ; Morawietz et al., 2020)

103 Soultz-sous-Forets GPK4 2005 (Cornet et al., 1997 ; Dorbath et al. 2009 ; Charlety et al. 2007 ; Vidal and Genter, 2018 ; Tischner et al. 2007 ; Vallier et al. 2018 ; Azzola et al. 2019 ; Glaas et al. 2021 ; Aichholzer et al. 2016 ; Dezayes et al. 2010 ; Dorbath et al. 2009 ; Morawietz et al., 2020)

90 Bruchsal (Meixner et al. 2016 ; Vidal and Genter, 2018; Agemar et al. 2014 ; Bär et al., 2020 ; Jodocy and Stober, 2009 ; Sabakatakis et al. 2008)

1 Tres Virgines (Urban and Lermo, 2012 ; Flores-Armenta et al. 2014 ; Verma et al. 2006 ; Antayhua-Vera et al. 2015 ; Tello-López and Torres-Rodrıguez, 2015 ; Prol-Ledesma and Morán-Zenteno, 2019 ; Gonzales-Partida et al. 2005 ; Prol-Ledesma et al. 2016 ; Flores et al. 2005 ; WSM (world Stress Map) Database; Guerrero et al. 2022)

73 Cerro Prieto (Glowacka et al. 1999 ; Trugman et al. 2014 ; Glowacka and Nava, 1996 ; Prol-Ledesman et al. 2016 ; Lyons and Van De Kamp, 1980;) Database; Herrera, 2005)

2 Podhale Zakopane (Kepinska, 2004 ; Kepinska, 2003 ; Kępińska and Jasnos, 2009 ; Jarosinski, 2006)

64 Mszczonow (Kepinska , 2015 ; Bujakowski and Wojnarowski, 2005 ; Pająk et al. 2020 ; Van Gessel et al. 2021, HIKE database)

65 Poddebice (Pająk et al. 2020 ; Van Gessel et al. 2021, HIKE database ; Kepinska, 2015 ; Królikowski, M. and Hajto, M., 2023)

66 Pyrzyce (Meyer and Kozlowski, 1995 ; Kepinska, 2015 ; IGSMiE PAN, 2019 ; Szczepański et al., 2006)

67 Stargard Szczezenski (Kepinska , 2015 ; Miecznik et al. 2015 ; Szczepański et al., 2006)

68 Uniejow (Kepinska , 2015 ; Sapinska-Sliwa et al. 2010 ; Pająk et al. 2020 ; Szczepański et al., 2006)

8 Habanero 1 2003 (Baisch et al. 2006 ; Holl and Barton, 2015 ; Humphreys et al. 2014 ; McNally, 1987; Vasarhelyi, 2003)

9 Habanero 1 2005 (Baisch et al. 2009 ; Holl and Barton, 2015 ; Humphreys et al. 2014 ; McNally, 1987; Vasarhelyi, 2003)

10 Habanero 4 2012 (Baisch et al. 2015 ; Holl and Barton, 2015 ; Humphreys et al. 2014 ; McNally, 1987; Vasarhelyi, 2003)

63 Pohang (PX-1 + PX-2) (Kim et al. 2018a/b; Grigoli et al. 2018 ; Hofmann et al. 2019 ; Farkas et al. 2021 ; Ellsworth et al. 2019 ; Zingg and Meier, 2019 ; Wassing et al., 2021)

157 Habanero 2 2005 (Baisch et al. 2016 ; Humphreys et al. 2014 ; Ayling et al. 2016 ; Holl and Barton, 2015 ; Wyborn, 2010 ; McNally, 1987; Vasarhelyi, 2003; Humphreys et al., 2014)

158 Habanero 3 2008 (Baisch et al. 2016 ; Humphreys et al. 2014 ; Ayling et al. 2016 ; Holl and Barton, 2015 ; Wyborn, 2010 ; McNally, 1987; Vasarhelyi, 2003)

17 Brady Hot Springs (Cardiff et al. 2018 ; Lutz et al. 2010 ; Benato et al. 2016 ; Lutz et al. 2011 ; Laboso, 2016 ; Dinçer et al. 2003 ; Abdaqadir and Alshkane, 2018)

81 Rotokawa (Sherburn et al. 2015 ; Sewell et al. 2015 ; Addison et al. 2017 ; Siratovich et al. 2014 ; Davidson et al. 2012 ; Dinçer et al. 2003 ; Hopp, 2019 ; GeoMechanics technologies, 2020)

77 Mokai (Sherburn et al. 2015 ; Bignall et al. 2010 ; McNamara et al. 2017 ; New Zealand Geothermal Association, 2023)

78 Ngatamariki (Sherburn et al. 2015 ; O'Brien, 2010 ; Allan et al. 2019 ; Cant et al. 2018 ; Wyering et al. 2014 ; McNamara et al. 2017 ; Moon et al., 2014 ; New Zealand Geothermal Association, 2023)

82 Wairakei-Tauhara (Sherburn et al. 2015 ; Bignall et al. 2010 ; Rosenberg et al. 2010 ; McNamara et al. 2017)

80 Ohaaki (Sherburn et al. 2015; Lee and Bacon, 2000; Rae et al. 2007; McNamara et al. 2014; Wood, 1996; O´Sullivan et al. 2021; McNamara et al. 2017; Wood et al. 2001; Rissmann et al. 2012 ; New Zealand Geothermal Association, 2023)

23 Nesjavellir (Flóvenz et al. 2015; Evans et al. 2012; Nouraliee, 2000; Bodvarsson et al. 1988; Batir, 2011; Juncu et al. 2019;)

143 Ribeira Grande (Franco et al. 2021 ; Franco, 2015 ; Carvalho et al. 2006 ; IPMA Database ; Rangel et al. 2017 ; Carmo et al., 2015)

142 Mutnovsky (Selyangin, 2019; Kiryukhin et al. 2015; Kiryukhin and Usacheva, 2017; Kiryukhin and Vereina, 2005; Dinçer et al. 2003)

137 Meshkin Shahr (Abdolalipoor et al. 2019; Akbar and Fathianpour, 2021; Rahimi et al. 2009; Faridi et al. 2017; Yousefi et al. 2019; Seyedrahimi-Niaraq et al. 2017; Porkhial et al. 2015)

127 Patuha (Elfina, 2017; Mehrabifard, 2018; Raharjo et al. 2016; Layman and Soemarinda, 2003)

3 Berlin (Rodriguez, 2005; Rivas et al. 2005; Kwiatek et al. 2014; Monterrosa and Geotermica Salvadorena, 2002; Henriquez, 2010; Renderos, 2002)

12 Rosemanowes 2A stimulation (Evans et al., 2012; Batchelor, 1982; Parker, 1999; Parker, 1989; Reinecker et al., 2021)

13 Rosemanowes 2B circulation (Evans et al., 2012; Richards et al. 1994; Parker, 1989; Batchelor, 1982; Atkins, 2013; Reinecker et al., 2021, Evans et al. 2012)

18 Coso (Trugman et al., 2015; Davatzes and Hickman, 2009; Kaven et al., 2011; Kaven et al., 2014; Davatzes et al., 2006; Rose et al., 2006; Kaven et al., 2011; Kaven et al., 2014; Adams et al., 2000)

144 Kizildere (Haklıdır et al.2021; Gokcen et al., 2004; Şimşek et al., 2005; Satman et al., 2005; Kaya et al., 2009; Yeltekin et al., 2002; Serpen and Aksoy, 2005; Heidbach et al., 2018)

115 Palinpinon I + II (S Negros) (Malate et al., 2008; Pastoriza, 2017; Austria and Bonsen, 2020; Rae et al., 2004; Dinçer et al., 2003; Magro et al., 2013; Olivar and Apuada, 2005)

110 Olkaria 1(East Production Field) (Fadel et al., 2021; Wamalwa et al., 2016; Koech, 2014; Simiyu, 2016; Simiyu and Keller, 2000; Mbithi, 2016; Strecker and Bosworth, 1991; Omenda, 1998)

50 Horstberg GeneSys (Orzol et al., 2005; Buijze et al., 2019; Tischner et al., 2010; Jung et al., 2019; Jung et al., 2019; Zoback, 2007; Tischner et al., 2013; Kehrer et al., 2007; Heidbach et al., 2018; Van Gessel et al. 2021, HIKE Database)

111 Olkaria IV (Domes Field) (Otieno, 2017; Fadel et al., 2021; Ambunya, 2014; Koech, 2014; Simiyu, 2016; Mbithi, 2016; Simiyu and Keller, 2000; Strecker and Bosworth, 1991; Omenda, 1998)

74 Salton Sea (Brodsky and Lajoie, 2013; Trugman et al., 2016; Younker et al., 1982; McGuire et al., 2015; Zoback, 2007; Barbour et al., 2016; Kaspereit et al., 2016)

79 Ngawha (Sherburn et al., 2015; Bromley and Bignall, 2016; McNamara et al., 2014; McNamara et al., 2017; Heidbach et al., 2018)

153 Obernberg (Baisch et al., 2016; Homuth, 2014; Goldbrunner, 2010; Elster et al. 2016; Goldbrunner and Goetzl, 2019; Sachpazis, 1990; Potten, 2020 ; Levi et al., 2021; Levi et al., 2019; Kröll et al. 2006)

152 Bad Blumau (Baisch et al., 2016; Goldbrunner, 2005; Goldbrunner, 2000; Alt-Epping et al., 2013; Elster et al. 2016 ; Heidbach et al., 2018)

36 Geinberg (Goldbrunner, 2005; Karytsas et al., 2009; Evans et al., 2012; Elster et al. 2016 ; Bauer et al., 2014; Goldbrunner, 2000; Sachpazis, 1990; Potten 2020; Levi et al., 2021)

55 Sonderborg (Mahler et al., 2013; Poulsen et al. 2019; Poulsen et al. 2017; Cobos et al. 2021; Røgen et al., 2015)

56 Margretheholm (Erlström et al., 2018; Poulsen et al. 2019; Geotherm Perform Database; GEUS Database; Moos et al. 1999; Horsrud 2001)

21 Húsmúli reinjection (Hellisheidi field) (Juncu et al., 2020; Batir 2011; Mahzari et al., 2021; Helgadottir et al., 2010; Snaebjornsdottir, et al., 2018; Franzson et al. 2005)

57 Thisted (Mahler et al., 1995; Hjuler et al., 2014; Mahler et al., 2013; Evans et al., 2012; GEUS Database; Moos et al. 1999; Horsrud 2001)

62 Palinpinon (Puhagan) (Malate et al., 2008; Bromley et al., 1987; Rae et al. 2004; Amistoso et al., 1993; Magro et al. 2013; Pastoriza 2017; Aqui et al. 2005)

39 Dürrnhaar (Seithel et al., 2019; Agemar et al., 2014a/b; Birner et al. 2012; Van Gessel et al. 2021, HIKE database)

22 Krafla (Flóvenz et al., 2015; Eggertsson et al., 2018; Evans et al., 2012; Armannsson et al., 1987; Weaver et al. 2020; Scott et al. 2019; Langella et al. 2017)

40 Kirchstockach (Wanner et al., 2017; Seithel et al., 2019; Agemar et al., 2014a/b; Birner et al., 2012; Dussel et al., 2016; Van Gessel et al. 2021, HIKE database)

41 Poing (Agemar et al., 2014a/b; Seithel et al. 2019; LIAG, 2018; Birner et al. 2012; Van Gessel et al. 2021, HIKE database)

43 Sauerlach (Agemar et al., 2014a/b; Seithel et al. 2015; Seithel et al. 2019; Birner et al., 2012; Van Gessel et al. 2021, HIKE database)

135 Bad Urach (Tenzer et al. 1999; Tenzer et al. 2004; Evans et al., 2012; Baisch et al., 2004; McDurmott et al., 2006; Kesonen, 2015; P3 Database Bär et al., 2020; Monsees 2021; Van Gessel et al. 2021, HIKE database)

134 Laugaland (Axelsson et al., 2000; Flovenz et al., 2015; Dinçer et al. 2003; Foged and Andreassen 2016)

24 Reykjanes (Flovenz et al. 2015; Armannsson et al. 2015; Evans et al. 2012; De Freitas et al. 2018; Franzson et al. 2002; Keilegalaven et al., 2021; Peter-Borie et al. 2018; Djama 2014; Khodayar et al., 2018; Duboeuf et al. 2022; Parks et al. 2020)

25 Svartsengi (Flovenz et al. 2015; Armannsson et al. 2015; Evans et al. 2012; De Freitas et al.2020; Mendez 1996; P3 Database Bär et al., 2020; Dinçer et al. 2003)

42 Pullach (Evans et al. 2012; Schneider and Lutz 2012; site of Bundesverband Geothermie; Birner et al. 2012; Van Gessel et al. 2021, HIKE database)

44 Simbach-Braunau (Goldbrunner, 2007; Elster et al. 2016; Leitner, 2013; Sachpazis, 1990; Potten, 2020; Levi et al. 2021; Van Gessel et al. 2021, HIKE database)

46 Gross Schoenebeck (Zimmerman et al. 2010; Kwiatek et al. 2010; Blöcher et al. 2018; Moeck et al. 2009; Huenges et al. 2006; Zoback, 2007; Jacquey et al. 2016; Zimmermann and Reinicke 2010)

49 Hannover GeneSys waterfrac (Tischner et al. 2013; Rioseco et al. 2013; Tiefegeothermie site; Tischner et al. 2010; Zoback, 2007)

51 Neubrandenburg (GEOTIS database, Agemar et al. 2014a/b; Hirst, 2016; Seibt and Kellner, 2003; Stück et al. 2011; Van Gessel et al. 2021, HIKE database;)

53 Neustadt-Glewe (GEOTIS database, Agemar et al. 2014a/b; Hirst, 2016; Seibt et al. 2005; Stück et al. 2011; Van Gessel et al. 2021, HIKE database)

54 Waren (GEOTIS database, Agemar et al. 2014a/b; Kabus and Jäntsch, 1995; UGII webpage; Hirst, 2016; Stück et al. 2011; Van Gessel et al. 2021, HIKE database)

91 Insheim stimulation (GEOTIS database, Agemar et al. 2014a/b; Pilger et al. 2017; Küperkoch et al. 2018; Vidal and Genter 2018; Buijze et al. 2019; P3 Database, Bär et al. 2020; Van Gessel et al. 2021, HIKE database; Meixner et al. 2016)

26 Hijiori HDR-1 1992 (Kaieda, 2015; Sasaki and Kaieda, 2002; Tenma et al. 2005; Kaieda, 2014; Kaieda, 2020; Matsunaga et al. 2005; Koseki, 2008; Vasco et al. 2002)

27 Hijiori HDR-1 1995 (Kaieda, 2015; Sasaki and Kaieda, 2002; Kaieda, 2014; Kaieda, 2020; Matsunaga et al. 2005; Koseki, 2008; Vasco et al. 2002)

28 Hijiori HDR-1 2000 long term circulation (Kaieda, 2015; Kaieda, 2014; Kaieda, 2020; Matsunaga et al. 2005; Koseki, 2008; Vasco et al. 2002)

29 Hijiori SKG-2 1988 (Kaieda, 2015; Sasaki and Kaieda, 2002; Kaieda, 2014; Kaieda, 2020; Matsunaga et al. 2005; Koseki, 2008; Vasco et al. 2002)

30 Ogachi OGC-1 1991 (Kaieda et al. 2005; Kaieda, 2015; Ito, 2003; Kaieda; 2012; Sasaki et al. 2018; Suzuki and Kaieda, 2000; Di Pippo, 2016; Ito and Kaieda, 2002)

31 Ogachi OGC-1 1992 (Kaieda et al. 2005; Kaieda, 2015; Ito, 2003; Kaieda; 2012; Sasaki et al. 2018; Suzuki and Kaieda, 2000; Di Pippo, 2016; Ito and Kaieda, 2002)

109 Illkirch (Boissavy et al. 2019; Bosia et al. 2021; Petterschmitt et al. 2018)

107 GeoVen (Schmittbuhl et al. 2021; Sanjuan et al. 2021; Boissavy et al. 2019; Gaucher et al. 2020)

Appendix 6. List Of Figures

Appendix 7. List Of Tables

Appendix 8. References

Abdaqadir, Z.K. and Alshkane, Y.M., 2018. Physical and mechanical properties of metamorphic rocks. Journal of Garmian University, 5(2), pp.160-173.

Abdolalipouradl, M., Khalilarya, S. and Jafarmadar, S., 2019. The thermodynamic analysis of a novel integrated transcritical CO2 with Kalina 11 cycles from Sabalan geothermal wells. Modares Mechanical Engineering, 19(2), pp.335-346. DOI: http://mme.modares.ac.ir/article-15-20581-en.html

A'Campo, Y.W.L., and Baisch, S., 2020. Risk assessment for UDG and EGS and an inventory of preventive and mitigating measures. Report for State Supervision of Mines. Witteveen Bos; 105911/20-005.135.

Adams, M.C., Moore, J.N., Bjornstad, S. and Norman, D.I., 2000. Geologic history of the Coso geothermal system. Transactions-geothermal resources council, pp.205-210.

Addison, S., Azwar, L., Clearwater, J., Hernandez, D., Mountain, B., Blair, A. and Siratovich, P., 2017. Improving the conceptual understanding through a recent injection of 200 GBq of iodine-125 at the Rotokawa geothermal field, New Zealand. In 42nd Workshop on Geothermal Reservoir Engineering Stanford University, February (pp. 1-12).

Adelinet, M., Fortin, J., Schubnel, A., and Guéguen, Y., 2013. Deformation modes in an Icelandic basalt: From brittle failure to localized deformation bands. Journal of Volcanology and Geothermal Research, 255, pp. 15-25. DOI: https://doi.org/10.1016/j.jvolgeores.2013.01.011

Agemar, T., Alten, J.A., Ganz, B., Kuder, J., Kühne, K., Schumacher, S. and Schulz, R., 2014a. The geothermal information system for Germany–GeotIS. Zeitschrift der deutschen Gesellschaft für Geowissenschaften, pp.129-144.

Agemar, T., Weber, J. and Schulz, R., 2014. Deep geothermal energy production in Germany. Energies, 7(7), pp.4397-4416. DOI: https://doi.org/10.3390/en7074397

Ahlers, S., Röckel, L., Hergert, T., Reiter, K., Heidbach, O., Henk, A., Müller, B., Morawietz, S., Scheck-Wenderoth, M., and Anikiev, D., 2022. The crustal stress field of Germany: a refined prediction. Geothermal Energy, 10, p.10. DOI: https://doi.org/10.1186/s40517-022-00222-6.

Aichholzer, C., Duringer, P., Orciani, S. and Genter, A., 2016. New stratigraphic interpretation of the Soultz-sous-Forêts 30-year-old geothermal wells calibrated on the recent one from Rittershoffen (Upper Rhine Graben, France). Geothermal Energy, 4(1), pp.1-26. DOI: https://doi.org/10.1186/s40517-016-0055-7

Akbar, S. and Fathianpour, N., 2021. Improving the conceptual–numerical model of Sabalan geothermal system using geological, geophysical and structural information. Geothermics, 90, p.102001. DOI: https://doi.org/10.1016/j.geothermics.2020.102001

Akin, S., 2008. Optimization of Re-Injection in Low Temperature Geothermal Reservoirs Using Neural Network and Kriging Proxies. In Proceedings of the 33th Workshop on Geothermal Reservoir Engineering, Stanford University, Stanford, CA, Paper SGP-TR-185 (on CDROM) (pp. 1-9).

Allan, G., Pogacnik, J., Siega, F. and Addison, S., 2019, February. Wellbore simulation to model calcite deposition on the Ngatamariki geothermal field, NZ. In Proceedings of 44th Workshop on Geothermal Reservoir Engineering.

AltaRock Energy, Inc., 2011. Induced Seismicity Mitigation Plan. 69 Pages.

Alt-Epping, P., Waber, H.N., Diamond, L.W. and Eichinger, L., 2013. Reactive transport modeling of the geothermal system at Bad Blumau, Austria: implications of the combined extraction of heat and CO2. Geothermics, 45, pp.18-30. DOI: https://doi.org/10.1016/j.geothermics.2012.08.002

Altmann, J.B., Müller, B.I.R., Müller, T.M., Heidbach, O., Tingay, M.R.P. and Weißhardt, A., 2014. Pore pressure stress coupling in 3D and consequences for reservoir stress states and fault reactivation. Geothermics, 52, pp.195-205. DOI: https://doi.org/10.1016/j.geothermics.2014.01.004

Ambunya, M. N., 2014. Natural-State Model Update of Olkaria Domes Geothermal Field. United Nations University. 38 P.

Aqui, A.R., Aragones, J.S. and Amistoso, A.E., 2005, April. Optimization of palinpinon-1 production field based on exergy analysis–the southern negros geothermal field, Philippines. In Proc. World Geothermal Congress.

ATKINS, 2013. Deep Geothermal Review Study Final Report Department of Energy & Climate Change (DECC). 156 P.

Austria, D.C. and Benson, P.M., 2020. Fracture, fluid and saturation effects on the seismic attributes of rocks from the Southern Negros geothermal field, Philippines. Journal of Volcanology and Geothermal Research, 408, p.107099. DOI: https://doi.org/10.1016/j.jvolgeores.2020.107099

Amistoso, A.E., Aquino, B.G., Aunzo, Z.P., Jordan, O.T., Ana, F.X.S., Bodvarsson, G.S. and Doughty, C., 1993. Reservoir analysis of the Palinpinon geothermal field, Negros Oriental, Philippines. Geothermics, 22(5-6), pp.555-574. DOI: https://doi.org/10.1016/0375-6505(93)90036-M

Antayhua-Vera, Y., Lermo-Samaniego, J., Quintanar-Robles, L. and Campos-Enríquez, O., 2015. Seismic activity and stress tensor inversion at Las Tres vírgenes volcanic and geothermal field (México). Journal of Volcanology and Geothermal Research, 305, pp.19-29. DOI: https://doi.org/10.1016/j.jvolgeores.2015.08.005

Arellano, V.M., García, A., Barragán, R.M., Izquierdo, G., Aragón, A. and Nieva, D., 2003. An updated conceptual model of the Los Humeros geothermal reservoir (Mexico). Journal of Volcanology and Geothermal Research, 124(1-2), pp.67-88. DOI: 10.1016/S0377-0273(03)00045-3

Armannsson, H., Gudmundsson, A. and Stringrimsson, S.S., 1987. Exploration and development of the Krafla geothermal area. Jökull 37, 1987.

Armenta, M.F., Montes, M.R. and Alcala, L.M., 2015, April. Wellbore modeling of production well H-1D using WellSim, Los Humeros geothermal field, Mexico. In Proceedings of the World Geothermal Congress.

Asef, M.R., and Farrokhrouz M., 2010. Governing Parameters for Approximation of Carbonates UCS. Electron J Geotech Eng, 15, pp.1581-1592.

Atkins, Department of Energy & Climate Change (DECC), 2013. Deep Geothermal Review Study, Final Report. 156 P.

Ayling, B.F., Hogarth, R.A. and Rose, P.E., 2016. Tracer testing at the Habanero EGS site, central Australia. Geothermics, 63, pp.15-26. DOI: https://doi.org/10.1016/j.geothermics.2015.03.008

Azzola, J., Valley, B., Schmittbuhl, J. and Genter, A., 2019. Stress characterization and temporal evolution of borehole failure at the Rittershoffen geothermal project. Solid Earth, 10(4), pp.1155-1180. DOI: https://doi.org/10.5194/se-10-1155-2019

Baisch, S., Weidler, R., Voeroes, R., Tenzer, H. and Teza, D., 2004, January. Improving hydraulic stimulation efficiency by means of real-time monitoring. In Proceedings of the 29th workshop on geothermal reservoir engineering, Stanford University (pp. 209-215).

Baisch, S., Weidler, R., Vörös, R., Wyborn, D. and de Graaf, L., 2006. Induced seismicity during the stimulation of a geothermal HFR reservoir in the Cooper Basin, Australia. Bulletin of the Seismological Society of America, 96(6), pp.2242-2256. DOI: https://doi.org/10.1785/0120050255

Baisch, S., Vörös, R., Weidler, R. and Wyborn, D., 2009. Investigation of Fault Mechanisms during Geothermal Reservoir Stimulation Experiments in the Cooper Basin, Australia. Bulletin of the Seismological Society of America, 99(1), pp.148-158. DOI: https://doi.org/10.1785/0120080055

Baisch, S., Rothert, E., Stang, H., Vörös, R., Koch, C. and McMahon, A., 2015. Continued geothermal reservoir stimulation experiments in the Cooper Basin (Australia). Bulletin of the Seismological Society of America, 105(1), pp.198-209. DOI: https://doi.org/10.1785/0120140208

Baisch, S., Koch, C., Stang, H., Pittens, B., Drijver, B., and Buik, N., 2016. Defining the Framework for Seismic Hazard Assessment in Geothermal Projects V0.1 – Technical Report, 1-65.

Baisch, S. and Vörös, R., 2019. Earthquakes near the Californië geothermal site: August 2015–November 2018. Report No. CLGG005. Q-con GmbH (Bad Bergzabern).

Bär, K., Reinsch, T. and Bott, J., 2020. The PetroPhysical Property Database (P 3)–a global compilation of lab-measured rock properties. Earth System Science Data, 12(4), pp.2485-2515. DOI: https://doi.org/10.5194/essd-12-2485-2020

Barbour, A.J., Evans, E.L., Hickman, S.H. and Eneva, M., 2016, February. Sources of subsidence at the Salton Sea geothermal field. In 41st Workshop on Geothermal Reservoir Engineering, Stanford University, Stanforf, California (Vol. 14, p. 15).

Baria, R., Baumgärtner, J., Gérard, A. and Garnish, J., 2000, May. The European HDR programme: main targets and results of the deepening of the well GPK2 to 5000 m. In Proceedings of the world geothermal congress (pp. 3643-3652).

Batchelor, A.S., 1982. The Stimulation of a Hot dry Rock Geothermal Reservoir in the Cornubian Granite, England. (No. SGP-TR-60; CONF-821214-34). Camborne School of Mines Geothermal Energy Project, Cornwall, England.

Batir, J.F., 2011. Stress field characterization of the Hellisheidi geothermal field and possibilities to improve injection capabilities (Doctoral dissertation).

Bauer, M., Freeden, W., Jacobi, H. and Neu, T., 2014. Ausblick: Herausforderungen, Chancen und Perspektiven. Handbuch Tiefe Geothermie: Prospektion, Exploration, Realisierung, Nutzung, pp.835-841.

Bauer, S.J., Barrow, P., Robbins, A. and Hileman, M., 2018. Mechanical and Fluid Flow Properties of Basaltic Andesite and Rhyolite Analogue Rocks. Sandia National Laboratories Technical Report (GDR Database).

Benato, S., Hickman, S., Davatzes, N.C., Taron, J., Spielman, P., Elsworth, D., Majer, E.L. and Boyle, K., 2016. Conceptual model and numerical analysis of the Desert Peak EGS project: Reservoir response to the shallow medium flow-rate hydraulic stimulation phase. Geothermics, 63, pp.139-156. DOI: https://doi.org/10.1016/j.geothermics.2015.06.008

Bender, 2011. Well proposals Honselersdijk, Wells HON-GT-01 and HON-GT-02, Report No. G888. PanTerra Geo consultants B.V. 50P.

Bignall, G., Rae, A. and Rosenberg, M., 2010, April. Rationale for targeting fault versus formation-hosted permeability in high-temperature geothermal systems of the Taupo Volcanic Zone, New Zealand. In Proceedings.

Birner, J., Fritzer, T., Jodocy, M., Savvatis, A., Schneider, M. and Stober, I., 2012. Hydraulic characterisation of the Malm aquifer in the South German Molasse basin and its impact on geothermal exploitations. Z geol Wiss, 40(2), pp.133-56.

Blöcher, M.G., Zimmermann, G., Moeck, I., Brandt, W., Hassanzadegan, A. and Magri, F., 2010. 3D numerical modeling of hydrothermal processes during the lifetime of a deep geothermal reservoir. Geofluids, 10(3), pp.406-421. DOI: https://doi.org/10.1111/j.1468-8123.2010.00284.x

Blöcher, G., Cacace, M., Jacquey, A.B., Zang, A., Heidbach, O., Hofmann, H., Kluge, C. and Zimmermann, G., 2018. Evaluating micro-seismic events triggered by reservoir operations at the geothermal site of Groß Schönebeck (Germany). Rock Mechanics and Rock Engineering, 51, pp.3265-3279. DOI: https://doi.org/10.1007/s00603-018-1521-2

Bodvarsson G.S., Bjornsson S., Gunnarsson A., Gunnlaugsson E., Sigurdsson O., Stefansson V., and Steingrimsson B.,1988. A summary of modeling studies of the Nesjavellir geothermal field, Iceland. 13th Workshop on Geothermal Reservoir Engineering, Stanford, CA, January 19-21.

Böhm, F., Savvatis, A., Beichel, K., and Linde, J., 2021. Risk minimization of fluid-induced seismicity in the South German Molasse Basin using the Schäftlarnstrasse project of Stadtwerke München as an example. EEK – Technologie, Transformation von fossilen und grünen Energieträgern, 137, pp.33-36.

Boissavy, C., Rocher, P., Laplaige, P. and Brange, C., 2016, September. Geothermal energy use, country update for France. In European Geothermal Congress (Vol. 11, p. 14).

Bosia, C., Mouchot, J., Ravier, G., Seibt, A., Jähnichen, S., Degering, D., Scheiber, J., Dalmais, E., Baujard, C. and Genter, A., 2021, February. Evolution of brine geochemical composition during operation of EGS geothermal plants (Alsace, France). In Proceedings of the 46th Workshop on Geothermal Reservoir Engineering, Stanford, CA, USA (pp. 15-17).

Boyle, K. and Zoback, M., 2014. The stress state of the Northwest Geysers, California geothermal field, and implications for fault-controlled fluid flow. Bulletin of the Seismological Society of America, 104(5), pp.2303-2312. DOI: https://doi.org/10.1785/0120130284

Boyd, O.S., 2018. Analysis of Seismic Moment Tensors, In-Situ Stress, and Finite-Source Scaling of Earthquakes at The Geysers Geothermal Field, California (Doctoral dissertation, UC Berkeley).

Breede, K., Dzebisashvili, K., Liu, X., and Falcone, G., 2013. A systematic review of enhanced (or engineered) geothermal systems: past, present and future. Geothermal Energy, 1, pp.1-27. DOI: https://doi.org/10.1186/2195-9706-1-4.

Brinkgreve, D., 2016. SodM End of Well ReportCAL-GT-04. CLG Geothermie B.V. 17 P.

Brodsky, E.E. and Lajoie, L.J., 2013. Anthropogenic seismicity rates and operational parameters at the Salton Sea Geothermal Field. Science, 341(6145), pp.543-546. DOI: https://doi.org/10.1126/science.1239213

Bromley, C. and Bignall, G., 2016. Ngawha Geothermal Field: Geology, Geophysics, Conceptual Model, Geochemical Monitoring Trends and Environmental Issues. JOGMEC-GNS Workshop, Tokyo.

Bromley, C.J., Pearson, C.F. and Rigor Jr, D.M., 1987. Microearthquakes at the Puhagan geothermal field, Philippines—A case of induced seismicity. Journal of volcanology and geothermal research, 31(3-4), pp.293-311. DOI: https://doi.org/10.1016/0377-0273(87)90073-4

Bromley, C.J., 2014. Seismicity and Subsidence: Examples of Observed Geothermal Deformation Synergies from New Zealand. In Proceedings 38th Workshop on Geothermal Resources, Engineering Stanford University, Stanford, SGP-TR-202.

Bromley, C.J., 2021. Induced Seismicity – a Perspective on Monitoring, Mechanisms and Public Acceptability for Hydrothermal Systems. In Proceedings of the World Geothermal Congress 2020, Reykjavik, April-October 2021.

Brown, D.W., 2009, February. Hot dry rock geothermal energy: important lessons from Fenton Hill. In Proceedings of the thirty-fourth workshop on geothermal reservoir engineering. Stanford: Stanford University.

Brown, J.M., 1989. Bedrock Geotechnical Properties Affecting Ground-water Movement in the US Coast Guard Reservation, Kodiak, Alaska. Alaska Division of Geological and Geophysical Surveys.

Bruno, M.S., Dusseault, M.B., Balaa, T.T., and Barrera, J.A., 1998. Geomechanical Analysis of Pressure Limits For Gas Storage Reservoirs. Proceedings North American Rock Mechanics Symposium, NARMS ’98, June 3-5, USA, PP.328-5.

Bruno, M.S., Lao, K., Diessl, J., Childers, B., Xiang, J., White, N., and van der Veer, E., 2014. Development of improved caprock integrity analysis and risk assessment techniques. Energy Procedia, 63, pp.4708-4744. DOI: https://doi.org/10.1016/j.egypro.2014.11.503.

Budach, I., Moeck, I., Lüschen, E. and Wolfgramm, M., 2018. Temporal evolution of fault systems in the Upper Jurassic of the Central German Molasse Basin: case study Unterhaching. International Journal of Earth Sciences, 107, pp.635-653. DOI: https://doi.org/10.1007/s00531-017-1518-1

Buijze, L., van Bijsterveldt, L., Cremer, H., Paap, B., Veldkamp, H., Wassing, B., van Wees, J.D., and ter Heege, J., 2019. Review of worldwide geothermal projects: mechanisms and occurrence of induced seismicity. TNO report, TNO 2019 R100043.

Buijze, L., van Bijsterveldt, L., Cremer, H., Paap, B., Veldkamp, H., Wassing, B.B.T., van Wees, J.D., van Yperen, G.C.N, and ter Heege, J.H., 2020. Review of induced seismicity in geothermal systems worldwide and implications for geothermal systems in the Netherlands. Netherlands Journal of Geosciences, 98, p.e13. DOI: https://doi.org/10.1017/njg.2019.6.

Bujakowski, W. and Wojnarowski, P., 2005. Recent Studies of the Low Cretaceous Geothermal Reservoir in Mszczonów, Poland. In Proceedings World Geothermal Congress.

Bundesverband Geothermie, Accessed in June 2023: https://www.geothermie.de/aktuelles/nachrichten.html

Caine, J.S., Evans, J.P., and Forster, C.B., 1996. Fault zone architecture and permeability structure. Geology, 24, pp. 1025-1028. DOI: https://doi.org/10.1130/0091-7613(1996)024%3C1025:FZAAPS%3E2.3.CO;2

Cant, J.L., Siratovich, P.A., Cole, J.W., Villeneuve, M.C. and Kennedy, B.M., 2018. Matrix permeability of reservoir rocks, Ngatamariki geothermal field, Taupo Volcanic Zone, New Zealand. Geothermal Energy, 6(1), pp.1-28. DOI: https://doi.org/10.1186/s40517-017-0088-6

Cardiff, M., Lim, D.D., Patterson, J.R., Akerley, J., Spielman, P., Lopeman, J., Walsh, P., Singh, A., Foxall, W., Wang, H.F. and Lord, N.E., 2018. Geothermal production and reduced seismicity:

Correlation and proposed mechanism. Earth and Planetary Science Letters, 482, pp.470-477. DOI: https://doi.org/10.1016/j.epsl.2017.11.037

Carmo, R., Madeira, J., Ferreira, T., Queiroz, G. And Hipo ́lito, A., 2015. Volcano-tectonic structures of Sa ̃o Miguel Island, Azores. The Geological Society of London. Chapter 6. 23 P.

Carvalho, M.R., Forjaz, V.H. and Almeida, C., 2006. Chemical composition of deep hydrothermal fluids in the Ribeira Grande geothermal field (São Miguel, Azores). Journal of Volcanology and Geothermal Research, 156(1-2), pp.116-134. DOI: https://doi.org/10.1016/j.jvolgeores.2006.03.015

Cauchie, L., Lengliné, O., and Schmittbuhl, J., 2020. Seismic asperity size evolution during fluid injection: case study of the 1993 Soultz-sous-Forets injection. Geophysical Journal International, 222, pp.968-980. DOI: https://doi.org/10.1093/gji/ggaa051.

Chang, K.W., and Segall, P., 2016. Seismicity on Basement Faults Induced by Simultaneous Fluid Injection–Extraction. Pure and Applied Geophysics, 173, pp.2621-2636. DOI: https://doi.org/10.1007/s00024-016-1319-7.

Chang, K.W., Yoon, H., Kim, Y.H., and Lee, M.Y., 2020. Operational and geological controls of coupled poroelastic stressing and pore-pressure accumulation along faults: induced earthquakes in Pohang, South Korea. Nature Research, 10, p.2073. DOI: https://doi.org/10.1038/s41598-020-58881-z.

Charléty, J., Cuenot, N., Dorbath, L., Dorbath, C., Haessler, H. and Frogneux, M., 2007. Large earthquakes during hydraulic stimulations at the geothermal site of Soultz-sous-Forêts. International Journal of Rock Mechanics and Mining Sciences, 44(8), pp.1091-1105. DOI: https://doi.org/10.1016/j.ijrmms.2007.06.003

Cladouhos, T.T., Petty, S., Swyer, M.W., Nordin, Y., Garrison, G., Uddenberg, M., Grasso, K., Stern, P., Sonnenthal, E., Foulger, G. and Julian, B., 2015. Newberry EGS Demonstration: Phase 2.2 Report (No. DOE/EE/2777/3). AltaRock Energy, Seattle, WA (United States). DOI: https://doi.org/10.2172/1214834

Cladouhos, T.T., Petty, S., Swyer, M.W., Uddenberg, M.E., Grasso, K. and Nordin, Y., 2016. Results from newberry volcano EGS demonstration, 2010–2014. Geothermics, 63, pp.44-61. DOI: https://doi.org/10.1016/j.geothermics.2015.08.009

Cobos, J.E., Knudby, C. and Søgaard, E.G., 2021. A geothermal plant from a time-scale perspective. Energies, 14(19), p.6096. DOI: https://doi.org/10.3390/en14196096

Condora, J., Unatrakarna, D., Wilson, M., and Asghari, K., 2011. A Comparative Analysis of Risk Assessment Methodologies for the Geologic Storage of Carbon Dioxide. Energy Procedia, 4, pp.4036-4043. DOI: https://doi.org/10.1016/j.egypro.2011.02.345.

Cornet, F.H., Helm, J., Poitrenaud, H. and Etchecopar, A., 1997. Seismic and aseismic slips induced by large-scale fluid injections. In Seismicity associated with mines, reservoirs and fluid injections (pp. 563-583). Birkhäuser Basel. DOI: https://doi.org/10.1007/978-3-0348-8814-1_12

Creative Commons (Creative Commons license Attribution-ShareAlike 4.0 International license), Accessed in June 2023: https://creativecommons.org/licenses/by-sa/4.0/deed.en.

Das, S., and Scholz, C.H., 1983. Why large earthquakes do not nucleate at shallow depths. Nature, 305, pp.621-623. DOI: https://doi.org/10.1038/305621a0

Davatzes, N.C., Hickman, S. and Team, E.H., 2006, January. Stress and faulting in the Coso Geothermal Field: Update and recent results from the East Flank and Coso Wash. In Proceedings 31st Workshop on Geothermal Reservoir Engineering (pp. 13-19).

Davatzes, N.C. and Hickman, S.H., 2009. Fractures, stress and fluid flow prior to stimulation of well 27-15, Desert Peak, Nevada, EGS Project. In Thirty-Fourth Workshop on Geothermal Reservoir Engineering.

Davatzes, N.C. and Hickman, S.H., 2011. Preliminary analysis of stress in the Newberry EGS well NWG 55-29 (No. DOE/EE-2777/3). AltaRock Energy, Inc., Seattle, WA (United States).

Davidson, J., Siratovich, P., Wallis, I., Gravley, D. and McNamara, D.D., 2012. Quantifying the stress distribution at the Rotokawa geothermal field, New Zealand. In New Zealand Geothermal Workshop 2012. New Zealand Geothermal Workshop.

Duboeuf, L., Dichiarante, A.M. and Oye, V., 2022. Interplay of large-scale tectonic deformation and local fluid injection investigated through seismicity patterns at the Reykjanes Geothermal Field, Iceland. Geophysical Journal International, 228(3), pp.1866-1886. DOI: https://doi.org/10.1093/gji/ggab423

De Freitas, M.A., 2018. Numerical simulation of the Svartsengi geothermal field, SW-Iceland. In 40th Anniversary Workshop.

De Freitas, M.E., Axelsson, G., and Einarsson, P., 2020. An Analysis of 40 Years of Subsidence due to Geothermal Production from the Svartsengi-Eldvörp Geothermal System in SW Iceland. Proceedings World Geothermal Congress 2020+1Reykjavik, Iceland, April -October 2021.

Deichmann, N., Kraft, T. and Evans, K.F., 2014. Identification of faults activated during the stimulation of the Basel geothermal project from cluster analysis and focal mechanisms of the larger magnitude events. Geothermics, 52, pp.84-97. DOI: https://doi.org/10.1016/j.geothermics.2014.04.001

Dempsey, D., Kelkar, S., Lewis, K., Hickman, S., Davatzes, N., Moos, D. and Zemach, E., 2013, June. Modeling shear stimulation of the desert peak EGS well 27-15 using a coupled thermal-hydrological-mechanical simulator. In 47th US Rock Mechanics/Geomechanics Symposium. OnePetro.

Denllinger, M., Majer, E., Freeman, K., Johnson, L.R., Jarpe, S., Nihei, K. and Walters, M., 2017. Final report: Monitoring the effect of injection of fluids from the Lake County pipeline on seismicity at The Geysers, California, geothermal field, United States. United States.

Dezayes, C., Genter, A. and Valley, B., 2010. Structure of the low permeable naturally fractured geothermal reservoir at Soultz. Comptes Rendus Geoscience, 342(7-8), pp.517-530. DOI: https://doi.org/10.1016/j.crte.2009.10.002

Dinçer, I., Acar, A., Çobanoğlu, I. and Uras, Y., 2004. Correlation between Schmidt hardness, uniaxial compressive strength and Young's modulus for andesites, basalts and tuffs. Bulletin of Engineering Geology and the Environment, 63, pp.141-148. DOI: https://doi.org/10.1007/s10064-004-0230-0

DiPippo, R., 2016. Geothermal Power Plants (4th Edition), 2016.

Djama, D.R., 2014. Borehole geology and alteration mineralogy of well rn-12, Reykjanes geothermal field, sw-Iceland. Orkustofnun, Grensasvegur 9,Reports 2014 IS-108 Reykjavik, Iceland.

Dorbath, L., Cuenot, N., Genter, A. and Frogneux, M., 2009. Seismic response of the fractured and faulted granite of Soultz-sous-Forêts (France) to 5 km deep massive water injections.

Geophysical Journal International, 177(2), pp.653-675. DOI: https://doi.org/10.1111/j.1365-246X.2009.04030.x

Drakos, P., 2010. Geothermal Technologies Program 2010 Peer Review. Energy Efficiency and Renewable Energy (EERE). US.

Drews, M.C., Hofstetter, P., Zosseder, K., Shipilin, V., and Stollhofen, H., 2020. Predictability and controlling factors of overpressure in the North Alpine Foreland Basin, SE Germany: an interdisciplinary postdrill analysis of the Geretsried- GEN-1 deep geothermal well. Geothermal Energy, 8, pp.1-28. DOI: https://doi.org/10.1186/s40517020001758.

Dussel, M., Lüschen, E., Thomas, R., Agemar, T., Fritzer, T., Sieblitz, S., Huber, B., Birner, J. and Schulz, R., 2016. Forecast for thermal water use from Upper Jurassic carbonates in the Munich region (South German Molasse Basin). Geothermics, 60, pp.13-30. DOI: https://doi.org/10.1016/j.geothermics.2015.10.010

Erlström, M., Boldreel, L.O., Lindström, S., Kristensen, L., Mathiesen, A., Andersen, M.S. and Nielsen, L.H., 2018. Stratigraphy and geothermal assessment of Mesozoic sandstone reservoirs in the Øresund Basin–exemplified by well data and seismic profiles. Bull Geol Soc Den, 66, pp.123-49.

Eggertsson, G.H., Lavallée, Y., Kendrick, J.E. and Markússon, S., 2018. Impact of thermo-mechanical stimulation on the reservoir rocks of the geothermal system at Krafla, Iceland. In 42rd Workshop on Geot Res Engineering. Standford University, California, USA.

Elfina, 2017. Updated Conceptual Model of The Patuha Geothermal Field, Indonesia. United Nations University. GTP (Geothermal Training Program). Reykjavik, Iceland.

Eliasson, T., Wallroth, T. and Sundquist, U., 1990. Circulation experiments in 1989 at Fjällbacka HDR test site. Göteborg, Sweden: Chalmers University of Technology. DOI: https://www.researchgate.net/publication/280932935

Ellsworth, W.L., Giardini, D., Townend, J., Ge, S. and Shimamoto, T., 2019. Triggering of the Pohang, Korea, earthquake (M w 5.5) by enhanced geothermal system stimulation. Seismological Research Letters, 90(5), pp.1844-1858. DOI: https://doi.org/10.1785/0220190102

Elster, D., Goldbrunner, J., Wessely, G., Niederbacher, P., Schubert, G., Berka, R., Philippitsch, R., and Hörhan, T., 2016. Erläuterungen zur geologischen Themenkarte Thermalwässer in Österreich, 1 : 500000. Geologische Bundesanstalt, Wien 2016.

Elsworth, D., Spiers, C.J. and Niemeijer, A.R., 2016. Understanding induced seismicity. Science, 354(6318), pp.1380-1381. DOI: https://doi.org/10.1126/science.aal2584

Evans, K.E., Zappone, A., Kraft, T., Deichmann, N., and Moia, F., 2012. A survey of the induced seismic responses to fluid injection in geothermal and CO2 reservoirs in Europe. Geothermics, 41, pp.30-54. DOI: https://doi.org/10.1016/j.geothermics.2011.08.002.

Evans, K.F., Moriya, H., Niitsuma, H., Jones, R.H., Phillips, W.S., Genter, A., Sausse, J., Jung, R. and Baria, R., 2005. Microseismicity and permeability enhancement of hydrogeologic structures during massive fluid injections into granite at 3 km depth at the Soultz HDR site. Geophysical Journal International, 160(1), pp.388-412. DOI: https://doi.org/10.1111/j.1365-246X.2004.02474.x

Fadel, I., Hecker, C., Kimata, J., Bonyo, E., van der Meijde, M., van der Werff, H. and van der Meer, F., 2021. Geoscientific monitoring of Olkaria's geothermal motor, Eos, 102.

Faridi, M., Burg, J.P., Nazari, H., Talebian, M. and Ghorashi, M., 2017. Active faults pattern and interplay in the Azerbaijan region (NW Iran). Geotectonics, 51(4), pp.428-437. DOI: https://doi.org/10.1134/S0016852117040033

Farkas, M.P., Hofmann, H., Zimmermann, G., Zang, A., Bethmann, F., Meier, P., Cottrell, M. and Josephson, N., 2021. Hydromechanical analysis of the second hydraulic stimulation in well PX-1 at the Pohang fractured geothermal reservoir, South Korea. Geothermics, 89, p.101990. DOI: https://doi.org/10.1016/j.geothermics.2020.101990

Farquharson, N., Schubert, A., and Steiner, U., 2016. Geothermal Energy in Munich (and Beyond). A Geothermal City Case Study. GRC Transactions, 40, pp.189-196.

Figueiredo, B., Tsang, C.-F., Rutqvist, J., and Niemi, A., 2015. A study of changes in deep fractured rock permeability due to coupled hydromechanical effects. International Journal of Rock Mechanics and Mining Sciences, 79, pp.70-85. DOI: https://doi.org/10.1016/j.ijrmms.2015.08.011.

Flores-Armenta, M., Ramírez-Montes, M. and Morales-Alcalá, L., 2014. Geothermal activity and development in Mexico–keeping the production going. Proceedings of the Geothermal Training Programme.

Flores, M., Davies, D., Couples, G. and Palsson, B., 2005, April. Stimulation of geothermal wells, can we afford it. In Proceedings world geothermal congress (Vol. 1).

Flóvenz, Ó.G., Ágústsson, K., Guðnason, E.Á. and Kristjánsdóttir, S., 2015, April. Reinjection and induced seismicity in geothermal fields in Iceland. In Proceedings world geothermal congress (pp. 1-15).

Foged, N.N., and Andrassen, K.A., 2016. Strength and deformation properties of volcanic rocks in Iceland. In Proceeding 17th Nordic Geotechnical Meeting, Reykjavik, 25th-28th May 2016.

Franco, A., 2015. Subsurface geology and hydrothermal alteration of Cachaços-Lombadas sector, Ribeira Grande geothermal field, (Sao Miguel Island, Azores). United Nations University. Reports.

Franco, A., Ortolá, R., Botelho, J., Pereira, V., Guimarães, T., Vieira, N. and Rita Martins, R., 2021. Forty Years of Power Generation at the Ribeira Grande Geothermal Field, Azores. Proceedings World Geothermal Congress 2021. Reykjavik, Iceland.

Franzson, H., Thordarson, S., Björnsson, G., Gudlaugsson, S.T., Richter, B., Fridleifsson, G.O. and Thorhallsson, S., 2002, January. Reykjanes high-temperature field, SW-Iceland. Geology and hydrothermal alteration of well RN-10. In Workshop on Geothermal Reservoir Engineering (Vol. 27, pp. 233-240).

Franzson, H., Kristjánsson, B.R., Gunnarsson, G., Björnsson, G., Hjartarson, A., Steingrímsson, B., Gunnlaugsson, E. and Gíslason, G., 2005, April. The Hengill-Hellisheiði geothermal field. Development of a conceptual geothermal model. In Proceedings world geothermal congress (pp. 1-7). Antalya.

Garcia, J., Walters, M., Beall, J., Hartline, C., Pingol, A., Pistone, S. and Wright, M., 2012, January. Overview of the northwest Geysers EGS demonstration project. In Proceedings of the thirty-seventh workshop on geothermal reservoir engineering (Vol. 30).

Garcia, J., Hartline, C., Walters, M., Wright, M., Rutqvist, J., Dobson, P.F. and Jeanne, P., 2016. The Northwest Geysers EGS demonstration project, California: Part 1: characterization and reservoir response to injection. Geothermics, 63, pp.97-119.

Galis, M., Ampuero, J.P., Mai, P.M., and Cappa, F., 2017. Induced Seismicity provides insight into why earthquake ruptures stop. Science advances, 3, p.eaap7528. DOI: https://doi.org/10.1126/sciadv.aap7528.

Gaucher, E., Jolivet, M. and Peter-Borie, M., 2020. Preliminary Results of the Seismicity Induced During the Stimulation of the Vendenheim Enhanced Geothermal System (France). In Proceedings World Geothermal Congress (p. 1).

GDR (Geothermal Data Repository Database), Accessed in June 2023: https://gdr.openei.org/home.

GeoMechanics Technologies, 2020. Surface Deformation Study at the Kawerau Field (2020-10), Internal Report, 93 p.

Geothermal Energy (Trudering-Riem Project), Accessed in June 2023: Messestadt-Riem: Geothermal energy Riem.

PERFORM (Geotherm Perform Database), Accessed in June 2023: https://www.geothermperform.eu/

GEUS (Geological Survey of Denmark and Greenland), Accessed on June 2023: https://www.geus.dk/produkter-ydelser-og-faciliteter/data-og-kort/national-boringsdatabase-jupiter.

Ghassemi, A., 2017. Geomechanics-Based Stochastic Analysis of Injection Induced Seismicity. Unites States DOE Report, OU-RM-DOE-17-F2; pp.330. DOI: https://doi.org/10.2172/1375732.

GitHub Inc. © 2023, www.github.com

Glaas, C., Genter, A., Girard, J.F., Patrier, P. and Vidal, J., 2018. How do the geological and geophysical signatures of permeable fractures in granitic basement evolve after long periods of natural circulation? Insights from the Rittershoffen geothermal wells (France). Geothermal Energy, 6(1), pp.1-25. DOI: https://doi.org/10.1186/s40517-018-0100-9

Glaas, C., Vidal, J. and Genter, A., 2021. Structural characterization of naturally fractured geothermal reservoirs in the central Upper Rhine Graben. Journal of Structural Geology, 148, p.104370. DOI: https://doi.org/10.1016/j.jsg.2021.104370

Glowacka, E. and Nava, F.A., 1996. Major earthquakes in Mexicali Valley, Mexico, and fluid extraction at Cerro Prieto geothermal field. Bulletin of the Seismological Society of America, 86(1A), pp.93-105. DOI: https://doi.org/10.1785/BSSA08601A0093

Glowacka, E., González, J. and Fabriol, H.U.B.E.R.T., 1999. Recent vertical deformation in Mexicali Valley and its relationship with tectonics, seismicity, and the exploitation of the Cerro Prieto geothermal field, Mexico. Pure and Applied Geophysics, 156, pp.591-614. DOI: https://doi.org/10.1007/s000240050314

Goebel, T.H.W., Weingarten, M., Chen, X., Haffener, J. and Brodsky, E.E., 2017. The 2016 Mw5. 1 Fairview, Oklahoma earthquakes: Evidence for long-range poroelastic triggering at> 40 km from fluid disposal wells. Earth and Planetary Science Letters, 472, pp.50-61. DOI: https://doi.org/10.1016/j.epsl.2017.05.011

Goebel, T.H.W., and Brodsky, E.E., 2018. The spatial footprint of injection wells in a global compilation of induced earthquake sequences. Science, 361, pp.899-904. DOI: https://doi.org/10.1126/science.aat5449.

Gokcen, G., Ozturk, H.K. and Hepbasli, A., 2004. Overview of Kizildere geothermal power plant in Turkey. Energy conversion and management, 45(1), pp.83-98. DOI: https://doi.org/10.1016/S0196-8904(03)00129-8

Goldbrunner, J.E., 2000. Hydrogeology of deep groundwaters in Austria. Mitt. Österr. Geol. Ges, 92(1999), pp.281-294.

Goldbrunner, J., 2005. Bad Blumau (Styria, Austria) The success story of combined use of geothermal energy. Magnesium (Mg++), 2, pp.6-4.

Goldbrunner, J.E., 2007. Entwicklungsstand, politisches Umfeld und Perspektiven der Tiefen Geothermie in Österreich. Erdöl Erdgas Kohle 123. Jg. 2007, Heft 2 75.

Goldbrunner, J., 2010, April. Austria–country update. In Proceedings World Geothermal Congress (pp. 1-13).

Goldbrunner, J.E. and Vasvari, V., 2016. Hydrogeology and geothermic simulation of the geothermal doublet at Waldkraiburg (Bavaria). Austrian Journal of Earth Sciences, 109(1). DOI: 10.17738/ajes.2016.0007

Goldbrunner, J. and Goetzl, G., 2019. Geothermal energy use, country update for Austria. European Geothermal Congress, Den Haag, The Netherlands.

González-Partida, E., Tritlla, J., Levresse, G., Venegas-Salgado, S., Ramírez-Silva, G., Camprubí, A. and Carrillo-Chavez, A., 2005. Fluid Inclusion Study from the Tres Virgenes Geothermal Field, Baja California Sur, Mexico.

Grad, M., and Polkowski, M., 2016. Seismic basement in Poland. International Journal of Earth Sciences, 105, pp.1199-1214. DOI: https://doi.org/10.1007/s00531-015-1233-8.

Granados, E., Henneberger, R., Klein, C., Sanyal, S., Bicudo da Ponte, C., and Forjaz, V., 2000. Development of Injection Capacity for the Expansion of the Ribeira Grande Geothermal Project, Sao Miguel, Acores, Portugal. In Proceedings World Geothermal Congress, Kyushu, 28th May-10th June 2000, pp.3065-3070.

Grigoli, F., Cesca, S., Rinaldi, A.P., Manconi, A., Lopez-Comino, J.A., Clinton, J.F., Westaway, R., Cauzzi, C., Dahm, T. and Wiemer, S., 2018. The November 2017 M w 5.5 Pohang earthquake: A possible case of induced seismicity in South Korea. Science, 360(6392), pp.1003-1006. DOI: https://doi.org/10.1126/science.aat2010

Gudmundsson, J.S., Olsen, G., and Thorhallsson, S., 1985. Proceedings of the tenth workshop on geothermal reservoir engineering, Stanford University.

Guerrero, F.J., Pérez-Zárate, D., Prol-Ledesma, R.M., Garza-Galindo, R., Reyes-Sandoval, A. and García-Zamorano, E.A., 2022. A numerical experiment for geological sequestration of CO2 in the pre-Comondú sandstones of Las Tres Virgenes geothermal area, Baja California Sur, Mexico. International Journal of Greenhouse Gas Control, 115, p.103630. DOI: https://doi.org/10.1016/j.ijggc.2022.103630

Guglielmi, Y., Cappa, F., and Amitrano, D., 2008. High-definition analysis of fluid-induced seismicity related to the mesoscale hydromechanical properties of a fault zone. Geophysical Research Letters, 35, L06306. DOI: https://doi.org/10.1029/2007GL033087.

Haklıdır, F.S.T., Şengün, R. and Aydın, H., 2021. Characterization and Comparison of geothermal fluids geochemistry within the Kızıldere Geothermal Field in Turkey: New findings with power capacity expanding studies. Geothermics, 94, p.102110. DOI: https://doi.org/10.1016/j.geothermics.2021.102110

Häring, M.O., Schanz, U., Ladner, F., and Dyer, B.C., 2008. Characterisation of the Basel 1 enhanced geothermal system. Geothermics, 37, pp.469-495. DOI: https://doi.org/10.1016/j.geothermics.2008.06.002.

Heap, M.J., and Violay, M.E.S., 2021. The mechanical behaviour and failure modes of volcanic rocks: a review. Bulletin of Volcanology, 83, p.33. DOI: https://doi.org/10.1007/s00445-021-01447-2.

ter Heege, J., van Bijsterveldt, L., Wassing, B., Osinga, S., Paap, B., and Kraaijpoel, D., 2020. Induced seismicity potential for geothermal projects targeting Dinantian carbonates in the Netherlands. Report TNO Appl. Geosciences: 148p., Utrecht.

Heidbach, O., Rajabi, M., Cui, X., Fuchs, K., Müller, B., Reinecker, J., Reiter, K., Tingay, M., Wenzel, F., Xie, F. and Ziegler, M.O., 2018. The World Stress Map database release 2016: Crustal stress pattern across scales. Tectonophysics, 744, pp.484-498. DOI: https://doi.org/10.1016/j.tecto.2018.07.007

Helgadóttir, H.M., Snaebjörnsdottir, S.O., Níelsson, S., Gunnarsdóttir, S.H., Matthíasdóttir, T., Hardarson, B.S., Einarsson, G.M. and Franzson, H., 2010, April. Geology and hydrothermal alteration in the reservoir of the Hellisheidi high temperature system, SW-Iceland. In Proceedings, World Geothermal Congress, Bali, Indonesia (pp. 25-29).

Henriquez, E.T., 2010, Petrologic Evaluation of the Southern Part of Berlin Geothermal Field, El Salvador.

Herrera, H.L., 2005. Actualización del modelo geológico conceptual del yacimiento geotérmico de Cerro Prieto, BC. Geotermia, p.37.

Hillers, G., T. Vuorinen, T.A., Uski, M.R., Kortström, J.T., Mäntyniemi, P.B., Tiira, T., Malin, P.E. and Saarno, T., 2020. The 2018 geothermal reservoir stimulation in Espoo/Helsinki, southern Finland: Seismic network anatomy and data features. Seismological Research Letters, 91(2A), pp.770-786. doi: https://doi.org/10.1785/0220190253

Hirst, C.A. The Geothermal Potential of Low Enthalpy Deep Sedimentary Basins in the UK. Durham theses, Durham University. Available at Durham E-Theses Online: http://etheses.dur.ac.uk/11979/

Hitzman, M., Leith, B., Petty, S., and Zoback, M., 2013. Induced Seismicity Potential in Energy Technologies. Nat. Academy Sci.: 248p. Washington D.C.

Hjuler, M.L., Nielsen, C.M., Frykman, P., Kristensen, L., Mathiesen, A.A., Bidstrup, T. and Nielsen, L.H., 2014. A multidisciplinary study of a geothermal reservoir below Thisted, Denmark. GEUS Bulletin, 31, pp.51-54.

Hofmann, H., Zimmermann, G., Farkas, M., Huenges, E., Zang, A., Leonhardt, M., Kwiatek, G., Martinez-Garzon, P., Bohnhoff, M., Min, K.B. and Fokker, P., 2019. First field application of cyclic soft stimulation at the Pohang Enhanced Geothermal System site in Korea. Geophysical Journal International, 217(2), pp.926-949. DOI: https://doi.org/10.1093/gji/ggz058

Holl, HG. and Barton, C., 2015. Habanero Field -Structure and State of Stress. Proceedings World Geothermal Congress. Melbourne, Australia.

Homuth, S., 2014. Aufschlussanalogstudie zur Charakterisierung oberjurassischer geothermischer Karbonatreservoire im Molassebecken. Thesis, Technische Universität Darmstadt.

Hopp, C., 2019. Seismic response to deep injection changes at Rotokawa geothermal field, New Zealand. Victoria University of Wellington. 29 P.

Horsrud, P., 2001. Estimating Mechanical Properties of Shale from Empirical Correlations. SPE Drilling and Completion, 16(2), 68–73.

Huenges, E., Trautwein, U., Legarth, B. and Zimmermann, G., 2006. Fluid pressure variation in a sedimentary geothermal reservoir in the North German Basin: case study Groß Schönebeck. Pure and applied geophysics, 163, pp.2141-2152. DOI: https://doi.org/10.1007/s00024-006-0122-2

Humphreys, B., Hodson-Clarke, A. and Hogarth, R., 2014. Habanero geothermal project field development plan. Geodynamics Ltd.: Brisbane, Australia.

IGSMiE PAN, 2019. Report on Risk assessment, Appendix 2: Risk factors influencing the success of geothermal heating projects in Poland –one of the GEORISK target country. Inputs from the geothermal district heating plants in Poland. Georisk. 39 P.

ITG (Informatonsportal Tiefe Geothermie), Accessed in June 2023. Ismaning | Informationsportal Tiefe Geothermie

IPMA (Portuguese Institute for Sea and Atmosphere), Accessed in June 2023: https://www.ipma.pt/en/.

IRSC (Iranian Seismological Center), Institute of Geophysics, University of Tehran, Accessed in June 2023: http://irsc.ut.ac.ir/.

Jacquey, A.B., Cacace, M., Blöcher, G., Watanabe, N., Huenges, E. and Scheck-Wenderoth, M., 2016. Thermo-poroelastic numerical modelling for enhanced geothermal system performance: Case study of the Groß Schönebeck reservoir. Tectonophysics, 684, pp.119-130. DOI: https://doi.org/10.1016/j.tecto.2015.12.020

Jeanne, R., Guglielmi, Y., Rutqvist, Y., Nussbaum, C., and Birkholzer, J., 2017. Field characterization of elastic properties across a fault zone reactivated by fluid injection. Geophysical Research: Solid Earth, 122, pp.6583-6598. DOI: https://doi.org/10.1002/2017JB014384.

Jeanne, P., Rutqvist, J., Vasco, D., Garcia, J., Dobson, P.F., Walters, M., Hartline, C. and Borgia, A., 2014, February. Development of a 3D hydrogeological and geomechanical model of an Enhanced Geothermal System using microseismic and ground deformation data from a 1-year injection program. In Proceedings, Thirty-Ninth Workshop on Geothermal Reservoir Engineering Stanford University. Stanford, California. DOI: https://doi.org/10.1016/j.geothermics.2014.01.013

Jodocy, M. and Stober, I., 2009. Geothermische Nutzhorizonte im baden-württembergischen Teil des Oberrheingrabens. Der Geothermiekongress.

Juhlin, C. and Sandstedt, H., 1989. Storage of nuclear waste in very deep boreholes. Svensk Karnbranslehantering AB, Sweden, 68.

Juncu, D., Árnadóttir, T., Geirsson, H. and Gunnarsson, G., 2019. The effect of fluid compressibility and elastic rock properties on deformation of geothermal reservoirs. Geophysical Journal International, 217(1), pp.122-134. DOI: https://doi.org/10.1093/gji/ggz011

Jung, R., Hassanzadegan, A. and Tischner, T., 2019. Determination of hydraulic properties of a large self-propped hydraulic fracture in the geothermal research borehole Horstberg Z1 in the Northwest German Basin. Geofluids, 2019.

Jupe, A.J., Green, A.S.P. and Wallroth, T., 1992, July. Induced microseismicity and reservoir growth at the Fjällbacka hot dry rocks project, Sweden. In International journal of rock mechanics and mining sciences & geomechanics abstracts (Vol. 29, No. 4, pp. 343-354). Pergamon. DOI: https://doi.org/10.1016/0148-9062(92)90511-W

Kaieda, H., Ito, H., Kiho, K., Suzuki, K., Suenaga, H. and Shin, K., 2005. Review of the Ogachi HDR project in Japan. In Proceedings of the world geothermal congress, April 2005.

Kaieda, I, 2012. Ogachi EGS Reservoir analysis. In GRC Transactions, Vol. 36, 2012.

Kaieda, I, 2014. Hijiori HDR Reservoir Evaluation by Micro-Earthquake Observation. GRC Transactions, Vol. 38, 2014.

Kaieda, H., 2015. Multiple reservoir creation and evaluation in the Ogachi and Hijiori HDR projects, Japan. World Geothermal Congress, 19–25 April 2015, Melbourne, Australia. Conference proceedings.

Kaieda, H., 2020. Lessons learned from the Ogachi and Hijiori HDR/EGS Projects, Japan. Proceedings World Geothermal Congress 2020+1Reykjavik, Iceland, April -October 2021.

Kabus, F. and Jäntsch, E., 1995.The geothermal heating plant at Waren-Papenberg: experience and modernisation. In World Geothermal Congress 18–31 May 1995, Florence, Italy. Conference proceedings: 2227–2232.

Karytsas, C., Mendrinos, D. & Goldbrunner, J., 2009. Production monitoring at the Geinberg geothermal site. Energy Sources Part A 31(17): 1537–1552. DOI: https://doi.org/10.1080/15567030802093971

Kaspereit, D., Mann, M., Sanyal, S., Rickard, B., Osborn, W. and Hulen, J., 2016. Updated conceptual model and reserve estimate for the Salton Sea geothermal field, Imperial Valley, California. Geotherm. Res. Council Trans, 40, pp.57-66.

Kaven, J.O., Hickman, S.H. and Davatzes, N.C., 2011, January. Micro-seismicity, fault structure and hydraulic compartmentalization within the Coso gethermal field, California. In Proceedings, Thirty-Sixth Workshop on Geothermal Resrvoir Engineering.

Kaven, J.O., Hickman, S.H. and Davatzes, N.C., 2014, February. Micro-seismicity and seismic moment release within the Coso Geothermal Field, California. In Proceedings of the 39th Workshop on Geothermal Reservoir Engineering (p. 10).

Kaya, T., Kindap, A. and Energy, Z., 2009. Kizildere–new geothermal power plant in Turkey. In Presentation at International Geothermal Days Conference & Summer School. Slovakia.

Kehrer, P., Orzol, J., Jung, R., Jatho, R. and Junker, R., 2007. The GeneSys project a contribution of GEOZENTRUM Hannover to the development of Enhanced Geothermal Systems (EGS). Zeitschrift der deutschen Gesellschaft für Geowissenschaften, pp.119-132.

Keilegavlen, E., Duboeuf, L., Dichiarante, A.M., Halldórsdóttir, S., Stefansson, I., Naumann, M., Guðnason, E.Á., Ágústsson, K., Eggertsson, G.H., Oye, V. and Berre, I., 2021. Hydro-mechanical simulation and analysis of induced seismicity for a hydraulic stimulation test at the Reykjanes geothermal field, Iceland. Geothermics, 97, p.102223. DOI: https://doi.org/10.1016/j.geothermics.2021.102223

Kelkar, S., WoldeGabriel, G. and Rehfeldt, K., 2016. Lessons learned from the pioneering hot dry rock project at Fenton Hill, USA. Geothermics, 63, pp.5-14. DOI: https://doi.org/10.1016/j.geothermics.2015.08.008

Kepinska, B., 2004. The Podhale geothermal system and heating project–an overview. International Geothermal Days Poland 2004. Zakopane, September 13-17, pp.1-16.

Kępińska, B. and Jasnos, J., 2009. Geothermal District Heating System in Podhale and Zakopane, Poland–a New and Environmentally Benign Solution for A Tourist Centre.

Kepinska, B., 2003. The Podhale Geothermal System Andspace-heating Project Poland –Case Study. The United Nations University. Geothermal Training Program. 29 P:

Kepinska, B., 2015. Geothermal energy country update report from Poland, 2010–2014. World Geothermal Congress, 19–25 April 2015, Melbourne, Australia. Conference proceedings.

Kesonen, A., 2015. Mechanical properties of Finnish rocks based on uniaxial compressive strength and tensile strength tests (Master's thesis).

Khodayar, M., Björnsson, S., Guðnason, E.Á., Níelsson, S., Axelsson, G. and Hickson, C., 2018. Tectonic control of the Reykjanes geothermal field in the oblique rift of SW Iceland: from regional to reservoir scales. Open Journal of Geology, 8(3), pp.333-382. DOI: https://doi.org/10.4236/ojg.2018.83021

Kim, K.H., Ree, J.H., Kim, Y., Kim, S., Kang, S.Y. and Seo, W., 2018. Assessing whether the 2017 M w 5.4 Pohang earthquake in South Korea was an induced event. Science, 360(6392), pp.1007-1009. DOI: https://doi.org/10.1126/science.aat6081

Kim, K.I., Min, K.B., Kim, K.Y., Choi, J.W., Yoon, K.S., Yoon, W.S., Yoon, B., Lee, T.J. and Song, Y., 2018. Protocol for induced microseismicity in the first enhanced geothermal systems project in Pohang, Korea. Renewable and Sustainable Energy Reviews, 91, pp.1182-1191. DOI: https://doi.org/10.1016/j.rser.2018.04.062

Kiryukhin, A.V., Rutqvist, J., and Maguskin M.A., 2015. Modeling of the Vertical Deformations During Exploitation of the Mutnovsky Geothermal Field, Kamchatka. In Proceedings World Geothermal Congress 2015, 19-25- April 2015, pp.1-10.

Kiryukhin, A.V., Polyakov, A.Y., Usacheva, O.O., and Kiryukhin P.A., 2018. Thermal-permeability structure and recharge conditions of the Mutnovsky high-temperature geothermal field (Kamchatka, Russia). Journal of Volcanology and Geothermal Research, 356, pp.36-55. DOI: https://doi.org/10.1016/j.jvolgeores.2018.02.010.

Kiryukhin, A.V. and Usacheva, O.O., 2017. Inversion modeling of the natural state and production history of Mutnovsky geothermal field in 1986-2006. Journal of Mining Institute, 224, pp.163-169. DOI: 10.18454/PMI.2017.2.163

Kiryukhin, A.V. and Vereina, O.B., 2005, February. Modelling of the fault type geothermal reservoir (Dachny site, Mutnovsky geothermal field). In Proceed. 30-th Workshop on Geothermal Reservoir Engineering, Stanford University, Stanford, Cal., Jan.

Klima- und Energiefonds, 2021. Leitfaden Energieforschung Jahresprogramm 2020, Vienna.

Kröll, A., Wagner, L., Wessely, G. and Zych, D., 2006. Strukturkarte der Molassebasis, GBA, Wien.

Koech, V.K., 2014. Numerical geothermal reservoir modelling and infield reinjection Design, constrained by tracer test data: case study for the Olkaria geothermal field in Kenya (Doctoral dissertation). 107 P.

Koros, W., O'Sullivan, M., Pogacnik, J., O'Sullivan, J. and Ryan, G., 2014, November. Coupled one-dimensional subsidence modelling using elasticplastic rheology. In Proceedings 36th New Zealand Geothermal Workshop (Vol. 24, p. 26).

Koseki, T., 2008. Geothermal resources in Yamagata prefecture, northeast Japan. Proceedings of the 8th Asian Geothermal Symposium, December 9-10, 2008.

Krawczyk, C.M., Stiller, M., Bauer, K., Norden, B., Henninges, J., Ivanova, A., and Huenges, E., 2019. 3D seismic exploration across the deep geothermal research platform Groß Schönebeck- north of Berlin/Germany. Geothermal Energy, 7, p.15. DOI: https://doi.org/10.1186/s405170190131x.

Kreemer, C., Blewitt, G. and Klein, E.C., 2014. A geodetic plate motion and Global Strain Rate Model. Geochemistry, Geophysics, Geosystems, 15, pp.3849-3889. DOI: https://doi.org/10.1002/2014GC005407

Królikowski, M. and Hajto, M., 2023. General technical overview – Poddębice – Geothermal Project in Poland Suported by EEA Financial Mechanism (agh.edu.pl)

Kruszewski, M., Hofmann, H., Alvarez, F.G., Bianco, C., Haro, A.J., Garduño, V.H., Liotta, D., Trumpy, E., Brogi, A., Wheeler, W. and Bastesen, E., 2021. Integrated stress field estimation and implications for enhanced geothermal system development in Acoculco, Mexico. Geothermics, 89, p.101931. DOI: https://doi.org/10.1016/j.geothermics.2020.101931

Kruszewski, M., Montegrossi, G., Parisio, F. and Saenger, E.H., 2022. Borehole observation-based in situ stress state estimation of the Los Humeros geothermal field (Mexico). Geomechanics for Energy and the Environment, 32, p.100392. DOI: https://doi.org/10.1016/j.gete.2022.100392.

Küperkoch, L., Olbert, K. and Meier, T., 2018. Long-term monitoring of induced seismicity at the Insheim geothermal site, Germany. Bulletin of the Seismological Society of America, 108(6), pp.3668-3683. DOI: https://doi.org/10.1785/0120170365

Kushnir, A.R., Heap, M.J., Baud, P., Gilg, H.A., Reuschlé, T., Lerouge, C., Dezayes, C. and Duringer, P., 2018. Characterizing the physical properties of rocks from the Paleozoic to Permo-Triassic transition in the Upper Rhine Graben. Geothermal Energy, 6(1), pp.1-32. DOI: https://doi.org/10.1186/s40517-018-0103-6

Kwiatek, G., Saarno, T., Ader, T., Bluemle, F., Bohnhoff, M., Chendorain, M., Dresen, G., Heikkinen, P., Kukkonen, I., Leary, P., Leonhardt, M., Malin, P., Martínez-Garzón, P., Passmore, K., Passmore, P., Valenzuela, S., and Wollin, C., 2019. Controlling fluid-induced seismicity during a 6.1-km-deep geothermal stimulation in Finland. Science, 5, pp.1-11. DOI: https://doi.org/10.1126/sciadv.aav7224.

Kwiatek, G., Bohnhoff, M., Dresen, G., Schulze, A., Schulte, T., Zimmermann, G. and Huenges, E., 2008, January. Microseismic event analysis in conjunction with stimulation treatments at the geothermal research well Gt GrSk4/05 in Groß Schönebeck/Germany. In Proceedings Thirty-Third Workshop on Geothermal Reservoir Engineering (pp. 28-30). Stanford University Stanford, California.

Kwiatek, G., Bohnhoff, M., Dresen, G., Schulze, A., Schulte, T., Zimmermann, G. and Huenges, E., 2010. Microseismicity induced during fluid-injection: A case study from the geothermal site at Groß Schönebeck, North German Basin. Acta Geophysica, 58, pp.995-1020. DOI: https://doi.org/10.2478/s11600-010-0032-7

Kwiatek, G., Bulut, F., Bohnhoff, M. and Dresen, G., 2014. High-resolution analysis of seismicity induced at Berlín geothermal field, El Salvador. Geothermics, 52, pp.98-111. DOI: https://doi.org/10.1016/j.geothermics.2013.09.008

Ito, H, and Kaieda, H., 2002. Review of 15 years the hot dry rock project with emphasis on geological features. Proceedings 24 New Zealand Geothermal Workshop 2002.

Ito, H., 2003. Inferred role of natural fractures, veins, and breccias in development of the artificial geothermal reservoir at the Ogachi Hot Dry Rock site, Japan. Journal of Geophysical Research: Solid Earth, 108(B9). DOI: https://doi.org/10.1029/2001JB001671

Jarosiński, M., 2006. Recent tectonic stress field investigations in Poland: a state of the art. Geological Quarterly, 50(3), pp.303-321.

Juncu, D., Árnadóttir, T., Geirsson, H., Guðmundsson, G.B., Lund, B., Gunnarsson, G., Hooper, A., Hreinsdottir, S. and Michalczewska, K., 2020. Injection-induced surface deformation and seismicity at the Hellisheidi geothermal field, Iceland. Journal of Volcanology and Geothermal Research, 391, p.106337. DOI: https://doi.org/10.1016/j.jvolgeores.2018.03.019

Laboso, R.C., 2016. Fault-controlled damage and permeability at the Brady geothermal system, Nevada, USA. Temple University.

Lal, M., 1999, April. Shale stability: drilling fluid interaction and shale strength. In SPE Asia Pacific Oil and Gas Conference and Exhibition. OnePetro.

Lang, J., Li, S.,, and Zhang, J., 2011. Wellbore Stability Modeling and Real-Time Surveillance for Deepwater Drilling to Weak Bedding Planes and Depleted Reservoirs. In Proceedings SPE/IADC Drilling Conference and Exhibition, Amsterdam, 1-3 March, 2011: 19p.; SPE/IADC 139708.

Langenbruch, C. and Zoback, M.D., 2016. How will induced seismicity in Oklahoma respond to decreased saltwater injection rates?. Science advances, 2(11), p.e1601542.

Lang, E.P., 1999. Geothermal project Straubing" thermal and mineral water for bathing and heating": 10 years of experience from the feasibility study to the start of operations. Bulletin d'hydrogéologie, (17), pp.245-251.

Langella, G., Paoletti, V., DiPippo, R., Amoresano, A., Steinunnardóttir, K. and Milano, M., 2017. Krafla geothermal system, northeastern Iceland: Performance assessment of alternative plant configurations. Geothermics, 69, pp.74-92. DOI: https://doi.org/10.1016/j.geothermics.2017.04.001

Layman, E.B. and Soemarinda, S., 2003, January. The Patuha vapor-dominated resource West Java, Indonesia. In Proceedings of the 28th Workshop on Geothermal Reservoir Engineering, Stanford University (pp. 56-65).

Leclère, H. and Fabbri, O., 2013. A new three-dimensional method of fault reactivation analysis. Journal of Structural Geology, 48, pp.153-161. DOI: https://doi.org/10.1016/j.jsg.2012.11.004

Lee, S. and Bacon, L., 2000. Operational history of the Ohaaki geothermal field, New Zealand. In Proc. World Geothermal Congress.

Lermo, J., Antayhua, Y., Quintanar, L. and Lorenzo, C., 2008. Estudio sismológico del campo geotérmico de Los Humeros, Puebla, México. Parte I: Sismicidad, mecanismos de fuente y distribución de esfuerzos. Geotermia, Rev. Mex. Geoenerg., (1), pp.25-41.

Leitner, U., 2013. Geothermie –Energie der Zukunft?Chancen und Möglichkeiten in Österreich. Diplomarbeit, University Vienna.

Levi, N., Habermueller, M., Exner, U., Piani, E., Wiesmayr, G. and Decker, K., 2019. The stress field in the frontal part of the Eastern Alps (Austria) from borehole image log data. Tectonophysics, 769, p.228175. DOI: https://doi.org/10.1016/j.tecto.2019.228175

Levi, N., Habermueller, M., Exner, U., Wiesmayr, G. and Decker, K., 2021. Active out-of-sequence thrusting in the Molasse Basin constrained by a multidisciplinary approach (Eastern Alps, Austria). Tectonophysics, 812, p.228911. DOI: https://doi.org/10.1016/j.tecto.2021.228911

LIAG (Leibniz-Institut für Angewandte Geophysik), 2018. Untersuchung der Seismizität am Standort des Geothermieprojekts Poing unter Einbeziehung von Strukturgeologie, Geohydraulik, Hydrochemie, Geomechanik und Dublettenbetrieb. Zusammenfassung. LIAG (Hannover).

Livingstone, S., de Wijs, H., Janssen, A. and Taylor, S., 2013. Final Well Report, Well: CAL-GT-03. Daldrup & Söhne AG. 195 P.

Lüschen, E., Wolfgramm, M., Fritzer, T., Dussel, M., Thomas, R. and Schulz, R., 2014. 3D seismic survey explores geothermal targets for reservoir characterization at Unterhaching, Munich, Germany. Geothermics, 50, pp.167-179. DOI: https://doi.org/10.1016/j.geothermics.2013.09.007

Lutz, S.J., Hickman, S., Davatzes, N., Zemach, E., Drakos, P. and Robertson-Tait, A., 2010, February. Rock mechanical testing and petrologic analysis in support of well stimulation activities at the Desert Peak Geothermal Field, Nevada. In Proceedings 35th workshop on geothermal reservoir engineering.

Lutz, S.J., Zutshi, A., Robertson-Tait, A., Drakos, P. and Zemach, E., 2011. Lithologies, hydrothermal alteration, and rock mechanical properties in wells 15-12 and BCH-3, Bradys hot springs geothermal field, Nevada. GRC Transactions, 35, pp.469-476.

Lyons, D.J. and Van De Kamp, P.C., 1980. Subsurface geological and geophysical study of the Cerro Prieto geothermal field.

Magro, G., Gherardi, F. and Bayon, F.E.B., 2013. Noble and reactive gases of Palinpinon geothermal field (Philippines): Origin, reservoir processes and geodynamic implications. Chemical geology, 339, pp.4-15. DOI: https://doi.org/10.1016/j.chemgeo.2012.09.036

Mahler, A. and og Naturgas, D.O., 1995, May. Geothermal plant with absorption heat pump in Thisted. Integration with heat and power plant and use for heat storage and removal of CO2. In Proc. World Geothermal Congress (pp. 2155-2159).

Mahler, A., Røgen, B., Ditlefsen, C., Nielsen, L.H. and Vangkilde-Pedersen, T., 2013, June. Geothermal energy use, country update for Denmark. In Proceedings of the European Geothermal Congress (pp. 1-12).

Mahzari, P., Stanton-Yonge, A., Sanchez-Roa, C., Saldi, G., Mitchell, T., Oelkers, E.H., Hjorleifsdottir, V., Snaebjornsdottir, S.O., Ratouis, T., Striolo, A. and Jones, A.P., 2021. Characterizing fluid flow paths in the Hellisheidi geothermal field using detailed fault mapping and stress-dependent permeability. Geothermics, 94, p.102127. DOI: https://doi.org/10.1016/j.geothermics.2021.102127

Malate, R.C.M., Aqui, A.R. and Orizonte, R.G., 2008. Sustaining and optimizing steam production in the Southern Negros geothermal production field, Philippines. Proceedings of the 8th Asian Geothermal Symposium, December 9-10, 2008.

Manzella, A., Giamberini, S., Montegrossi, G., Scrocca, D., Chiarabba, C., Valkering, P., Delvaux, S., Harcouët-Menou, V., Branchu, F., Maury, J., Maurel, C., Bozkurt, C., Nádor, A., Guðjónsdóttir. S.R., Guðmundsdóttir, M., Ravier, G., Cuenot, N., Bonciani, D., Torsello, L., Luchini, M., Batini, F., and Dumas, P., 2021. Compilation of Recommendations on environmental regulations. 142p., Geoenvi.

Martínez-Garzón, P., Kwiatek, G., Sone, H., Bohnhoff, M., Dresen, G. and Hartline, C., 2014. Spatiotemporal changes, faulting regimes, and source parameters of induced seismicity: A case study from The Geysers geothermal field. Journal of Geophysical Research: Solid Earth, 119(11), pp.8378-8396. DOI: https://doi.org/10.1002/2014JB011385

Martínez-Garzón, P., Kwiatek, G., Bohnhoff, M., and Dresen, G., 2016. Impact of fluid injection on fracture reactivation at The Geysers geothermal field. Journal of Geophysical Research: Solid Earth, 121, pp.7432-7449. DOI: https://doi.org/10.1002/2016JB013137.

Maruyama, T., 1963. On the Force Equivalents of Dynamical Elastic Dislocations with Reference to the Earthquake Mechanism. Bulletin of the Earthquake Research Institute, University of Tokyo, 41, pp.467-486.

Matsunaga, I., Niitsuma, H., and Oikawa, Y., 2005. Review of the HDR Development at Hijiori Site, Japan. Proceedings World Geothermal Congress 2005 Antalya, Turkey, 24-29 April 2005.

Maver, K.G., Mamador, C., and Baillard, F., 2020. Accelerating E&P decisions by applying AI to unstructured data. First Break, 38, pp.67-70. DOI: https://doi.org/10.3997/1365-2397.fb2020091.

Mazzoldi, A., Rinaldi, A.P., Borgia, A. and Rutqvist, J., 2012. Induced seismicity within geological carbon sequestration projects: Maximum earthquake magnitude and leakage potential from undetected faults. International journal of greenhouse gas control, 10, pp.434-442.

MacLeod, N.S., Sherrod, D.R., Chitwood, L.A. and Jensen, R.A., 1995. Geologic Map of Newberry Volcano, Deschutes, Klamath, and Lake Counties. US Geological Survey, Oregon. Miscellaneous Investigations Series Map I-2455, scale, 1(62,500).

McDermott, C.I., Randriamanjatosoa, A.R., Tenzer, H. and Kolditz, O., 2006. Simulation of heat extraction from crystalline rocks: the influence of coupled processes on differential reservoir cooling. Geothermics, 35(3), pp.321-344. DOI: https://doi.org/10.1016/j.geothermics.2006.05.002

Mbithi, U.K., 2016. Interpretation of feed zones to map sub-surface permeability structures and natural state simulation: A case study of Olkaria Domes geothermal system in Kenya (Doctoral dissertation).

McGarr, A., 2014. Maximum magnitude earthquakes induced by fluid injection. Journal of Geophysical Research: solid earth, 119, pp.1008-1019. DOI: https://doi.org/10.1002/2013JB010597.

McGuire, J.J., Lohman, R.B., Catchings, R.D., Rymer, M.J. and Goldman, M.R., 2015. Relationships among seismic velocity, metamorphism, and seismic and aseismic fault slip in the Salton Sea Geothermal Field region. Journal of Geophysical Research: Solid Earth, 120(4), pp.2600-2615. DOI: https://doi.org/10.1002/2014JB011579

McNally, G. H. N., 1987. Estimation of coal measures rock strength using sonic and neutron logs. Geoexploration, 24, 381–395.

McNamara, D.D., Faulkner, D. and McCarney, E., 2014, February. Rock properties of greywacke basement hosting geothermal reservoirs, New Zealand: preliminary results. In 39th Workshop on Geothermal Reservoir Engineering. Stanford University.

McNamara, D.D., Massiot, C. and Milicich, S.M., 2017. Characterizing the subsurface structure and stress of New Zealand's geothermal fields using borehole images. Energy Procedia, 125, pp.273-282. DOI: https://doi.org/10.1016/j.egypro.2017.08.176

Megies, T. and Wassermann, J., 2014. Microseismicity observed at a non-pressure-stimulated geothermal power plant. Geothermics, 52, pp.36-49. DOI: https://doi.org/10.1016/j.geothermics.2014.01.002

Mehrabifard, A., 2018. Reinjection experiment at the Patuha geothermal field, West Java, Indonesia: a field experience and numerical analysis. Dissertation of Master's Degree in Engineering Seoul, South Korea The Graduate School Seoul National University.

Mehrabifard, A., Amini, A., Gorjian, M., Rogers, S., Eberhardt, E., and Damjanac, B., 2021. The mechanistical study of the effects of rock stiffness and wellbore orientation with respect to SHmax on induced seismicity: a numerical study. In Proceedings GeoConvention 2021, 13-15 September 2021, p.6.

Meixner, J., Schill, E., Grimmer, J.C., Gaucher, E., Kohl, T. and Klingler, P., 2016. Structural control of geothermal reservoirs in extensional tectonic settings: an example from the Upper Rhine Graben. Journal of Structural Geology, 82, pp.1-15. DOI: https://doi.org/10.1016/j.jsg.2015.11.003

Mendez, N.R.R., 1996. Borehole geology and hydrothermal alteration of well sv-14, Svartsengi, sw-Iceland. Geothermal training programme Orkustofnun, Grensasvegur 9, IS-108 Reykjavik, Iceland.

Meyer, Z. and Kozlowski, J., 1995. Pyrzyce - First Geothermal Heating System in Poland. Maczna 4; 70-780 Szczecin. Poland.

Miecznik, M., Sowiżdżał, A., Tomaszewska, B. and Pająk, L., 2015. Modelling geothermal conditions in part of the Szczecin Trough–the Chociwel area. Geologos, 21(3), pp.187-196. DOI: https://doi.org/10.1515/logos-2015-0013

Mielke, P., Weinert, S., Bignall, G., and Sass, I., 2016. Thermo-physical rock properties of greywacke basement rock and intrusive lavas from the Taupo Volcanic Zone, New Zealand. J Mielke, P., Weinert, S., Bignall, G. and Sass, I., 2016. Thermo-physical rock properties of greywacke basement rock and intrusive lavas from the Taupo Volcanic Zone, New Zealand. Journal of Volcanology and Geothermal Research, 324, pp.179-189. DOI: http://dx.doi.org/10.1016/j.jvolgeores.2016.06.002.

Mijnlieff, H.F., 2020. Introduction to the geothermal play and reservoir geology of the Netherlands. Netherlands Journal of Geosciences, 99, p.e2. DOI: https://doi.org/10.1017/njg.2020.2

Milicich, S.D., Wilson, C.J.N., Bignall, G., Pezaro, B., Charlier, B.L.A., Wooden, J.L. and Ireland, T.R., 2011, November. Buried rhyolite in the Kawerau Geothermal Field, Taupo Volcanic Zone, New Zealand: sources of a rejuvenated geothermal system. In Proceedings, New Zealand Geothermal Workshop (pp. 21-23).

Mills, T., and Humphreys, B., 2013. Habanero Pilot Project – Australia's First EGS Power Plant. In Proceedings 35th New Zealand Geothermal Workshop, 17-20 November 2013, Rotorua, p.4.

Moeck I.S., 2014. Catalog of geothermal play types based on geologic controls. Renewable and Sustainable Energy Reviews, 37, pp.867-882. DOI: http://dx.doi.org/10.1016/j.rser.2014.05.032.

Moeck, I., Kwiatek, G., and Zimmermann, G., 2009. Slip tendency analysis, fault reactivation potential and induced seismicity in a deep geothermal reservoir. Journal of Structural Geology, 31, pp.1174-1182. DOI: https://doi.org/10.1016/j.jsg.2009.06.012.

Mohamed, F.R., Rasmussen, A., Wendt, A.S., and Murineddu, A., 2008. High resolution 3D Mechanical Earth Model using seismic neural netmodeling: Integrating geological, petrophysical and geophysical data. In Proceedings 0th EAGE Conference, Exhibition, 9-12 June 2008, Rome, p.5.

Monsees, A.C., 2021. Diagenetic controls on fluid flow and mechanical properties in Rotliegend reservoir sandstones (p. 188). KIT Scientific Publishing.

Monterrosa, M.E. and SA, G.S., 2002, January. Reservoir modelling for the Berlin geothermal field El Salvador. In Proceedings.

Moon, H., Clearwater, J., Franz, P., Wallis, I. and Azwar, L., 2014. Sensitivity analysis, parameter estimation and uncertainty propagation in a numerical model of the Ngatamariki geothermal field, New Zealand. In Proc. 39th Workshop on Geothermal Reservoir Engineering.

Moos, D., Zoback, M.D. and Bailey, L., 2001. Feasibility study of the stability of openhole multilaterals, Cook Inlet, Alaska. SPE Drilling & Completion, 16(03), pp.140-145.

Morawietz, S., Heidbach, O., Reiter, K., Ziegler, M., Rajabi, M., Zimmermann, G., Müller, B., and Tingay, M., 2020. An openaccess stress magnitude database for Germany and adjacent regions. Geothermal Energy-, 8, pp.1-39. DOI: https://doi.org/10.1186/s40517020001785.

Mouchot, J., Genter, A., Cuenot, N., Scheiber, J., Seibel, O., Bosia, C., Ravier, G., Mouchot, J., Genter, A. and Cuenot, N., 2018, February. First year of operation from EGS geothermal plants in Alsace, France: Scaling issues. In Proceedings of the 43rd Workshop on Geothermal Reservoir Engineering, Stanford, CA, USA (pp. 12-14).

Mukuhira, Y., Dinske, C., Asanuma, H., Ito, T. and Häring, M.O., 2017. Pore pressure behavior at the shut-in phase and causality of large induced seismicity at Basel, Switzerland. Journal of Geophysical Research: Solid Earth, 122(1), pp.411-435. DOI: 10.1002/2016JB013338

NZGA (New Zealand Geothermal Association), Accessed in June 2023: New Zealand Geothermal Fields (nzgeothermal.org.nz)

NLOG (Dutch Oil and Gas Portal), Dutch Ministry of Infrastructure and the Environment, TNO-AGE, NLOG.NL and the TNO Advisory Group for Economic Affairs, Accessed in May 2023: https://www.nlog.nl/en/boreholes.

Norbeck, J.H., McClure, M.W. and Horne, R.N., 2018. Field observations at the Fenton Hill enhanced geothermal system test site support mixed-mechanism stimulation. Geothermics, 74, pp.135-149. DOI: https://doi.org/10.1016/j.geothermics.2018.03.003

Nouraliee, J., 2000. Borehole geology and hydrothermal alteration of well NJ-20, Nesjavellir high--temperature area, SW Iceland. United Nations University Geothermal Training Programme, Report, 15, pp.303-330.

O'Brien, J.M., 2010. Hydrogeochemical Characteristics of the Ngatamariki Geothermal Field and a Comparison with the Orakei Korako Thermal Area, Taupo Volcanic Zone, New Zealand. DOI: http://dx.doi.org/10.26021/6642

Olivar, R.E.R. and Apuada, N.A., 2005. Hydro-Geophysical Model of the Southern Negros Geothermal Project, Central Philippines Based on Magnetotellurics Resistivity. Ankarra: Proceedings World Geothermal Congress.

Omenda, P.A., 1998. The geology and structural controls of the Olkaria geothermal system, Kenya. Geothermics, 27(1), pp.55-74. DOI: https://doi.org/10.1016/S0375-6505(97)00028-X

Orlic, B., 2008. Some Geomechanical Aspects of Geological CO2 Sequestration. In Proceedings 12th International Conference of International Association for Computer Methods and Advanced in Geomechanics (IACMAG), 1-6 October 2008, Goa, p.9.

Orlic, B., ter Heege, J., and Wassing, B., 2011. Assessing the integrity of fault- and top seals at CO2 storage sites. Energy Procedia, 4, pp.4798-4805. DOI: https://doi.org/10.1016/j.egypro.2011.02.445.

Orzol, J., Jung, R., Jatho, R., Tischner, T. and Kehrer, P., 2005, April. The GeneSys-Project: Extraction of geothermal heat from tight sediments. In Proceedings World Geothermal Congress (pp. 24-29).

O'Sullivan, M.J., Renaud, T., Gravatt, M.J., Riffault, J., Popineau, J., O'Sullivan, J.P., Ruiz, N.C. and Sophy, M., 2021, November. An updated numerical model of the ohaaki geothermal field. In Proceedings 43rd New Zealand Geothermal Workshop (Vol. 23, p. 25).

Otieno, S.O., 2017. Interpretation Of Drawdown Test Data from Olkaria Domes Geothermal Field – A Case Study of Ow-907b, Ow-912b And Ow-917. United Nations University. Geothermal Training Program.

Pagani, M., Garcia-Pelaez, J., Gee, R., Johnson, K., Poggi, V., Silva, V., Simionato, M., Styron, R., Viganò, D., Danciu, L. and Monelli, D., 2020. The 2018 version of the global earthquake model: Hazard component. Earthquake Spectra, 36(1_suppl), pp.226-251.

Palmström, A., 2011. Uniaxial compressive strength (sc) and deformation modulus of rocks Table. Average values from tests of rock samples (rockmass.net)

Parker, R., 1989. Hot dry rock geothermal energy. Phase 2B final report of the Camborne School of Mines project, 1392.

Parker, R., 1999. The rosemanowes HDR project 1983–1991. Geothermics, 28(4-5), pp.603-615. DOI: https://doi.org/10.1016/S0375-6505(99)00031-0

Parks, M., Sigmundsson, F., Sigurðsson, Ó., Hooper, A., Hreinsdóttir, S., Ófeigsson, B. and Michalczewska, K., 2020. Deformation due to geothermal exploitation at Reykjanes, Iceland. Journal of Volcanology and Geothermal Research, 391, p.106438. DOI: https://doi.org/10.1016/j.jvolgeores.2018.08.016

Pastoriza, L.R., 2017. The geological characterization and permeability evaluation of fractures in the southern negros geothermal field, negros island, Philippines, Durham theses, Durham University. 589 P.

Pawey, S., Schultz, R., Playter, T., Corlett, H., Shipman, T., Lyster, S., and Hauck, T., 2018. The geological susceptibility of induced earthquakes in the Duvernay play. Geophysical Research Letters, 45, 1786-1793. DOI: https://doi.org/10.1002/2017GL076100.

Pearson, K., 1895. VII. Note on regression and inheritance in the case of two parents. proceedings of the royal society of London, 58 (347-352), 240-242.

PEPS (Petroleum Exploration and Production System South Australia), Accessed in May 2023: https://peps.sa.gov.au/wells/2277/list.

Pernecker, G., and Uhlig, S., 2002. Low-enthalpy power generation with ORC turbogenerator; The Altheim project, upper Austria. GHC Bulletin, 23, pp.26-30.

Peter-Borie, M., Loschetter, A., Merciu, I.A., Kampfer, G. and Sigurdsson, O., 2018. Borehole damaging under thermo-mechanical loading in the RN-15/IDDP-2 deep well: towards validation of numerical modeling using logging images. Geothermal Energy, 6(1), pp.1-33. DOI: https://doi.org/10.1186/s40517-018-0102-7

Peterschmitt, A., Hehn, R., Bosia, C., Cuenot, N., Sam, A., Genter, A., 2018. A comprehensive report on risk assessment and workflow for soft stimulations, DESTRESS Technical Report.

Pham, M., Klein, C., Ponte, C., Cabeças, R., Martins, R., and Rangel, G., 2010. Production/Injection Optimization Using Numerical Modeling at Ribeira Grande, São Miguel, Azores, Portugal. In Proceedings World Geothermal Congress 2010, 25-29 April 2010, Bali, P.6.

Phillips, W.S., House, L.S. and Fehler, M.C., 1997. Detailed joint structure in a geothermal reservoir from studies of induced microearthquake clusters. Journal of Geophysical Research: Solid Earth, 102(B6), pp.11745-11763. DOI: https://doi.org/10.1029/97JB00762

PHIVOLCS (Philippine Institute of Volcanology and Seismology), Accessed in May 2023: https://www.phivolcs.dost.gov.ph/.

Pilger, M., Eulenfeld, T., Brüstle, A., Wegler, U., Plenefisch, T. & Schmidt, B., 2017. Mikroseismische Aktivität geothermischer Systeme 2 – Vom Einzelsystem zur grossräumigen Nutzung. Einzelprojekt 1 – Seismische Monitoringskonzepte und bruchmechanische Bewertungen für komplexe Geothermiefelder am Beispiel Südpfalz. Report No. 0325662A. Bundesanstalt für Geowissenschaften und Rohstoffe (Hannover).

Porkhial, S., Abdollahzadeh Bina, F., Radmehr, B. and Johari Sefid, P., 2015. Interpretation of the injection and heat up tests at Sabalan geothermal field, Iran. In Proceedings world geothermal congress, Melbourne, Australia, 19-25 April.

Porter, R.T.J., Striolo, A., Mahgerefteh, H., and Walker, J.F., 2019. Addressing the risks of induced seismicity in subsurface energy operations. Wiley Interdisciplinary Reviews: Energy and Environment, 8, P.e324. DOI: https://doi.org/10.1002/wene.324.

Potten, M., 2020. Geomechanical characterization of sedimentary and crystalline geothermal Reservoirs. Thesis, Techniche Universität München.

Poulsen, S.E., Balling, N., Bording, T.S., Mathiesen, A. and Nielsen, S.B., 2017. Inverse geothermal modelling applied to Danish sedimentary basins. Geophysical Journal International, 211(1), pp.188-206.

Poulsen, S.E., Bjørn, H., Mathiesen, A., Nielsen, L.H., Vosgerau, H., Vangkilde-Pedersen, T., Ditlefsen, C. and Røgen, B., 2019, June. Geothermal Energy Use, Country Update for Denmark. In Proceedings of the Proceedings European Geothermal Congress, Den Haag, The Netherlands (Vol. 14).

Prol-Ledesma, R.M., Arango-Galvan, C. and Torres-Vera, M.A., 2016. Rigorous analysis of available data from cerro prieto and las tres virgenes geothermal fields with calculations for expanded electricity generation. Natural Resources Research, 25, pp.445-458. DOI: https://doi.org/10.1007/s11053-016-9295-2

Prol-Ledesma, R.M. and Morán-Zenteno, D.J., 2019. Heat flow and geothermal provinces in Mexico. Geothermics, 78, pp.183-200. DOI: https://doi.org/10.1016/j.geothermics.2018.12.009

Python Software Foundation. Python Language Reference, version 3.9. Available at http://www.python.org

Rae, A.J., Cooke, D.R., Phillips, D. and Zaide-Delfin, M., 2004. The nature of magmatism at Palinpinon geothermal field, Negros Island, Philippines: implications for geothermal activity and regional tectonics. Journal of Volcanology and Geothermal Research, 129(4), pp.321-342. DOI: https://doi.org/10.1016/S0377-0273(03)00280-4

Rae, A.J., Rosenberg, M.D., Bignall, G., Kilgour, G.N. and Milicich, S.D., 2007, November. Geological results of production well drilling in the western steamfield, Ohaaki geothermal system: 2005–2007. In Proceedings of the 29th New Zealand Geothermal Workshop, Auckland, New Zealand (pp. 19-21).

Raharjo, I.B., Allis, R.G. and Chapman, D.S., 2016. Volcano-hosted vapor-dominated geothermal systems in permeability space. Geothermics, 62, pp.22-32. DOI: https://doi.org/10.1016/j.geothermics.2016.02.005

Rahimi, H., Hamzehloo, H. and Kamalian, N., 2009. Estimation of coda and shear wave attenuation in the volcanic area in SE Sabalan Mountain, NW Iran. Acta Geophysica, 58(2), p.244. DOI: https://doi.org/10.2478/s11600-009-0023-8

Raleigh, C.B., Healy, J.H., and Bredehoef, J.D., 1976. An Experiment in Earthquake Control at Rangely, Colorado. Science, 191, pp.1230-1237. DOI: https://doi.org/10.1126/science.191.4233.1230

Rangel, G., Guimarães, T., Hackett, L., Henneberger, R., Pham, M., RENOVÁVEIS, E. and SA, P.D., 2017. Well field optimization and expansion guided by tracer testing and numerical reservoir modelling, Ribeira Grande geothermal field, Açores, Portugal. Geothermal Resources Council Transactions, 41(9), pp.93-96.

Rathje, E.M., Clayton, P., Cox, B., Grigoratos, I., Khosravikia, F., Meibai, L., Yust, M., and Savvaidis, A., 2020. Seismic Hazard and Risk Assessment for Induced Seismicity. Presentation.

Regenauer Lieb, K., Bunger, A., Hui, T.C., Dyskin, A., Fusseis, F., Gaede, O., Jeffrey, R., Karrech, A., Kohl, T., Jie, L., Lyakhovsky, V., Pasternak, E., Pognorney, R., Poulet, T., Rahman, S., Schrank, C., Trefry, M., Veveakis, M., Bisheng, W., Yuen, D., Wellmann, F., and Xi, Z., 2015. Deep Geothermal: The 'Moon Landing' Mission in the Unconventional Energy and Minerals Space. Report Idaho National Laboratory: 22p.

Reinecker, J., Gutmanis, J., Foxford, A., Cotton, L., Dalby, C. and Law, R., 2021. Geothermal exploration and reservoir modelling of the United Downs deep geothermal project, Cornwall (UK). Geothermics, 97, p.102226. DOI: https://doi.org/10.1016/j.geothermics.2021.102226

Reith, D., 2018. Dynamic simulation of a geothermal reservoir: case study of the Dinantian carbonates in the Californië geothermal wells, Limburg, NL. URL: http://resolver.tudelft.nl/uuid:e38ecf05-dfc1-4bcc-b995-875e178609dc

Renderos, R.E., 2002. Chemical characterization of the thermal fluid discharge from well production tests in the Berlín geothermal field, El Salvador. United Nations University.

Richards, H.G., Parker, R.H., Green, A.S.P., Jones, R.H., Nicholls, J.D.M., Nicol, D.A.C., Randall, M.M., Richards, S., Stewart, R.C. & Willis-Richards, J., 1994. The performance and characteristics of the experimental hot dry rock geothermal reservoir at Rosemanowes, Cornwall. Geothermics 23(2): 73–109. DOI: https://doi.org/10.1016/0375-6505(94)90032-9

Richter, B., 2010, April. Geothermal Energy Plant Unterhaching, Germany. In Proceedings World Geothermal Congress.

Rinaldi, A.P. and Rutqvist, J., 2019. Joint opening or hydroshearing? Analyzing a fracture zone stimulation at Fenton Hill. Geothermics, 77, pp.83-98. DOI: https://doi.org/10.1016/j.geothermics.2018.08.006

Rioseco, E.M., Löhken, J., Schellschmidt, R. and Tischner, T., 2013. 3-D geomechanical modeling of the stress field in the North German basin: case study GeneSys-borehole GT1 in Hanover Groß-Buchholz. 38th Workshop on Geothermal Reservoir Engineering, 11–13 February 2013, Stanford, California. Conference proceedings.

Rissmann, C., Christenson, B., Werner, C., Leybourne, M., Cole, J. and Gravley, D., 2012. Surface heat flow and CO2 emissions within the Ohaaki hydrothermal field, Taupo Volcanic Zone, New Zealand. Applied geochemistry, 27(1), pp.223-239. DOI: https://doi.org/10.1016/j.apgeochem.2011.10.006

Rivas, J., 2003. Seismic monitoring of a well stimulation operation at the Berlin geothermal field. El Salvador. GRC Transactions, 27, pp.365-368.

Rivas, J.A., Castellón, J.A. and Maravilla, J.N., 2005, April. Seven years of reservoir seismic monitoring at Berlın Geothermal Field, Usulután, El Salvador. In Proceedings of the World Geothermal Congress (pp. 24-29).

Robertson-Tait, A. and Morris, C., 2003. Progress and Future Plans at the Desert Peak East EGS Project. Geothermal Resources Council Transactions, Vol. 27.

Rojas, A.E.O., Dussel, M. and Moeck, I., 2017. Borehole geophysical characterisation of a major fault zone in the geothermal Unterhaching Gt 2 well, South German Molasse Basin. Zeitschrift der Deutschen Gesellschaft für Geowissenschaften, 169(3), pp.445-463.

Røgen, B., Ditlefsen, C., Vangkilde-Pedersen, T., Nielsen, L. H., & Mahler, A. (2015). Geothermal Energy Use, 2015 Country Update for Denmark. In Abstract volume (CD-Rom only) (pp. 1079). World Geothermal Congress.

Rose, P., Hickman, S., McCulloch, J., Davatzes, N., Moore, J.M., Kovac, K., Adams, M., Mella, M., Wannamaker, P., Julian, B., Foulger, G., Swenson, D., Gosavi, S., Bhat, A., Richards-Dinger, K., Monastero, F., Weidler, R., Baisch, S., Ghassemi, A., Kohl, T., and Megel, T., 2006. FinalReport for the Portion of the Project Focused on the East Compartment of the Coso Geothermal Field, Volume 1, Creation of an Enhanced Geothermal System through Hydraulic and Thermal Stimulation, Project No. DE-FC07-01ID14186. 484 P.

Rosenberg, M., Wallin, E., Bannister, S., Bourguignon, S., Sherburn, S., Jolly, G., Mroczek, E., Milicich, S., Graham, D., Bromley, C. and Reeves, R., 2010. Tauhara stage II geothermal project: geoscience report. GNS Science Consultancy Report, 138, p.2010.

Rutqvist, J., and Oldenburg, C., 2007. Analysis of cause and mechanism for injection-induced seismicity at the Geysers Geothermal Field, California. Lawrence Berkeley National Laboratory; URL: https://escholarship.org/uc/item/5264q9cd.

Rutqvist, J., Rinaldi, A.P., Cappa, F. and Moridis, G.J., 2013. Modeling of fault reactivation and induced seismicity during hydraulic fracturing of shale-gas reservoirs. Journal of Petroleum Science and Engineering, 107, pp.31-44. DOI: https://doi.org/10.1016/j.petrol.2013.04.023

Rutqvist, J., Jeanne, P., Dobson, P.F., Garcia, J., Hartline, C., Hutchings, L., Singh, A., Vasco, D.W. and Walters, M., 2016. The Northwest Geysers EGS demonstration project, California–part 2: modeling and interpretation. Geothermics, 63, pp.120-138. DOI: https://doi.org/10.1016/j.geothermics.2015.08.002

Saadati, M., Forquin, P., Weddfelt, K., Larsson, P.L. and Hild, F., 2018. On the mechanical behavior of granite material with particular emphasis on the influence from pre-existing cracks and defects. Journal of Testing and Evaluation, 46(1), pp.33-45. DOI: 10.1520/JTE20160072

Sabatakakis, N., Koukis, G., Tsiambaos, G. and Papanakli, S., 2008. Index properties and strength variation controlled by microstructure for sedimentary rocks. Engineering geology, 97(1-2), pp.80-90. DOI: https://doi.org/10.1016/j.enggeo.2007.12.004

Sachpazis, C.I., 1990. Correlating Schmidt hardness with compressive strength and Young's modulus of carbonate rocks. Bulletin of Engineering Geology and the Environment, 42(1), pp.75-83.

Saiang, C. and Miskovsky, K., 2011, October. Effect of heat on the mechanical properties of selected rock types–a laboratory study. In 12th ISRM congress. OnePetro.

Sanjuan, B., Negrel, G., Le Lous, M., Poulmarch, E., Gal, F. and Damy, P.C., 2020, April. Main geochemical characteristics of the deep geothermal brine at Vendenheim (Alsace, France) with constraints on temperature and fluid circulation. In World Geothermal Congress 2020.

Sapińska-Śliwa, A., Wojnarowski, P. and Gonet, A., 2010. Analysis of Uniejów geothermal water reservoirs modeling in view of various aspects of geothermal water and heat management. In Proceedings of World Geothermal Congress (pp. 25-29).

Sasaki, S. and Kaieda, H., 2002. Determination of stress state from focal mechanisms of microseismic events induced during hydraulic injection at the Hijiori hot dry rock site. The Mechanism of Induced Seismicity, pp.489-516.

Sasaki, K., Tezuka, S., Takizawa, K., Kaneko, T., Asano, K., Asai, H., Nakanishi, S., and Akasaka, C., 2018. Mineralogical and Hydraulic Characteristics of the Wasabizawa Geothermal Field, Akita Prefecture, Japan. PROCEEDINGS, 43rd Workshop on Geothermal Reservoir Engineering Stanford University, Stanford, California, February12-14, 2018SGP-TR-213.

Satman, A., Sarak, H., Onur, M. and Korkmaz, E.D., 2005, April. Modeling of production/reinjection behavior of the Kizildere geothermal field by a two-layer geothermal reservoir Lumped-Parameter Model. In World Geothermal Congress.

Schill, E., Guglielmetti, L., Klingler, P., Abdelfettah, Y. and Alcolea, A., 2012, January. The role of structural changes for geothermal projects in the area of Basel. In Proceedings of the Thirty-Seventh Workshop on Geothermal Reservoir Engineering. Stanford, California: Stanford University.

Schmid, CH. J., Schon, J., Savatis, A. And Gratze¡, R., 2012. Welltest Honselersd¡jk GT1, Documentation of well test analysis, technical report. Green Well Westland BV. 22 P.

Schmittbuhl, J., Lambotte, S., Lengliné, O., Grunberg, M., Jund, H., Vergne, J., Cornet, F., Doubre, C. and Masson, F., 2021. Induced and triggered seismicity below the city of Strasbourg, France from November 2019 to January 2021. Comptes Rendus. Géoscience, 353(S1), pp.561-584. DOI: https://doi.org/10.5802/crgeos.71

Schneider, M. and Lutz T., (2012). Wissenschaftliche und technische Grundlagen zur strukturgeologischen und hydrogeologischen Charakterisierung tiefer geothermisch genutzter Grundwasserleiter am Beispiel des süddeutschen Molassebeckens. Report oft he Freie Universität Berlin.

Scholz, C.H., 2019. The mechanics of earthquakes and faulting.- 3rd ed., 515p.; New York (Cambridge Univ. Press). DOI: https://doi.org/10.1017/9781316681473.

Scott, S.W., Covell, C., Júlíusson, E., Valfells, Á., Newson, J., Hrafnkelsson, B., Pálsson, H. and Gudjónsdóttir, M., 2019. A probabilistic geologic model of the Krafla geothermal system constrained by gravimetric data. Geothermal Energy, 7(1), pp.1-30. DOI: https://doi.org/10.1186/s40517-019-0143-6

Schulz, I., Steiner, U. and Schubert, A., 2017. Erfolgsfaktoren bei Projekten der Tiefengeothermie–Erfahrungen aus dem Bayerischen Molassebecken. Erdöl Erdgas Kohle, 133(2), p.2017.

Segall, P., and Fitzgerald, S.D., 1998. A note on induced stress changes in hydrocarbon and geothermal reservoirs. Tectonophysics, 289, pp.117-128. DOI: https://doi.org/10.1016/S0040-1951(97)00311-9

Seibt, P. and Kellner, T., 2003. Practical experience in the reinjection of cooled thermal waters back into sandstone reservoirs. Geothermics, 32(4-6), pp.733-741. DOI: https://doi.org/10.1016/S0375-6505(03)00071-3

Seibt, P., Kabus, F., Hoth, P., 2005. The Neustadt-Glewe geothermal power plant – practical experience in the reinjection of cooled thermal waters into sandstone aquifers. In: Proceedings World Geothermal Conference, Antalya, Turkey, April 24–29, p. 4.

Seibt, P., and Wolfgramm, M., 2008. Practical Experience in the Reinjection of Thermal Waters into Sandstone. Proc. Workshop for Decision Makers on Direct Heating Use of Geothermal Resources in Asia, 11-18 May 2008, Tianjin: 18p.

Seithel, R., Steiner, U., Müller, B., Hecht, C., and Kohl, T., 2015. Local stress anomaly in the Bavarian Molasse Basin. Geothermal Energy, 3, pp.1-22. DOI: https://doi.org/10.1186/s40517-014-0023-z.

Seithel, R., Peters, M., Lesueur, M., and Kohl, T., 2017. Stress heterogeneity above and within a deep geothermal reservoir: From borehole observations to geomechanical modelling. In EGU General Assembly Conference Abstracts (p. 7159).

Seithel, R., Gaucher, E., Mueller, B., Steiner, U. and Kohl, T., 2019. Probability of fault reactivation in the Bavarian Molasse Basin. Geothermics, 82, pp.81-90. DOI: https://doi.org/10.1016/j.geothermics.2019.06.004

Selyangin, O.B., 2019, November. Structure, substance and near-surface magmatic chambers of Mutnovsky and Gorely volcanoes (Mutnovsky geothermal region, Kamchatka). II. Mutnovsky volcano. In IOP Conference Series: Earth and Environmental Science (Vol. 367, No. 1, p. 012020). IOP Publishing. **DOI:** 10.1088/1755-1315/367/1/012020

Serpen, U. and Aksoy, N., 2005. Reinjection problems in overpressured geothermal reservoirs. In Proceedings.

Sewell, S.M., Cumming, W., Bardsley, C.J., Winick, J., Quinao, J., Wallis, I.C., Sherburn, S. and Bourguignon, S., 2015. Interpretation of microseismicity at the Rotokawa Geothermal Field, 2008 to 2012. Interpretation, 19, p.25.

Seyedrahimi-Niaraq, M., Doulati Ardejani, F., Noorollahi, Y. and Porkhial, S., 2017. Development of an updated geothermal reservoir conceptual model for NW Sabalan geothermal field, Iran. Geothermal Energy, 5, pp.1-22. DOI: https://doi.org/10.1186/s40517-017-0073-0

Shah, A.K. and Keller, G.R., 2017. Geologic influence on induced seismicity: Constraints from potential field data in Oklahoma. Geophysical Research Letters, 44(1), pp.152-161. DOI: https://doi.org/10.1002/2016GL071808

Sherburn, S., Bromley, C., Bannister, S., Sewell, S. and Bourguignon, S., 2015, April. New Zealand geothermal induced seismicity: an overview. In Proceedings of the World Geothermal Congress.

Siler, D.L., Faulds, J.E., and Hinz, N.H., 2015. Earthquake-Related Stress Concentrations and Permeability Generation in Geothermal Systems. GRC Transactions, 39, pp.437-444.

Simiyu, S.M., 2016. Application of micro-seismic methods to geothermal exploration: Examples from the Kenya Rift. Proceedings of the Short Course VIII on Exploration for Geothermal Resources, Lake Naivasha, Kenya, 31.

Simiyu, S.M. and Keller, G.R., 2000. Seismic monitoring of the Olkaria Geothermal area, Kenya Rift valley. Journal of Volcanology and Geothermal Research, 95(1-4), pp.197-208. DOI: https://doi.org/10.1016/S0377-0273(99)00124-9

Şimşek, Ş., Yıldırım, N. and Gülgör, A., 2005. Developmental and environmental effects of the Kızıldere geothermal power project, Turkey. Geothermics, 34(2), pp.234-251. DOI: https://doi.org/10.1016/j.geothermics.2004.12.005

Siratovich, P.A., Heap, M.J., Villenueve, M.C., Cole, J.W. and Reuschlé, T., 2014. Physical property relationships of the Rotokawa Andesite, a significant geothermal reservoir rock in the Taupo Volcanic Zone, New Zealand. Geothermal Energy, 2(1), pp.1-31. DOI: https://doi.org/10.1186/s40517-014-0010-4

Snæbjörnsdóttir, S.Ó., Tómasdóttir, S., Sigfússon, B., Aradóttir, E.S., Gunnarsson, G., Niemi, A., Basirat, F., Dessirier, B., Gislason, S.R., Oelkers, E.H. and Franzson, H., 2018. The geology and hydrology of the CarbFix2 site, SW-Iceland. Energy Procedia, 146, pp.146-157.

Stadt Unterschleissheim, Accessed in June 2023: GTU - Geothermie Unterschleißheim AG - Stadt Unterschleissheim

Strecker, M. and Bosworth, W., 1991. Quaternary stress-field change in the Gregory Rift, Kenya. Eos, 72(3), pp.17-21.

Stück, H., Siegesmund, S. and Rüdrich, J., 2011. Weathering behaviour and construction suitability of dimension stones from the Drei Gleichen area (Thuringia, Germany). Environmental Earth Sciences, 63, pp.1763-1786. DOI: https://doi.org/10.1007/s12665-011-1043-7

Sunberg, J., 1988. Thermal Properties of Soils and Rocks.- 325p.; Göteborg (Geologiska Institutionen Publ. A57).

Suzuki, K. and Kaieda, H., 2000. Geological structure around the Ogachi Hot Dry Rock test site using seismic reflection and CSAMT surveys. In Proceedings World Geothermal Congress 2000, Kyushu--Tohoku, Japan, May 28-June 10.

Szczepański, A., Sadurski, A., Hajto, M., Papiernik, B., Szewczyk, J., Sokołowski, A., Strzetelski, W., Haładus, A., Kania, J., Rajchel, L. and Feldman-Olszewska, A., 2006. Atlas of Geothermal Resources of Paleozoic Formations in the Polish Lowlands, W. Ministry of Environment. ZSE AGH, Kraków.

Teatini, P., Gambolati, G., Ferronato, M., Settari, A., and Walters, D., 2011. Land uplift due to subsurface fluid injection. Journal of Geodynamics, 51, pp.1-16. DOI: https://doi.org/10.1016/j.jog.2010.06.001.

Tello-López, M.R. and Torres-Rodrıguez, M.A., 2015. Behavior of the production characteristics of the wells in the Las Tres Vırgenes, BCS, Geothermal Field, México. In Proceedings World Geothermal Congress 2015 (pp. 19-25).

Tenma, N., Yamaguchi, T., and Zyvoloski, G., 2005. Variation of the Characteristics of the Shallow Reservoir at the Hijiori Test Site between 90-days Circulation Test and Long-Term Circulation Test Using FEHM Code. Proceedings World Geothermal Congress 2005 Antalya, Turkey, 24-29 April 2005.

Tenzer, H., 1995. Fracture Mapping and Determination of Horizontal Stress Field by Borehole Measurements in HDR Drillholes Soultz, Urach. In World Geothermal Congress (pp. 2649-2655).

Tenzer, H., Schanz, U., and Homeier G., 1999. HDR research programme and results of drill hole Urach 3 to depth of 4440 m – The key for realisation of a HDR programme in southern Germany and northern Switzerland. In Proceedings of the world geothermal congress, 28-30 September 1999, Basel, P.10.

Tenzer, H., Schanz, U., Stang, H., Baisch, S. and Weidler, R., 2004. Potential for geothermal power production from deep hot crystalline rock at Bad Urach (Southern Germany). Zeitschrift für angewandte Geologie, 50(2), pp.43-49.

Tch, A., 2017. The mostly complete chart of Neural Networks, explained. - Towards Data Science, Accessed on May 02, 2023: https://towardsdatascience.com/the-mostly-complete-chart-of-neural-networks-explained-3fb6f2367464.

Tischner, T., Schindler, M., Jung, R. and Nami, P., 2007, January. HDR project Soultz: Hydraulic and seismic observations during stimulation of the 3 deep wells by massive water injections. In Proceedings, 32nd workshop on Geothermal Engineering, Stanford University, Stanford, California (pp. 22-24)

Tischner, T., Evers, H., Hauswirth, H., Jatho, R., Kosinowski, M. and Sulzbacher, H., 2010, April. New concepts for extracting geothermal energy from one well: the GeneSys-Project. In Proceedings of the world geothermal congress, Bali (Vol. 2530).

Tischner, T., Krug, S., Pechan, E., Hesshaus, A., Jatho, R., Bischoff, M. and Wonik, T., 2013, February. Massive hydraulic fracturing in low permeable sedimentary rock in the GeneSys project. In Proceedings of the Thirty-Eighth Workshop on Geothermal Reservoir Engineering, SGP-TR-198, Stanford University, Stanford, CA, USA (pp. 11-13).

Trautwein, U. and Huenges, E., 2005. Poroelastic behaviour of physical properties in Rotliegend sandstones under uniaxial strain. International Journal of Rock Mechanics and Mining Sciences, 42(7-8), pp.924-932. DOI: https://doi.org/10.1016/j.ijrmms.2005.05.016

Trugman, D.T., Borsa, A.A. and Sandwell, D.T., 2014. Did stresses from the Cerro Prieto Geothermal Field influence the El Mayor-Cucapah rupture sequence? Geophysical Research Letters, 41(24), pp.8767-8774. DOI: https://doi.org/10.1002/2014GL061959

Trugman, D.T., Shearer, P.M, Borsa, A.A., and Fialko, Y., 2016. A comparison of long-term changes in seismicity at The Geysers, Salton Sea, and Coso geothermal fields. Journal of Geophysical Research: Solid Earth, 121, 225-247. DOI: https://doi.org/10.1002/2015JB012510.

Tuğrul, A. and Zarif, İ.H., 1998. The influence of mineralogical textural and chemical characteristics on the durability of selected sandstones in Istanbul, Turkey. Bulletin of Engineering Geology and the Environment, 57, pp.185-190.

Tut Haklıdır, F.S., Sengün, R., and Aydın, H., 2021. Characterization and Comparison of geothermal fluids geochemistry within the Kızıldere Geothermal Field in Turkey: New findings with power capacity expanding studies. Geothermics, 94, pp.1-23. DOI: https://doi.org/10.1016/j.geothermics.2021.102110.

UGII (Unscheinbarer Glanz im Informationsnetz), Accessed in June 2023: http://www.ugii.net/umwelt/schriften/12-jk-waren.html

Ulrich, S., Dyer, B., Ladner, F. and Häring, M.O., 2007. Part 2: Microseismic aspects of the Basel 1 geothermal reservoir. In 5th Swiss Geoscience Meeting, Genova2007 (Website: http://www.geothermal.ch/english/downloads.html)

Umweltbundesamt, Energieverbrauch für fossile und erneuerbare Wärme. Accessed in July 2023: https://www.umweltbundesamt.de/daten/energie/energieverbrauch-fuer-fossile-erneuerbare-waerme.

Ungemach, P., 1983. Geothermal Field Development in the European Community: Objectives, Achivements and Problem Areas.- Proc. Ninth Workshop Geothermal Reservoir Engineering, December 1983, Stanford: 5-15.

Ura-Binczyk, E., Banas, J., Mazurkiewicz, B., Solarski, W., Lewandowska, M., Roguska, A., M. Andrzejczuk, M., Balcer, M., Kulik, S., Zarnowiec, P., and Kaca, W., 2019. On-site monitoring and laboratory characterization of corrosion processes in the geothermal water of Polish Lowland. Geothermics, 77, pp.267-277. DOI: https://doi.org/10.1016/j.geothermics.2018.10.002.

Urban, E. and Lermo, J.F., 2012. Relationship of local seismic activity, injection wells and active faults in the geothermal fields of Mexico. In Proceedings of Thirty-Seventh Workshop on Geothermal Reservoir Engineering, Stanford University, Stanford, CA, SGP-TR-194.

Urban, E. and Lermo, J.F., 2013, February. Local seismicity in the exploitation of Los Humeros geothermal field, Mexico. In 38th Workshop on Geothermal Reservoir Engineering (pp. 11-13).

Urban, E. and Lermo, J., 2017. Fracture and stress evaluation using well logs and microseismicity, in the exploitation of Los Humeros geothermal field, Mexico. Trans. Geotherm. Resour. Counc, 41, pp.1756-1780.

USGS (United State Geological Survey) Earthquake Catalog, Accessed in May 2023: https://earthquake.usgs.gov/earthquakes/search/.

Valley, B. and Evans, K.F., 2007, January. Stress state at Soultz-sous-Forêts to 5 km depth from wellbore failure and hydraulic observations. In Proceedings, 32nd workshop on geothermal reservoir engineering (pp. 17481-17469).

Valley, B. and Evans, K.F., 2019. Stress magnitudes in the Basel enhanced geothermal system. International Journal of Rock Mechanics and Mining Sciences, 118, pp.1-20. DOI: https://doi.org/10.1016/j.ijrmms.2019.03.008

Vallier, B., Magnenet, V., Schmittbuhl, J. and Fond, C., 2018. THM modeling of hydrothermal circulation at Rittershoffen geothermal site, France. Geothermal Energy, 6, pp.1-26. DOI: https://doi.org/10.1186/s40517-018-0108-1

van Eijs, R.M.H.E., Mulders, F.M.M., Nepveu, M., Kenter, C.J., and Scheffers, B.C., 2006. Correlation between hydrocarbon reservoir properties and induced seismicity in the Netherlands. Engineering Geology, 84, pp.99-111. DOI: https://doi.org/10.1016/j.enggeo.2006.01.002.

Van Gessel, S., Middelburg, H., Hintersberger, E., Larsen, T., Ben Rhouma, S., Diepolder, G., and Di Manna, P., 2020. Towards a comprehensive European fault database for induced seismic hazard research. EGU General Assembly 2020, Online, 4–8 May 2020, EGU2020-21420. DOI: https://doi.org/10.5194/egusphere-egu2020-21420.

Van Wees, J.D., Buijze, L., Van Thienen-Visser, K., Nepveu, M., Wassing, B.B.T., Orlic, B. and Fokker, P.A., 2014. Geomechanics response and induced seismicity during gas field depletion in the Netherlands. Geothermics, 52, pp.206-219. DOI: https://doi.org/10.1016/j.geothermics.2014.05.004

Vasarhelyi, B., 2003. Some observations regarding the strength and deformability of sandstones in dry and saturated conditions. Bulletin of Engineering Geology and the Environment, 62, pp.245-249. DOI: https://doi.org/10.1007/s10064-002-0186-x

Veldkamp, J.G., Mijnlieff, H., Bloemsma, M., Donselaar, R., Henares, S., Redjosentono, A. and Weltje, G.J., 2015. Permian Rotliegend reservoir architecture of the Dutch Koekoekspolder Geothermal Doublet. World Geothermal Congress, 19–25 April 2015, Melbourne, Australia. In Conference proceedings.

Verma, S.P., Pandarinath, K., Santoyo, E., González-Partida, E., Torres-Alvarado, I.S. and Tello-Hinojosa, E., 2006. Fluid chemistry and temperatures prior to exploitation at the Las Tres Vírgenes geothermal field, Mexico. Geothermics, 35(2), pp.156-180. DOI: https://doi.org/10.1016/j.geothermics.2006.02.002

Verweij, J.M., Simmelink, H.J., Underschultz, J. and Witmans, N., 2012. Pressure and fluid dynamic characterisation of the Dutch subsurface. Netherlands Journal of Geosciences, 91(4), pp.465-490. DOI: https://doi.org/10.1017/S0016774600000342

Van Gessel, S., Hintersberger, E., v. Ede, R., ten Veen, J., Doornenbal, H., Diepolder, G.W., den Dulk, M., Hamiti, S., Vukzaj, N., Çako, R., Prendi, E., Ceroni, M., Mara, A., Barros, R., Tovar, A., Britze, P., Baudin, T., Stück, H., Jähne-Klingberg, F., Jahnke, C., Höding, T., Malz, A., Kristjánsdóttir, S., Þorbergsson, A, Di Manna, P., D'Ambrogi, C., Congi, M., Lazauskienė, J., Andriuškevičienė, G., Baliukevičius, A., Jarosiński, M., Gogołek, T., Stępień, U., Krzemińska, E., Salwa, S., Habryn, R., Aleksandrowski, P., Szynkaruk, E., Konieczyńska, M., Ressurreição, R., Machado, S., Moniz, C., Sampaio, J., Dias, R., Carvalho, J., Fernandes, J., Ramalho, E., Filipe, A., Celarc, B., Atanackov, J., Jamšek Rupnik, P., Shevchenko, A., Melnyk, I., and Lapshyna, A., 2021. The HIKE European Fault Database (EFDB) compiled in the framework of the GeoERA project HIKE (2018-2021). https://egdi.geology.cz/record/basic/5edf7bd4-9270-4188-b69d-7ddd0a010833

Vasco, D.W., Karasaki, K. and Nakagome, O., 2002. Monitoring production using surface deformation: the Hijiori test site and the Okuaizu geothermal field, Japan. Geothermics, 31(3), pp.303-342. DOI: https://doi.org/10.1016/S0375-6505(01)00036-0

Victor Aníbal Rodríguez S., 2005. Analysis of temperature and pressure measurements and production data for Berlín geothermal field, El Salvador. United Nations University.

Vidal, J. and Genter, A., 2018. Overview of naturally permeable fractured reservoirs in the central and southern Upper Rhine Graben: Insights from geothermal wells. Geothermics, 74, pp.57-73. DOI: https://doi.org/10.1016/j.geothermics.2018.02.003

Vilarrasa, V., Carrera, J., Olivella, S., Rutqvist, J., and Laloui, L., 2019. Induced seismicity in geologic carbon storage. Solid Earth, 10, pp.871-892. DOI: https://doi.org/10.5194/se-10-871-2019.

Vondrak, A., De Weerd, A.V., Leeuwen, L.V., Brautigam, K. and Brautigam, K., 2014. Update doubletvoorstel HON-GT-03 enHON-GT-04(G1121). PanTerra Geoconsultants B.V. Netherland. 89 p. (from NLOG database)

Vörös, R. and Baisch, S., 2019. Seismic hazard assessment for the CLG-Geothermal System–study update March 2019. Report No. CLG006. Q-con GmbH (Bad Bergzabern).

Vrouwe, B.J. and Rutten, R.F.X., 2012. Welltest Analyse HON-GT-O2, Project Number: 0311-OEM2495. Greenwell Westland B.V. 34 P.

Wallis, I.C., McNamara, D., Rowland, J.V. and Massiot, C., 2012, January. The nature of fracture permeability in the basement greywacke at Kawerau Geothermal Field, New Zealand. In Proceedings, Thirty-Seventh Workshop on Geothermal Reservoir Engineering (pp. 1-9). Stanford University Stanford, CA.

Wallis, I., Rowland, J., Dempsey, D., Allan, G., Sidik, R., Martikno, R., McLean, K., Sihotang, M., Azis, H., and Baroek, M., 2020. Approaches to Imaging Feedzone Diversity with Case Studies from Sumatra, Indonesia and the Taupo Volcanic Zone, New Zealand.- Proc. 42nd New Zealand Geothermal Workshop, 24-26 November 2020, Waitingi.

Wallis, I.C., Rowland, J.V., Cumming, W., and Dempsey, D., 2017. The subsurface geometry of a natural geothermal reservoir. Proc. 39th New Zealand Geothermal Workshop, 21-25 November 2017, Rotorua.

Wamalwa, R.N., Waswa, A.K., Nyamai, C.N., Mulwa, J. and Ambusso, W.J., 2016. Evaluation of the factors controlling concentration of non-condensable gases and their possible impact on the performance of geothermal systems: case study of Olkaria wells in the Kenyan rift valley. International journal of geosciences, 7(3), pp.257-279.

Wassing, B.B.T., Gan, Q., Candela, T. and Fokker, P.A., 2021. Effects of fault transmissivity on the potential of fault reactivation and induced seismicity: Implications for understanding induced seismicity at Pohang EGS. Geothermics, 91, p.101976. DOI: https://doi.org/10.1016/j.geothermics.2020.101976

Weaver, J., Eggertsson, G.H., Utley, J.E., Wallace, P.A., Lamur, A., Kendrick, J.E., Tuffen, H., Markússon, S.H. and Lavallée, Y., 2020. Thermal liability of hyaloclastite in the Krafla geothermal reservoir, Iceland: the impact of phyllosilicates on permeability and rock strength. Geofluids, 2020, pp.1-20. DOI: https://doi.org/10.1155/2020/9057193

Weydt, L.M., Bär, K., Colombero, C., Comina, C., Deb, P., Lepillier, B., Mandrone, G., Milsch, H., Rochelle, C.A., Vagnon, F. and Sass, I., 2018. Outcrop analogue study to determine reservoir properties of<? xmltex\break?> the Los Humeros and Acoculco geothermal fields, Mexico. Advances in Geosciences, 45, pp.281-287. DOI: https://doi.org/10.5194/adgeo-45-281-2018

White, S.P., 1995. Inverse modelling of the Kawerau geothermal reservoir, NZ (No. GEO-PROC-95-02). NZ Institute for Industrial Research and Development, Lower Hutt, NZ. DOI:10.2172/895955

Vidal, J. and Genter, A., 2018. Overview of naturally permeable fractured reservoirs in the central and southern Upper Rhine Graben: Insights from geothermal wells. Geothermics, 74, pp.57-73. DOI: https://doi.org/10.1016/j.geothermics.2018.02.003

Willson, S.M., Last, N.C., Zoback, M.D. and Moos, D., 1999, April. Drilling in South America: a wellbore stability approach for complex geologic conditions. In Latin American and Caribbean petroleum engineering conference. OnePetro.

Wolfgramm, M., Bartels, J., Hoffmann, F., Kittl, G., Lenz, G., Seibt, P., Schulz, R., Thomas, R. and Unger, H.J., 2007, May. Unterhaching geothermal well doublet: structural and hydrodynamic reservoir characteristic; Bavaria (Germany). In European Geothermal Congress (Vol. 30).

Wood, C.P., 1996. Basement geology and structure of TVZ geothermal fields, New Zealand. In Proceedings of the 18th New Zealand Geothermal Workshop (pp. 157-162). The University of Auckland, Auckland, New Zealand Geothermal Institute.

Wood, C.P., Brathwaite, R.L. and Rosenberg, M.D., 2001. Basement structure, lithology and permeability at Kawerau and Ohaaki geothermal fields, New Zealand. Geothermics, 30(4), pp.461-481. DOI: https://doi.org/10.1016/S0375-6505(01)00003-7

Worum, G., van Wees, J.D., Bada, G., van Balen, R.T., Cloetingh, S. and Pagnier, H., 2004. Slip tendency analysis as a tool to constrain fault reactivation: A numerical approach applied to three-dimensional fault models in the Roer Valley rift system (southeast Netherlands). Journal of Geophysical Research: Solid Earth, 109(B2). DOI: https://doi.org/10.1029/2003JB002586

Wyborn, D., 2010, April. Update of development of the geothermal field in the granite at Innamincka, South Australia. In Proceedings of the World Geothermal Congress, Bali, Indonesia (Vol. 2530, p. 2529).

Wyering, L.D., Villeneuve, M.C., Wallis, I.C., Siratovich, P.A., Kennedy, B.M., Gravley, D.M. and Cant, J.L., 2014. Mechanical and physical properties of hydrothermally altered rocks, Taupo Volcanic Zone, New Zealand. Journal of Volcanology and Geothermal Research, 288, pp.76-93. DOI: https://doi.org/10.1016/j.jvolgeores.2014.10.008

Yeltekin, K., Parlaktuna, M. and Akin, S., 2002, January. Modeling of Kizildere geothermal reservoir, Turkey. In Proceedings of the 27th Workshop on Geothermal Reservoir Engineering, Stanford University, Stanford, CA, paper SGP-TR-171 (on CDROM) pp (pp. 1-8).

Younker, L.W., Kasameyer, P.W. and Tewhey, J.D., 1982. Geological, geophysical, and thermal characteristics of the Salton Sea Geothermal Field, California. Journal of Volcanology and Geothermal Research, 12(3-4), pp.221-258. https://doi.org/10.1016/0377-0273(82)90028-2

Yousefi, H., Roumi, S., Ármannsson, H. and Noorollahi, Y., 2019. Cascading uses of geothermal energy for a sustainable energy supply for Meshkinshahr City, Northwest, Iran. Geothermics, 79, pp.152-163. DOI: https://doi.org/10.1016/j.geothermics.2019.01.012

Zang, A., Oye, V., Jousset, P., Deichmann, N., Gritto, R., McGarr, A., Majer, E., and Bruhn, D., 2014. Analysis of induced seismicity in geothermal reservoirs – An overview. Geothermics, 52, pp.6-21. DOI: http://doi.org/10.1016/j.geothermics.2014.06.005.

Zemach, E., Drakos, P., Robertson-Tait, A. and Lutz, S.J., 2010, April. Feasibility evaluation of an "in-field" EGS project at Desert Peak, Nevada, USA. In Proceedings World Geothermal Congress.

Zhang, Y., and Zhao, G.F., 2020. A global review of deep geothermal energy exploration: from a view of rock mechanics and engineering. Geomechanics and Geophysics for Geo-Energy and Geo-Resources, 6, pp.1-26. DOI: https://doi.org/10.1007/s40948-019-00126-z.

Ziegler, M.O. and Heidbach, O., The 3D stress state from geomechanical–numerical modelling and its uncertainties: a case study in the Bavarian Molasse Basin. Geotherm Energy. 2020; 8: 11. DOI: https://doi.org/10.1186/s40517-020-00162-z

Ziegler, M. O., Heidbach, O., Reinecker, J., Przybycin, A. M., and Scheck-Wenderoth, M. 2016. A multi-stage 3-D stress field modelling approach exemplified in the Bavarian Molasse Basin, Solid Earth, 7, 1365–1382. DOI: https://doi.org/10.5194/se-7-1365-2016, 2016.

Zimmermann, G., Moeck, I. and Blöcher, G., 2010. Cyclic waterfrac stimulation to develop an enhanced geothermal system (EGS)—conceptual design and experimental results. Geothermics, 39(1), pp.59-69. DOI: https://doi.org/10.1016/j.geothermics.2009.10.003

Zimmermann, G. and Reinicke, A., 2010. Hydraulic stimulation of a deep sandstone reservoir to develop an Enhanced Geothermal System: Laboratory and field experiments. Geothermics, 39(1), pp.70-77. DOI: https://doi.org/10.1016/j.geothermics.2009.12.003

Zingg, O. and Meier, P., 2019. Summary of the Investigations Conducted Following the November 2017 Earthquake in Pohang, South Korea, and Implications for the Haute-Sorne Multi-stage-stimulation EGS Project, Switzerland. GRC-Transactions, Vol. 43.

Zoback, M.D., 2007. Reservoir geomechanics. Cambridge University Press.